

Program subject to change until 12/16/2019.



105[™] Scientific Assembly and Annual Meeting December 1–6 | McCormick Place, Chicago





Practical MR Imaging

Friday, Dec. 6 8:30AM - 10:00AM Room: E353B



AMA PRA Category 1 Credits ™: 1.50 ARRT Category A+ Credit: 1.75

LEARNING OBJECTIVES

1) Discuss application of optimized non-vascular thoracic MR protocols for troubleshooting problematic mediastinal masses. 2) Use case based discussion to highlight which indeterminate mediastinal masses could benefit from further tissue characterization provided by MR. 3) Describe MR imaging appearances of select indeterminate and complex cystic mediastinal masses. 4) Harness the tissue characterization properties of MRI to add diagnostic specificity to assessment of pleural lesions beyond that of CT. 5) Understand how higher soft tissue contrast of MR can make CT-occult lesions visible. 6) Recognize how the higher soft tissue contrast of MR than CT can: a) add precision to lesion compartment localization, narrowing the differential diagnosis b) better show integrity of tissue planes and invasion across them. 7) To give an overview over the diagnostic scope of lung MRI for pathologies of lung parenchyma and airway disease. 8) To review the diagnostic yield of MRI for the detection and characterisation of lung nodules. 9) To introduce MRI as potential first choice modality for imaging pulmonary disease in young or pregnant patients. 10) To discuss the potential role of lung MRI as an alternative or adjunct modality, e.g. in COPD or interstitial lung diseases. 11) List most common benign and malignant cardiac masses. 12) Assemble key magnetic resonance imaging sequences into a protocol to assess cardiac masses.13) Recognize magnetic resonance imaging features of select benign and malignant cardiac masses.

Sub-Events

RC801A Troubleshooting Problematic Mediastinal Masses with MR Imaging

Participants

Rachna Madan, MD, Boston, MA (Presenter) Nothing to Disclose

For information about this presentation, contact:

rmadan@bwh.harvard.edu

LEARNING OBJECTIVES

1) Discuss application of optimized non-vascular thoracic MR protocols for troubleshooting problematic mediastinal masses. 2) Use case based discussion to highlight which indeterminate mediastinal masses could benefit from further tissue characterization provided by MR. 3) Describe MR imaging appearances of select indeterminate and complex cystic mediastinal masses.

RC801B The Value of MRI for Diagnosis of Pleural Disease

Participants

Jeanne B. Ackman, MD, Weston, MA (*Presenter*) Spouse, Stockholder, Everest Digital Medicine; Spouse, Consultant, Everest Digital Medicine; Spouse, Stockholder, Cynvenio Biosystems, Inc; Spouse, Scientific Advisory Board, Cynvenio Biosystems, Inc; Spouse, Consultant, PAREXEL International Corporation

LEARNING OBJECTIVES

1) Harness the tissue characterization properties of MRI to add diagnostic specificity to assessment of pleural lesions beyond that of CT. 2) Understand how higher soft tissue contrast of MR can make CT-occult lesions visible. 3) Recognize how the higher soft tissue contrast of MR than CT can: a) add precision to lesion compartment localization, narrowing the differential diagnosis b) better show integrity of tissue planes and invasion across them.

RC801C MR Imaging of the Lung: Added Value for Your Thoracic Imaging Practice

Participants Juergen Biederer, MD, Heidelberg, Germany (*Presenter*) Nothing to Disclose

For information about this presentation, contact:

juergen.biederer@uni-heidelberg.de

LEARNING OBJECTIVES

1) To give an overview over the diagnostic scope of lung MRI for pathologies of lung parenchyma and airway disease. 2) To review the diagnostic yield of MRI for the detection and characterisation of lung nodules. 3) To introduce MRI as potential first choice modality for imaging pulmonary disease in young or pregnant patients. 4) To discuss the potential role of lung MRI as an alternative or adjunct modality, e.g. in COPD or interstitial lung diseases.

ABSTRACT

MRI of the lung can play an interesting role and be added value to your thoracic imaging practice besides X-ray and CT. The sensitivity of MRI for infiltrates is at least similar to X-ray and CT, lung nodule detection is superior to X-ray and slightly inferior to CT and favorable options for tissue characterization (exclusion of malignancy) and functional imaging capacities (perfusion, ventilation, respiratory motion) are available with standardized protocols. Given this, MRI may serve as a radiation-free alternative in patients who should not be exposed to ionizing radiation (children and young subjects, pregnant patients), e.g. as your first

choice modality in patients with cystic fibrosis. It may well serve as an adjunct to other modalities for comprehensive lung imaging in COPD and some cases of interstitial lung diseases, e.g. sarcoidosis (dark lymph node sign). In young patients, MRI may well be used for the long term follow-up of malignancy (e.g. seminoma) or inflammatory disease (e.g. GPA/Wegener's disease). As an adjunct or alternative to other modalities, MRI can be helpful in lung cancer staging and follow-up (differentiation of atelectasis and lung cancer) or the characterization of lung nodules ('actionable nodules' with contrast uptake, high NPV in nodules with no or low contrast uptake, fatty content in hamartoma). MRI might even be suitable for the early detection of lung cancer, either as the primary screening tool or for the ad-hoc diagnostic work-up of detected lesions on site.

RC801D Magnetic Resonance Imaging of Cardiac Masses

Participants

Nila J. Akhtar, MD, Rochester, MN (Presenter) Nothing to Disclose

LEARNING OBJECTIVES

1) List most common benign and malignant cardiac masses. 2) Assemble key magnetic resonance imaging sequences into a protocol to assess cardiac masses. 3) Recognize magnetic resonance imaging features of select benign and malignant cardiac masses.

RC801E MR Imaging of Aortopathies

Participants

Cristina Fuss, MD, Portland, OR (Presenter) Spouse, Officer, ViewRay, Inc

LEARNING OBJECTIVES

1) To familiarize the learner with the most common familiar aortopathies, their clinical background, imaging appearance on MRI and specific considerations for MR acquisition planning.

ABSTRACT

Familial aortopahties comprise a grounp of inherited disorders of aortic aneurysms and/or dissection including. These include Thoracic Aortic Aneurysms and Aortic Dissections (TAAD), Marfan syndrome, Loeys-Dietz syndrome, and Ehlers-Danlos syndrome, only to name the most common ones.

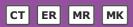






Avulsion Injuries of the Upper and Lower Extremities

Friday, Dec. 6 8:30AM - 10:00AM Room: E451B



AMA PRA Category 1 Credits ™: 1.50 ARRT Category A+ Credit: 1.75

Participants

Zehava S. Rosenberg, MD, Hoboken, NJ (Director) Nothing to Disclose

Sub-Events

RC804A Upper Extremity

Participants Lee F. Rogers, MD, Tucson, AZ (*Presenter*) Nothing to Disclose

For information about this presentation, contact:

lfrogers@comcast.net

LEARNING OBJECTIVES

1) Obtain appropriate radiographs, AP, lateral and obliques; oblique views are essential as certain fractures may be visible only on this projection. 2) Certain fractures and dislocations are notorious for being overlooked; know these injuries and be certain to identify or exclude them. 3) Certain ligamentous avulsion of the digits are associated with characteristic deformities allowing a definitive diagnosis of the underlying abnormality. 4) Be aware of the potential for satisfaction of search and the potential of diagnostic oversights in certain injuries; once such an injury is noted look closely for the commonly associated injury. 5) When the clinical diagnosis is not apparent or uncertain on the initial radiographs, do not hesitate to obtain CT or MRI to confirm or exclude an injury.

RC804B Avulsion Injuries of the Pelvis and Hip

Participants

Omer A. Awan, MD, Baltimore, MD (Presenter) Nothing to Disclose

LEARNING OBJECTIVES

1) Outline the spectrum of avulsive injuries in the pelvis and hip. 2) Delineate imaging characteristics of pelvic and hip avulsive injuries, with emphasis on radiography and MRI. 3) Elucidate practical and clinical applications to pelvic and hip avulsive injuries.

ABSTRACT

n/a

RC804C Knee

Participants Thomas L. Pope, MD, Denver, CO (*Presenter*) Nothing to Disclose

For information about this presentation, contact:

thomaspopemd@gmail.com

LEARNING OBJECTIVES

1) Delineate the most common avulsion injuries in the knee. 2) Outline the most common imaging features of avulsion injuries in the knee. 3) Describe the complimentary role of radiography, CT and MR imaging in the diagnosis of avulsion injuries of the knee. 4) Provide some hints on keys to avoid missing these lesions in your clinical practice.

RC804D Foot and Ankle

Participants

Zehava S. Rosenberg, MD, Hoboken, NJ (Presenter) Nothing to Disclose

LEARNING OBJECTIVES

1) Familiarize the radiologist with radiographic findings of common avulsion injuries of the ankle and foot with emphasis on frequently missed entities. 2) Provide cross sectional imaging correlation for all the described entities. 3) Provide the radiologist with tools for distinguishing radiographic evidence of pathology from mimickers of disease.





Call in the Troops, or Walk on By? Management of Unexpected Findings in Neuro/Head & Neck (Interactive Session)

Friday, Dec. 6 8:30AM - 10:00AM Room: E450B



AMA PRA Category 1 Credits ™: 1.50 ARRT Category A+ Credit: 1.75

Participants

Deborah R. Shatzkes, MD, New York, NY (*Moderator*) Nothing to Disclose Pejman Jabehdar Maralani, MD, FRCPC, Toronto, ON (*Moderator*) Nothing to Disclose

For information about this presentation, contact:

pejman.maralani@utornoto.ca

Sub-Events

RC805A Unexpected Intracranial Findings

Participants

Alireza Radmanesh, MD, New York, NY (Presenter) Nothing to Disclose

LEARNING OBJECTIVES

1) Identify and describe the most frequently encountered unexpected/incidental intracranial findings. 2) Characterize some potentially significant consequences of incidental intracranial findings. 3) Identify and implement the best available recommendations to handle incidental intracranial findings.

RC805B Unexpected Skull Base Findings

Participants

Tabassum A. Kennedy, MD, Saint Louis, MO (Presenter) Nothing to Disclose

For information about this presentation, contact:

tkennedy@uwhealth.org

LEARNING OBJECTIVES

1) Recognize common anatomic variants of the skull base. 2) Recommend the appropriate next step in evaluating a patient with an unexpected skull base lesion. 3) Generate a short differential for common skull base lesions based on anatomic location.

RC805C Unexpected Spine Findings

Participants Jason F. Talbott, MD, PhD, Novato, CA (*Presenter*) Nothing to Disclose

For information about this presentation, contact:

jason.talbott@ucsf.edu

LEARNING OBJECTIVES

1) Gain familiarity with 4 basic craniospinal metrics that will enable the radiologist to readily identify unexpected congenital anomalies of the spine and craniovertebral junction. 2) Identify and the top blindspots in spine CT and MRI for frequently missed and clinically significant incidental findings. 3) Review clinical recommendations for the most frequent incidental findings on spine imaging.

ABSTRACT

With the progressive increase in spine imaging, unexpected findings not related to the initial clinical indication for imaging are increasingly recognized. While many of these findings are incidental and require no further management recommendations, some incidental findings are of clinical significance. Thus, it is paramount that the radiologist is familiar with the imaging appearance of clinically significant incidental findings of the spine. It is equally important that the radiologist's diagnostic search pattern of the spine includes areas where incidental, but clinically significant spine findings are frequently observed. This presentation will prepare the radiologist to identify the most frequent and clinically significant incidental findings on cross-sectional spine studies including un-expected congenital, infectious, and traumatic pathologies. Appropriate clinical recommendations will also be discussed.

RC805D Unexpected Neck Findings

Participants Philip R. Chapman, MD, Birmingham, AL (*Presenter*) Nothing to Disclose

LEARNING OBJECTIVES

1) Identify and describe the most frequently encountered unexpected/incidental findings in neck. 2) Characterize some potentially significant consequences of incidental neck findings. 3) Identify and implement the best available recommendations to handle incidental intracranial findings. 4) Improve awareness of learn search strategies for identifying incidental or unexpected findings in the neck.





Body CT Angiography: 2019 Update

Friday, Dec. 6 8:30AM - 10:00AM Room: E351



AMA PRA Category 1 Credits ™: 1.50 ARRT Category A+ Credit: 1.75

Participants

Alan H. Stolpen, MD,PhD, Iowa City, IA (*Moderator*) Nothing to Disclose Gregory Kicska, MD, PhD, Seattle, WA (*Moderator*) Nothing to Disclose

For information about this presentation, contact:

alan-stolpen@uiowa.edu

Sub-Events

RC812A Thoracic CTA

Participants Gregory Kicska, MD, PhD, Seattle, WA (*Presenter*) Nothing to Disclose

For information about this presentation, contact:

kicskag@uw.edu

LEARNING OBJECTIVES

1) Diagnosis of aortic dissection, intramural hematoma and aortic aneurysm. 2) To discuss imaging features that suggest prognosis in acute aortic syndromes. 3) To discuss common pitfalls in diagnosis.

RC812B Abdominal CTA

Participants Eric E. Williamson, MD, Rochester, MN (*Presenter*) Nothing to Disclose

For information about this presentation, contact:

Williamson.eric@mayo.edu

LEARNING OBJECTIVES

1) Identify common clinical indications for abdominal CT angiography, 2) Describe techniques for performing abdominal CTA, 3) Discuss how recent developments in CT have influenced these techniques and the resulting imaging findings.

RC812C Peripheral CTA

Participants Alan H. Stolpen, MD, PhD, Iowa City, IA (*Presenter*) Nothing to Disclose

For information about this presentation, contact:

alan-stolpen@uiowa.edu

LEARNING OBJECTIVES

1) Identify common clinical indications for peripheral CTA. 2) Describe protocols for performing and strategies for reviewing peripheral CTA. 3) Recognize a variety of vascular pathologies. 4) Understand the strengths, weaknesses and pitfalls of peripheral CTA.





Pediatric Neuroemergencies

Friday, Dec. 6 8:30AM - 10:00AM Room: E451A



AMA PRA Category 1 Credits ™: 1.50 ARRT Category A+ Credit: 1.75

Sub-Events

RC813A Pediatric Brain Emergencies: Traumatic

Participants V. Michelle Silvera, MD, Boston, MA (*Presenter*) Nothing to Disclose

RC813B Pediatric Brain Emergencies: Non-traumatic

Participants

Sarah S. Milla, MD, Atlanta, GA (Presenter) Nothing to Disclose

For information about this presentation, contact:

sarah.milla@emory.edu

LEARNING OBJECTIVES

1) Review causes of atraumatic pediatric brain emergencies. 2) Illustrate "teaching points" and things not to miss. 3) Discuss optimal imaging techniques for lesion detection.

ABSTRACT

The topic of 'Nontraumatic Brain Emergencies' include several causes of significant morbidity and mortality in children. Vascular causes, such as stroke and sinus thrombosis will be discussed, with illustrative cases to demonstrate tips for interpreting neuroimaging in children of all ages. Infectious and subtle neoplastic cases will also be reviewed to highlight 'what not to miss' in this 20 minute review.

RC813C Pediatric Head and Neck Emergencies

Participants Alok I. Jaju, MD, Chicago, IL (*Presenter*) Nothing to Disclose

For information about this presentation, contact:

ajaju@luriechildrens.org

LEARNING OBJECTIVES

1) Identify the pediatric head and neck pathologies that can present in the emergency setting. 2) Describe the complications and routes of spread of pediatric head and neck infections. 3) Recommend the best imaging technique and next step in management for common head and neck emergencies.

Active Handout: Alok Indraprakash Jaju

http://abstract.rsna.org/uploads/2019/19000103/Active RC813C.pdf

RC813D Pediatric Spine Emergencies

Participants Maura E. Ryan, MD, Chicago, IL (*Presenter*) Nothing to Disclose

LEARNING OBJECTIVES

1) To identify and understand the significance of critical imaging findings in pediatric spine emergencies in both traumatic and atraumatic settings.

Active Handout:Maura E. Ryan

http://abstract.rsna.org/uploads/2019/19000104/Active RC813D.pdf







The Neoadjuvant Patient

Friday, Dec. 6 8:30AM - 10:00AM Room: E352



AMA PRA Category 1 Credits ™: 1.50 ARRT Category A+ Credit: 1.75

Participants

Eric L. Rosen, MD, Seattle, WA (Moderator) Nothing to Disclose

For information about this presentation, contact:

zuleyml@upmc.edu

LEARNING OBJECTIVES

1) To discuss three clinically significant areas involving care of the breast cancer patient undergoing neoadjuvant therapy. 2) To apply in everyday clinical practice the principles and conclusions learned.

Sub-Events

RC815A State-of-the-Art: An Evidence-based Approach

Participants

Eric L. Rosen, MD, Seattle, WA (Presenter) Nothing to Disclose

RC815B Ongoing Trials and Future Directions

Participants

Jessica W. Leung, MD, Houston, TX (Presenter) Scientific Advisory Board, Subtle Medical

LEARNING OBJECTIVES

1) To learn the design of some of the ongoing clinical trials involving care of the breast cancer patient receiving neoadjuvant therapy. 2) To describe the imaging components of these trials. 3) To understand the role that imaging plays in these trials.

RC815C Ultrasound Evaluation of the Axilla in the Neoadjuvant Patient

Participants

Steven P. Poplack, MD, Saint Louis, MO (Presenter) Nothing to Disclose

LEARNING OBJECTIVES

1) Identify the key US criteria that are predictive of axillary lymph node metastases. 2) Appraise the accuracy of axillary US in the setting of Invasive Breast Cancer. 3) Describe the role of axillary US in the surgical management of the axilla after neoadjuvant treatment.





Taking Action to Promote Gender Inclusion in Radiology: A Roadmap for Progress (Sponsored by the RSNA Professionalism Committee)

Friday, Dec. 6 8:30AM - 10:00AM Room: E253CD

LM

AMA PRA Category 1 Credits ™: 1.50 ARRT Category A+ Credit: 1.75

Participants

Anastasia L. Hryhorczuk, MD, Ann Arbor, MI (*Moderator*) Nothing to Disclose Kate Hanneman, MD, FRCPC, Toronto, ON (*Moderator*) Medical Advisory Board, sanofi-aventis Group

For information about this presentation, contact:

laurabancroftmd@gmail.com

LEARNING OBJECTIVES

1) Implement strategies to address unconscious bias and improve gender disparity in radiology. 2) Discuss strategies that can be used to promote engagement and retention of radiologist with young families. 3) Describe professional development programs that can be utilized to support women in radiology. 4) Demonstrate the ability to identify and address sexual misconduct and discrimination.

ABSTRACT

In 2017, the number of women enrolling in American medical schools surpassed men for the first time. However, women continue to comprise a minority of the radiology workforce, with women representing only 27% of the radiology residents and 23% of attending physicians in the United States. How can radiologists construct an inclusive workplace that actively recruits and retains an increasingly diverse population of physicians? This refresher course, sponsored by the RSNA Professionalism Committee, will suggest concrete, practical, and actionable ways to build a culture that recognizes and values equitable gender diversity in radiology, both with respect to recruiting and hiring women and to developing and sustaining professional careers.

Sub-Events

RC816A Unconscious Bias in Recruiting Female Radiologists

Participants

Katarzyna J. Macura, MD, PhD, Catonsville , MD (*Presenter*) Author with royalties, Reed Elsevier; Research Grant, Profound Medical Inc; Research Grant, GlaxoSmithKline plc; Research Grant, Siemens AG

For information about this presentation, contact:

kmacura@jhmi.edu

LEARNING OBJECTIVES

1) Discuss unconscious bias as a natural phenomenon that needs to be managed. 2) Mitigate bias in recruitment, promotion, and attitudes to others in the workplace.

ABSTRACT

Addressing the gender disparity in radiology requires an understanding of and willingness to tackle unconscious biases-the pervasive tendencies to make assumptions about people based on gender, race and other characteristics rooted in unconscious feelings.

RC816B Sexual Misconduct in Radiology

Participants Anastasia L. Hryhorczuk, MD, Ann Arbor, MI (*Presenter*) Nothing to Disclose

For information about this presentation, contact:

ahryhorc@med.umich.edu

LEARNING OBJECTIVES

1) To discuss the pervasiveness of sexual harassment and misconduct in radiology. 2) To describe education and management skills that have been deployed in other work environments to address harassment and discrimination.

ABSTRACT

As discussions of sexual misconduct and gender discrimination continue to merit significant attention in society at large, radiologists, too, are being forced to grapple with harassment and bias in the workplace.

RC816C Work-Life Balance for Radiologists with Young Families

Kate Hanneman, MD, FRCPC, Toronto, ON (Presenter) Medical Advisory Board, sanofi-aventis Group

LEARNING OBJECTIVES

1) To discuss the challenges that face young and dual-career families in radiology and strategies to promote work life balance, engagement and retention of radiologists during and after parental leave.

ABSTRACT

For young women and men in radiology, the beginning of a career often coincides with starting a family. As young physicians are trying to gain their footing at work, external and family pressures may begin to encroach on career advancement. Are radiology workplaces enthusiastically supporting individuals who are facing new challenges once they have already entered the career pipeline?

RC816D Informal Programs for Mentoring Women in Radiology

Participants

Ella A. Kazerooni, MD, Ann Arbor, MI (Presenter) Nothing to Disclose

LEARNING OBJECTIVES

1) To discuss the importance of professional development and the role of informal programs for mentoring women in radiology. 2) Explore strategies for developing these initiatives as new programs in academic institutions.

ABSTRACT

Women remain underrepresented in leadership positions in radiology and academic medicine. Once women gain faculty positions in radiology, professional development and sponsorship are essential to providing them with the tools needed to progress through their career.

RC816E Formal Programs for Mentoring Women in Radiology

Participants

Lucy B. Spalluto, MD, Nashville, TN (Presenter) Nothing to Disclose

LEARNING OBJECTIVES

1) To discuss the implementation and evaluation of a formal leadership program designed to improve access to opportunities for women's faculty development and advancement in radiology.

ABSTRACT

Formal faculty development and mentorship programs are also important, fostering career development opportunities and the executive skills necessary for women to achieve academic career success and assume leadership positions.





Emerging Technology: Theranosis-Molecularly Targeted Therapies 2019

Friday, Dec. 6 8:30AM - 10:00AM Room: E260



AMA PRA Category 1 Credits ™: 1.50 ARRT Category A+ Credit: 1.75

FDA Discussions may include off-label uses.

Participants

Rathan M. Subramaniam, MD, PhD, Dunedin, New Zealand (Moderator) Nothing to Disclose

For information about this presentation, contact:

rathan.subramaniam@utsouthwestern.edu

LEARNING OBJECTIVES

1) To review the established and emerging molecularly targeted radionuclide therapies for human solid tumors.

Sub-Events

RC817A Thyroid Cancer: 131-I Na Therapy

Participants Arif Sheikh, MD, New York, NY (*Presenter*) Nothing to Disclose

For information about this presentation, contact:

arif.sheikh@mountsinai.org

LEARNING OBJECTIVES

1. To review the basic approaches of radioiodine therapy in thyroid cancer management 2. To evaluate the integration of radioiodine imaging and therapy in thyroid cancer 3. Understanding radioiodine therapy as the general model for theranostics

RC817B Phaeochromocytomas and Paragangliomas: 131-I MIBG Therapy

Participants

Lilja B. Solnes, MD, Baltimore, MD (Presenter) Advisory Board, Progenics Pharmaceuticals, Inc

RC817C Neuroendocrine Tumors: 177Lu-DOTATATE Therapy

Participants

Rathan M. Subramaniam, MD, PhD, Dunedin, New Zealand (Presenter) Nothing to Disclose

For information about this presentation, contact:

rathan.subramaniam @utsouthwestern.edu

LEARNING OBJECTIVES

1) To learn the indications and patient selections for 177Lu DOTATATE therapy. 2) To review the 177Lu DOTATATE therapy procedures, toxicity monitoring and patient care follow-up. 3) To review therapy response methods for 177Lu DOTATATE treatments.

RC817D Prostate Cancer: 177Lu-PSMA Therapy

Participants Ayse T. Karagulle Kendi, MD, Rochester, MN (*Presenter*) Investigator, Endocyte, Inc

For information about this presentation, contact:

kendi.ayse@mayo.edu

LEARNING OBJECTIVES

1) Brief review of clinical background. 2) Discuss basic principles of Lu-PSMA therapy. 3) Describe therapy methods. 4) Explain side effects. 5) Review clinical impact/outcomes of Lu-PSMA therapy.





Radiomics: From Image to Radiomics

Friday, Dec. 6 8:30AM - 10:00AM Room: E350



AMA PRA Category 1 Credits ™: 1.50 ARRT Category A+ Credit: 1.75

Participants

Sandy Napel, PhD, Stanford, CA (*Coordinator*) Medical Advisory Board, Fovia, Inc; Scientific Advisor, EchoPixel, Inc; Scientific Advisor, RADLogics, Inc

LEARNING OBJECTIVES

1) Learn about the role of image annotations in radiology and their relevance to enabling interoperability and for communicating results and value for machine learning and decision support. 2) Become acquainted with important standards and tools that support the creation, management, and use of image annotations. 3) See case examples of image annotations in practice to enable developing applications that help the practice of radiology. 4) Understand the categories of, and the specific radiomic image features that can be computed from images. 5) Understand the effect and implications of image acquisition and reconstruction on radiomic image features. 6) Learn about workflows that drive the creation of predictive models from radiomic image features. 7) Understand the methods for and the potential value of correlating radiological images with genomic data for research and clinical care. 8) Learn how to access genomic and imaging data from databases such as The Cancer Genome Atlas (TCGA) and The Cancer Imaging Archive (TCIA) databases, respectively. 9) Learn about methods and tools for annotating regions within images and link them with semantic and computational features.10) Learn about methods and tools for analyzing molecular data, generating molecular features and associating them with imaging features. 11) Learn how deep learning can revolutionize interpretation of medical images.

Sub-Events

RC825A Image Annotation and Semantic Labeling

Participants

Daniel L. Rubin, MD, Stanford, CA (Presenter) Consultant, F. Hoffmann-La Roche Ltd

For information about this presentation, contact:

daniel.l.rubin@stanford.edu

LEARNING OBJECTIVES

1) To learn about the role of image annotations in radiology and their relevance to enabling interoperability and for communicating results and value for machine learning and decision support. 2) To become acquainted with important standards and tools that support the creation, management, and use of image annotations. 3) To see case examples of image annotations in practice to enable developing applications that help the practice of radiology.

RC825B Image feature Computation and Considerations

Participants

Sandy Napel, PhD, Stanford, CA (*Presenter*) Medical Advisory Board, Fovia, Inc; Scientific Advisor, EchoPixel, Inc; Scientific Advisor, RADLogics, Inc

For information about this presentation, contact:

snapel@stanford.edu

LEARNING OBJECTIVES

1) To understand the categories of, and the specific radiomic image features that can be computed from images. 2) To understand the effect and implications of image acquisition and reconstruction on radiomic image features. 3) To learn about workflows that drive the creation of predictive models from radiomic image features.

RC825C Correlating Image features with Multi-Omics Data

Participants Olivier Gevaert, PhD, Stanford, CA (*Presenter*) Nothing to Disclose

For information about this presentation, contact:

ogevaert@stanford.edu

LEARNING OBJECTIVES

1) Understand the methods for and the potential value of correlating radiological images with genomic data for research and clinical care. 2) Learn how to access genomic and imaging data from databases such as The Cancer Genome Atlas (TCGA) and The Cancer Imaging Archive (TCIA) databases, respectively. 3) Learn about methods and tools for annotating regions within images and link them with semantic and computational features. 4) Learn about methods and tools for analyzing molecular data, generating

molecular features and associating them with imaging features. 5) Introduction into how deep learning can revolutionize interpretation of medical images: challenges and opportunities.

ABSTRACT

Radiogenomics is an emerging field that integrates medical images and genomic data for the purposes of improved clinical decision making and advancing discovery of critical disease processes. In cancer, both imaging and genomic data are becoming publicly available through The Cancer Imaging Archive (TCIA) and The Cancer Genome Atlas (TCGA) databases, respectively. The TCIA/TCGA provide examples of matched molecular and image data for five cancer types, namely breast, lung, brain, prostate and kidney. The data in TCGA includes various omics data such as gene expression, microRNA expression, DNA methylation and mutation data. Quantitative image analysis from MRI, CT and/or PET images in TCIA has now become widespread and these image features represent concepts such as tumor volume, shape, edge sharpness, voxel-value histogram statistics, image textures, and specialized features developed for particular acquisition modes. Similarly, images are being annotated with semantic descriptors by radiologists using controlled terminologies to record the visual characteristics of the diseases. The availability of these linked imaging-genomic data provides exciting new opportunities to recognize imaging phenotypes that emerge from molecular characteristics of disease and that can potentially serve as biomarkers of disease and its response to treatment. They also provide an opportunity to discover key molecular processes associated with distinct image features, within one cancer type and across different cancer types. More recently, deep learning approaches have become very popular to analyze medical images. Deep learning has the advantage that no features have to be engineered beforehand, and everything is learned from the image. This workshop will describe datasets and tools that enable research at the intersection of imaging and genomics, and focus on the opportunities and challenges to develop future applications that leverage this knowledge for diagnostic decision support and treatment planning.







Engaging Patients: Opportunities and Challenges for Radiology

Friday, Dec. 6 8:30AM - 10:00AM Room: E261

ΗР

AMA PRA Category 1 Credits ™: 1.50 ARRT Category A+ Credit: 1.75

Participants

Ramin Khorasani, MD, Roxbury Crossing, MA (Moderator) Nothing to Disclose

Sub-Events

RC827A Price Transparency

Participants Gelareh Sadigh, MD, Atlanta, GA (*Presenter*) Nothing to Disclose

For information about this presentation, contact:

gsadigh@emory.edu

LEARNING OBJECTIVES

1) Define health-related financial toxicity and healthcare price transparency. 2) Differentiate cost vs charges vs paid price. 3) Assess impact of financial burden from cost of treatment on patient-reported outcomes. 4) Assess impact of healthcare price transparency tools on patients' spending. 5) Apply knowledge gained from this session in their encounter with patients.

RC827B Patient Reported Data and Its Impact on Quality and Safety

Participants

Keith D. Hentel, MD, MS, Briarcliff, NY (Presenter) Nothing to Disclose

RC827C Patient Portals to Access Results: Opportunities and Challenges

Participants

Teresa Martin-Carreras, MD , Philadelphia, PA (*Presenter*) Nothing to Disclose

For information about this presentation, contact:

Teresa.Martin-Carreras@pennmedicine.upenn.edu

RC827D Eliminating Ordered but Not Performed Imaging in Your Practice: What Are the Safety Risks and Solutions?

Participants Ronilda Lacson, MD, PhD, Brookline, MA (*Presenter*) Nothing to Disclose

For information about this presentation, contact:

rlacson@rics.bwh.harvard.edu

LEARNING OBJECTIVES

1) To quantify the incidence of diagnostic imaging that are ordered but not performed in clinical practice. 2) To identify factors that affect failure in scheduling and performance of diagnostic imaging orders. 3) To learn potential solutions for eliminating unperformed diagnostic imaging orders in practice.





Abdominal/Pelvic MRI in the Emergent Setting

Friday, Dec. 6 8:30AM - 10:00AM Room: E263



AMA PRA Category 1 Credits ™: 1.50 ARRT Category A+ Credit: 1.75

Participants

John R. Leyendecker, MD, Dallas, TX (Moderator) Nothing to Disclose

LEARNING OBJECTIVES

1) Understand the advantages and disadvantages of MRI in the acute setting for the diagnosis of acute genitourinary disorders. 2) Identify the diagnostic criteria for ovarian torsion and also predict ovarian viability with MRI. 3) Contrast the strengths of different MRI sequences for the diagnosis of pyelonephritis. 4) Apply a rapid, noncontrast MRI protocol for the imaging of acute abdominopelvic pain that is accurate for the diagnosis of acute genitourinary disorders. 5) Discuss clinical and imaging features of a spectrum of entities that present with acute female pelvic pain including complications of fibroids, pelvic inflammatory disease and complicated cysts. 6) Highlight the pathogenesis and pertinent MR imaging features of adnexal (ovarian and tubal) torsion. 7) Assess the relative advantages and disadvantages for MR vs. other imaging modalities for suspected appendicitis in adults. 8) Assess the ability of MR for making alternative diagnoses to acute appendicitis in the setting of non-traumatic abdominal pain. 9) Consider the implications for the potential increased use of MR in the ED for non-traumatic abdominal pain. 10) Identify patients who will benefit from MR enterography in the acute setting. 11) Protocol and perform MR enterography in the acute setting. 12) Identify and report acute findings of Crohn's disease on MR enterography. 13) Discuss the most common indications for abdominal or pelvic MRI in pediatric patients in the emergent setting. 14) Demonstrate and discuss the most frequently encountered MRI imaging manifestations of these conditions. 15) Review the most appropriate MRI protocols for evaluation of pediatric patients presenting to the Emergency Department with acute abdominal or pelvic pain. 16) Discuss available techniques for achieving patient cooperation and limiting exam time in pediatric patients. 17) Understand MRI safety concerns in the setting of pregnancy. 18) Understand indications for emergency MRI during pregnancy. 19) Implement an imaging protocol for emergency MRI during pregnancy. 20) Understand MRI appearance of common acute disease processes during pregnancy.

Sub-Events

RC829A MRI for Acute Genitourinary Disorders

Participants

Bobby T. Kalb, MD, Tucson, AZ (Presenter) Nothing to Disclose

LEARNING OBJECTIVES

1) Understand the advantages and disadvantages of MRI in the acute setting for the diagnosis of acute genitourinary disorders. 2) Identify the diagnostic criteria for ovarian torsion and also predict ovarian viability with MRI. 3) Contrast the strengths of different MRI sequences for the diagnosis of pyelonephritis. 4) Apply a rapid, noncontrast MRI protocol for the imaging of acute abdominopelvic pain that is accurate for the diagnosis of acute genitourinary disorders.

RC829B MRI for Acute Pelvic Pain in Women

Participants Christine O. Menias, MD, Chicago, IL (*Presenter*) Royalties, Reed Elsevier

For information about this presentation, contact:

menias.christine@mayo.edu

LEARNING OBJECTIVES

1) Discuss clinical and imaging features of a spectrum of entities that present with acute female pelvic pain including complications of fibroids, pelvic inflammatory disease and complicated cysts. 2) Highlight the pathogenesis and pertinent MR imaging features of adnexal (ovarian and tubal) torsion.

RC829C MRI for Acute Appendicitis and Differential Diagnosis

Participants

Perry J. Pickhardt, MD, Madison, WI (*Presenter*) Stockholder, SHINE Medical Technologies, Inc; Stockholder, Elucent Medical; Advisor, Bracco Group;

LEARNING OBJECTIVES

1) Assess the relative advantages and disadvantages for MR vs. other imaging modalities for suspected appendicitis in adults. 2) Assess the ability of MR for making alternative diagnoses to acute appendicitis in the setting of non-traumatic abdominal pain. 3) Consider the implications for the potential increased use of MR in the ED for non-traumatic abdominal pain.

RC829D MRI for Crohn's Disease in the Acute Setting

For information about this presentation, contact:

dgrand@lifespan.org

LEARNING OBJECTIVES

1) Identify patients who will benefit from MR enterography in the acute setting. 2) Protocol and perform MR enterography in the acute setting. 3) Identify and report acute findings of Crohn's disease on MR enterography.

RC829E MRI for Acute Pediatric Disorders

Participants

Sarah D. Bixby, MD, Boston, MA (Presenter) Nothing to Disclose

For information about this presentation, contact:

sarah.bixby@childrens.harvard.edu

LEARNING OBJECTIVES

1) Discuss the most common indications for abdominal or pelvic MRI in pediatric patients in the emergent setting. 2) Demonstrate and discuss the most frequently encountered MRI imaging manifestations of these conditions. 3) Review the most appropriate MRI protocols for evaluation of pediatric patients presenting to the Emergency Department with acute abdominal or pelvic pain. 4) Discuss available techniques for achieving patient cooperation and limiting exam time in pediatric patients.

RC829F Emergency MRI During Pregnancy

Participants

Gaurav Khatri, MD, Irving, TX (Presenter) Nothing to Disclose

LEARNING OBJECTIVES

1) Understand MRI safety concerns in the setting of pregnancy. 2) Understand indications for emergency MRI during pregnancy. 3) Implement an imaging protocol for emergency MRI during pregnancy. 4) Understand MRI appearance of common acute disease processes during pregnancy.

Active Handout:Gaurav Khatri

http://abstract.rsna.org/uploads/2019/19001016/Active RC829F.pdf





Radiology Benchmark: Productivity, Quality, and Compensation

Friday, Dec. 6 8:30AM - 10:00AM Room: E353A



AMA PRA Category 1 Credits ™: 1.50 ARRT Category A+ Credit: 1.75

Participants

Vincent P. Mathews, MD, Hartland, WI (Moderator) Nothing to Disclose

For information about this presentation, contact:

vmathews@mcw.edu

Sub-Events

RC832A Measuring Radiology Productivity

Participants Sanjay Saini, MD, Boston, MA (*Presenter*) Nothing to Disclose

For information about this presentation, contact:

ssaini@mgh.harvard.edu

LEARNING OBJECTIVES

1. WHY: Understand the economic rationale for measuring labor productivity 2. WHAT: Describe the options for measuring radiologist productivity 3. HOW: Discuss Implementation strategies in physician operations

RC832B Measuring Radiology Quality

Participants Lauren P. Golding, MD, Summerfield, NC (*Presenter*) Nothing to Disclose

For information about this presentation, contact:

laurengoldingmd@gmail.com

LEARNING OBJECTIVES

1) Understand the role of Quality in the Merit Based Incentive Payment System. 2) Become familiar with the collection types available for reporting quality measures into MIPS. 3) Understand the history of Qualified Clinical Data Registries. 4) Learn how to implement radiology specific QCDR into your practice.

RC832C Radiology Compensation Benchmarks

Participants Vincent P. Mathews, MD, Hartland, WI (*Presenter*) Nothing to Disclose

For information about this presentation, contact:

vmathews@mcw.edu

LEARNING OBJECTIVES

1) To learn about the implementation of fair market value compensation plans. 2) To understand the importance of utilizing appropriate benchmarks for clinical productivity measures.

RC832D The Financial Impact of Payment Reform on Radiology

Participants

Suresh K. Mukherji, MD, Carmel, IN (Presenter) Nothing to Disclose

LEARNING OBJECTIVES

Review the different financial reforms that have affected radiology.
 Explain the effects these reforms have had on radiology.
 Discuss future strategies that can help mitigate the downward trends on radiology reimbursement.





Carotid and Renal Doppler (Hands-on)

Friday, Dec. 6 8:30AM - <u>10:00AM Room: E264</u>



AMA PRA Category 1 Credits ™: 1.50 ARRT Category A+ Credit: 1.75

FDA Discussions may include off-label uses.

Participants

Gowthaman Gunabushanam, MD, New Haven, CT (*Presenter*) Nothing to Disclose Shweta Bhatt, MD, Rochester, NY (*Presenter*) Nothing to Disclose Wui K. Chong, MD, Houston, TX (*Presenter*) Nothing to Disclose Corinne Deurdulian, MD, Encino, CA (*Presenter*) Speaker, Samsung Electronics Co, Ltd Vikram S. Dogra, MD, Pittsford, NY (*Presenter*) Nothing to Disclose Ulrike M. Hamper, MD, Baltimore, MD (*Presenter*) Nothing to Disclose Davida Jones-Manns, Owings Mills, MD (*Presenter*) Nothing to Disclose Mark E. Lockhart, MD, Birmingham, AL (*Presenter*) Author, Oxford University Press; Author, Reed Elsevier; Editor, John Wiley & Sons, Inc; Deputy Editor, Journal of Ultrasound in Medicine Nira Beck-Razi, MD, Haifa, Israel (*Presenter*) Nothing to Disclose Margarita V. Revzin, MD, New Haven, CT (*Presenter*) Consultant, Koninklijke Philips NV; ; Leslie M. Scoutt, MD, Birmingham, AL (*Presenter*) Speaker, Koninklijke Philips NV Ravinder Sidhu, MD, Rochester, NY (*Presenter*) Nothing to Disclose Sadhna Verma, MD, Cincinnati, OH (*Presenter*) Nothing to Disclose

For information about this presentation, contact:

margarita.revzin@yale.edu

drsadhnaverma@gmail.com

nirabeckr@gmail.com

leslie.scoutt@yale.edu

ravinder_sidhu@urmc.rochester.edu

wkchong@mdanderson.org

corinne.deurdulian@usc.edu

LEARNING OBJECTIVES

1) Describe the technique and optimally perform carotid Doppler ultrasound. 2) Describe the technique and optimally perform renal Doppler ultrasound. 3) Review qualitative and quantitative criteria for diagnosing abnormalities in carotid and renal ultrasound Doppler examinations.

ABSTRACT

This hands-on course will provide participants with a combination of didactic lectures and an extended 'live' scanning opportunity on normal human volunteers, as follows: Didactic lectures (30 minutes): Carotid Doppler ultrasound: scanning technique, diagnostic criteria and interesting teaching cases. Renal Doppler ultrasound: scanning technique, diagnostic criteria and interesting teaching cases. Mentored scanning (60 minutes): Following the didactic lectures, the participants will proceed to a scanning area with normal human volunteers and ultrasound machines from different manufacturers. Participants will be able to perform live scanning with direct assistance, as needed, by faculty. Faculty will be able to offer feedback, help participants improve their scanning technique as well as answer any questions. Time permitting, faculty will also be available to answer general questions relating to all aspects of vascular ultrasound, not just limited to carotid and renal Doppler studies.







AI, Radiomics, Text Mining, and More: 2019's Key Advances in Imaging Informatics

Friday, Dec. 6 8:30AM - 10:00AM Room: E450A



AMA PRA Category 1 Credits ™: 1.50 ARRT Category A+ Credit: 1.75

Participants

William Hsu, PhD, Los Angeles, CA (*Moderator*) Research Grant, Siemens AG William Hsu, PhD, Los Angeles, CA (*Presenter*) Research Grant, Siemens AG Po-Hao Chen, MD, MBA, Philadelphia, PA (*Presenter*) Nothing to Disclose

For information about this presentation, contact:

whsu@mednet.ucla.edu

LEARNING OBJECTIVES

1) Identify the year's most important advances in imaging informatics. 2) Describe the ways in which Artificial Intelligence (AI) and machine learning are impacting radiology. 3) Define how radiomics, radiogenomics, and 'big data' have added to our knowledge of radiology.

ABSTRACT

The field of imaging informatics continues to advance rapidly. Machine learning, a form of artificial intelligence (AI), has improved the ability to detect image features, make diagnoses, and assess prognosis from image data. Radiomics - which generates highdimensionality datasets from radiology images - provides insights to support precision medicine. Novel approaches have improved sharing of images and image-derived findings with patients and clinicians. Current research efforts go beyond pixel data to integrate imaging with other biomedical data, standardize imaging workflows, and improve the quality and utility of image-derived information in clinical practice. This session reviews key advances in imaging informatics research published this past year.







SPIS61

International Symposium on Cardiothoracic Imaging

Friday, Dec. 6 8:30AM - 12:00PM Room: E353C



AMA PRA Category 1 Credits ™: 3.50 ARRT Category A+ Credits: 4.00

FDA Discussions may include off-label uses.

Participants

Jeremy J. Erasmus, MD, Houston, TX (*Director*) Nothing to Disclose Carol C. Wu, MD, Houston, TX (*Director*) Author, Reed Elsevier

For information about this presentation, contact:

carolcwu@gmail.com

LEARNING OBJECTIVES

1) Define the role of imaging in the diagnosis and characterization of cardiothoracic diseases. 2) Describe available advanced imaging techniques in the evaluation of cardiothoracic diseases.

Sub-Events

SPIS61A Diffuse Lung Disease

Friday, Dec. 6 8:30AM - 9:20AM Room: E353C

Participants

Noriyuki Tomiyama, MD,PhD, Suita, Japan (*Moderator*) Nothing to Disclose Santiago E. Rossi, MD, Buenos Aires City, Argentina (*Moderator*) Speaker, Boehringer Ingelheim GmbH; Speaker, Novartis AG

SPIS61B Introduction to Idiopathic Pulmonary Fibrosis: What Radiologists Need to Know

Friday, Dec. 6 8:30AM - 9:20AM Room: E353C

Participants

Santiago E. Rossi, MD, Buenos Aires City, Argentina (Presenter) Speaker, Boehringer Ingelheim GmbH; Speaker, Novartis AG

For information about this presentation, contact:

santirossi@cdrossi.com

LEARNING OBJECTIVES

1) To introduce most common imaging features of ILD. 2) To introduce ATS / ERS / JRS /ALAT guidelines.

SPIS61C Imaging Diagnosis of Idiopathic Pulmonary Fibrosis: Status and Challenges

Friday, Dec. 6 8:30AM - 9:20AM Room: E353C

Participants

Qihang Chen, MD, Beijing, China (Presenter) Nothing to Disclose

LEARNING OBJECTIVES

1) To compare the white paper of the Flerschner society with ATS/ERS/JRS/LATA guidelines. 2) To differentiate the honeycomb and mimic honeycomb. 3) To introduce the status of diagnosis of IPF in China.

SPIS61D Staging and Prognostication of Idiopathic Pulmonary Fibrosis

Friday, Dec. 6 8:30AM - 9:20AM Room: E353C

Participants

Nicola Sverzellati, MD, Parma, Italy (*Presenter*) Consultant, PAREXEL International Corporation; Consultant, Biomedic System; Consultant, F. Hoffmann-La Roche Ltd; Consultant, Boehringer Ingelheim GmbH; Consultant, Galapagos; Advisory Board, F. Hoffmann-La Roche Ltd; Advisory Board, Boehringer Ingelheim GmbH; Speaker, F. Hoffmann-La Roche Ltd; Speaker, Boehringer Ingelheim GmbH;

LEARNING OBJECTIVES

1) To understand the most accurate visual and computer-based CT indexes for IPF staging and prognostication. 2) To describe some of the current technologies and cutting edge perspective for objective quantification of IPF on CT.

SPIS61E Quantitative Assessment of Interstitial Lung Disease on CT

Participants

Joon Beom Seo, MD, PhD, Seoul, Korea, Republic Of (Presenter) Nothing to Disclose

For information about this presentation, contact:

joonbeom.seo@gmail.com

LEARNING OBJECTIVES

1) To understand why quantitative assessment of interstitial lung disease on CT is necessary. 2) To know the basic technical concept of various software methods for quantification of interstitial lung disease. 3) To acknowledge the potential clinical values of using quantitative imaging biomarkers in practice.

SPIS61F Lung Nodules and Cancer

Friday, Dec. 6 9:25AM - 10:15AM Room: E353C

Participants Claudio Silva Fuente-Alba, MD, MsC, Santiago, Chile (*Moderator*) Nothing to Disclose Carol C. Wu, MD, Houston, TX (*Moderator*) Author, Reed Elsevier

For information about this presentation, contact:

carolcwu@gmail.com

LEARNING OBJECTIVES

1) Compare and contrast lung cancer screening strategies in the United States and Asia. 2) Describe the role of computer softwares, CT and MRI in the detection and characterization of lung nodules.

SPIS61G Lung Cancer Screening in the US

Friday, Dec. 6 9:25AM - 10:15AM Room: E353C

Participants Carol C. Wu, MD, Houston, TX (*Presenter*) Author, Reed Elsevier

For information about this presentation, contact:

carolcwu@gmail.com

LEARNING OBJECTIVES

1) Describe current lung cancer screening strategies in the United States. 2) Explain the underlying rationales for lung cancer screening strategies in the United States.

SPIS61H Lung Cancer Screening in Asia

Friday, Dec. 6 9:25AM - 10:15AM Room: E353C

Participants Yeun-Chung Chang, MD, Taipei, Taiwan (*Presenter*) Nothing to Disclose

LEARNING OBJECTIVES

1) To understand the incidence and some screening programs of lung cancer in Asia. 2) To know the characteristic CT findings of screen detected lung cancer in Asian and how it is managed.

ABSTRACT

Lung cancer is the leading cause of cancer death worldwide so dose it in Asia. There is a much higher prevalence of epidermal growth factor receptor (EGFR) mutation, predominantly among patients with adenocarcinoma and never-smokers. Some reports of lung cancer screening in Asia show a cancer detection rate about 1.0-2.5% in Asia. CT characteristic of lung cancer with EGFR mutation and clinical management of the screen detected lung cancer in Taiwan will be described.

Active Handout: Yeun-Chung Chang

http://abstract.rsna.org/uploads/2019/19001623/Active SPIS61H.pdf

SPIS611 Pulmonary Nodules: Impact of Computer Support

Friday, Dec. 6 9:25AM - 10:15AM Room: E353C

Participants

Cornelia M. Schaefer-Prokop, MD, Amersfoort, Netherlands (*Presenter*) Researcher, Thirona; Researcher, Varian Medical Systems, Inc; Spouse, Speaker, Bracco Group; Spouse, Speaker, Bayer AG; Spouse, Speaker, Canon Medical Systems Corporation; Spouse, Speaker, Siemens AG; Spouse, Research support, Siemens AG; Spouse, Research support, Canon Medical Systems Corporation; Spouse, Researcher, Thirona; Spouse, Researcher, Varian Medical Systems, Inc

LEARNING OBJECTIVES

1) To learn about available computer tools for detection and characterization of pulmonary nodules. 2) To understand the potential but also shortcomings of current computer tools for nodules. 3) To learn about various models for malignancy risk assessment and how they are implemented in computer tools.

SPIS61J Role of PET and MRI for Lung Nodule Characterization

Participants

Yoshiharu Ohno, MD, PhD, Toyoake, Japan (*Presenter*) Research Grant, Canon Medical Systems Corporation; Research Grant, DAIICHI SANKYO Group; ;

For information about this presentation, contact:

yohno@fujita-hu.ac.jp

LEARNING OBJECTIVES

1) To deliver the updates of PET, PET/CT and MRI for lung nodule characterization and management of pulmonary nodule.

ABSTRACT

In this lecture, I will talk about 1) lung nodule detection capability, 2) morphological evaluation of lung nodule characterization and 3) quantitative potential for lung nodule characterization on PET, PET/CT and MRI. I hope this lecture will contribute your daily clinical practice.

SPIS61K Infection

Friday, Dec. 6 10:25AM - 11:10AM Room: E353C

Participants

Tomas C. Franquet, MD, Barcelona, Spain (*Moderator*) Nothing to Disclose Ioannis Vlahos, MRCP,FRCR, Houston, TX (*Moderator*) Director, Grayscale Ltd; Co-owner, Grayscale Ltd

SPIS61L Imaging of Community-acquired Pneumonia

Friday, Dec. 6 10:25AM - 11:10AM Room: E353C

Participants

Tomas C. Franquet, MD, Barcelona, Spain (Presenter) Nothing to Disclose

For information about this presentation, contact:

tfranquet@santpau.cat

LEARNING OBJECTIVES

1) To become familiar with the variable imaging findings related to CAP. 2) To discuss the role of HRCT in the diagnosis of CAP. 3) To discuss a general approach to CAP diagnosis using the predominant imaging pattern.

ABSTRACT

Community-acquired pneumonia refers to an acute infection of the lung in patients who did not meet any of the criteria for HCAP and associated with at least some symptoms of acute infection, accompanied by the presence of an acute infiltrate on a chest radiograph. Chest radiography remains an important component of the evaluation of patient with a suspicion of pneumonia, and usually is the first examination to be obtained. The diagnosis of CAP is based on the presence of select clinical features and is supported by imaging of the lung, usually by chest radiography. Infection of the lower respiratory tract typically presents radiologically as one of three patterns: a) focal nonsegmental or lobar pneumonia, b) multifocal bronchopneumonia or lobular pneumonia, and c) focal or diffuse 'interstitial' pneumonia. Bacterial and viral micro-organisms are the most common etiologic agents responsible for CAP. Identification of causative micro-organisms in CAP remains challenging and in 30% to 65% of cases .

SPIS61M Thoracic Manifestations of HIV Infection

Friday, Dec. 6 10:25AM - 11:10AM Room: E353C

Participants Hongjun Li, Beijing, China (*Presenter*) Nothing to Disclose

For information about this presentation, contact:

lihongjun00113@126.com

LEARNING OBJECTIVES

1) To understand the imaging characteristics of HIV infection related thoracic manifestations. 2) To emphasize the importance and urgency in medication of HIV related thoracic manifestations. 3) To introduce the research development of HIV infection pulmonary disease

ABSTRACT

Pulmonary lesions in HIV/AIDS patients are most common with opportunistic infections and tumors. Pulmonary infection is a common complication and cause of death in HIV/AIDS patients. The pathogens mainly include Pneumocystis jirovecii, Cryptococcus, Mycobacterium tuberculosis and so on. Imaging findings are varied and nonspecific. HIV/AIDS complicated with Pneumocystis pneumoniae pneumonia is typically characterized by a frosted glass-like shadow symmetrically distributed around the hilar; pulmonary cryptococcosis is characterized by a single, multiple nodule or mass near the pleura with wide base. The nodule cavity is a characteristic CT manifestation of pulmonary cryptococcosis. The imaging patterns of tuberculosis in HIV-infected patients are upper lung consolidation and multiple nodules, which may cavitate. Centrilobular nodules are presented in endobronchial spread of turberculosis. Kaposi sarcoma (KS) is the most common AIDS-defining malignancy. A characteristic CT finding in AIDS-related KS is the presence of bilateral and symmetric ill-defined nodules in a peribronchovascular distribution (flame-shaped lesions) and ground-glass opacities may be seen surrounding the nodules. AIDS-related lymphoma is another common malignancy in HIV infected patients are powerful and effective tool of examination for AIDS- related lung lesions. The diagnosis combined with clinical and laboratory tests

is helpful to medical treatment.

SPIS61N Pulmonary Tuberculosis and Nontuberculous Mycobacterial (NTM) Infection: An Overview

Friday, Dec. 6 10:25AM - 11:10AM Room: E353C

Participants Kyung S. Lee, MD, PhD, Seoul, Korea, Republic Of (*Presenter*) Nothing to Disclose

For information about this presentation, contact:

kyungs.lee@samsung.com

LEARNING OBJECTIVES

1) To deliver the updates in pulmonary tuberculosis and nontuberculous mycobacterial (NTM) pulmonary infection in terms of pathogenesis and imaging findings.

ABSTRACT

In this overview of pulmonary tuberculosis and nontuberculous mycobacterial (NTM) infection, this speaker will talk about 1. Mode of tuberculous pulmonary infection, 2. Identification of latent tuberculous infection, 3. Serial CT features in primary multidrug-resistant pulmonary tuberculosis, 4. Prevalence of nontuberculous mycobacterial (NTM) infection in US and Canada, 5. Clinical and radiological findings of Mycobacterium avium-intracellulare (MAC) infection, 6. Natural course of MAC pulmonary infection, 7. Chronic pulmonary aspergillosis in NTM infection.

SPIS610 Cardiovascular Imaging

Friday, Dec. 6 11:15AM - 12:00PM Room: E353C

Participants

Yung-Liang Wan, MD, Tao-Yuan, Taiwan (*Moderator*) Nothing to Disclose Marie-Pierre Revel, Paris, France (*Moderator*) Nothing to Disclose

For information about this presentation, contact:

ylw0518@CGMH.ORG.TW

SPIS61P Aortic Intramural Hematoma: The Prognostic Impact of CT Features

Friday, Dec. 6 11:15AM - 12:00PM Room: E353C

Participants Ming-Ting Wu, MD, Kaohsiung, Taiwan (*Presenter*) Nothing to Disclose

For information about this presentation, contact:

wu.mingting@gmail.com

LEARNING OBJECTIVES

1) The learn the CT features of aortic intramural hematoma. 2) The learn the types of focal contrast enhancement in the hematoma and their differential prognosis impacts. 3) The learn the CT predictors of poor prognosis of aortic intramural hematoma.

ABSTRACT

Aortic intramural hematoma (AIMH) is one major component of acute aortic syndrome, esp. in Asia. We will review the CT characteristic of AIMH, including the inframural focal contrast enhancement. Two types of the intramural lesions will be introduced. One is ulcer-like projection, one is intramural blood pool. Their prognosis is different. We will also review the prognosis predictor of AIMH, and the nature course of the AIMH on the follow-up CT.

SPIS61Q Role of CT in Pulmonary Hypertension

Friday, Dec. 6 11:15AM - 12:00PM Room: E353C

Participants Marie-Pierre Revel, Paris, France (*Presenter*) Nothing to Disclose

For information about this presentation, contact:

marie-pierre.revel@aphp.fr

LEARNING OBJECTIVES

1) Detect CT signs of pulmonary hypertension. 2) Identify CT features suggesting a thromboembolic origin. 3) Differentiate the various causes of pulmonary hypertension on CT.

ABSTRACT

CT allows depicting pulmonary hypertension (PH), helps identifying its cause and therefore plays a crucial role in the diagnostic work-up of PH. CT features of pulmonary hypertension include dilatation of the main pulmonary artery, with a diameter greater than or equal to 29 mm, a ratio to the aortic diameter greater than 1:1 and a segmental artery-to-bronchus ratio greater than 1:1 in at least three lobes. On ECT-gated CT, loss of pulmonary artery distensibility with a cut-off value of 16.5% has 86% sensitivity and 96% specificity. CT is especially useful for detecting signs of chronic thromboembolic pulmonary hypertension , that must be recognized and distinguished from idiopathic pulmonary artery hypertension. These signs include wall adherent thrombi, bands webs or chronic arteril occlusion, mosaic perfusion and systemic collateral supply.Signs of pulmonary edema, such as thickening of the interlobular septa, centrilobular ground glass, medisatinal lymph node enlargement and plural effusion are seen on CT in PH due to venoocclusive disease, left heart diseases or fibrosing mediastinitis. Signs of lung parenchyma diseases can be identified on CT. PH

is a late complication in patients with lung fibrosis, sarcoidosis or COPD but may affect systemic sclerosis patients with limited lung parenchyma involvement. Congenital cardiac abnormalities with untreated right-to-left shunting resulting in Eisenmenger syndrome can also be identified, especially ventricular septal defect. Conversely, signs of peripheral arteriovenous shunting in hepatopulmonary syndrome are more difficult to assess.

SPIS61R Comprehensive Multi-chamber Cardiac Function Evaluation by CT

Friday, Dec. 6 11:15AM - 12:00PM Room: E353C

Participants

Jongmin J. Lee, MD, PhD, Daegu, Korea, Republic Of (Presenter) Nothing to Disclose

LEARNING OBJECTIVES

1) The global cardiac function depends on four cardiac chambers' function and their interactions. 2) Left and right ventricular function evaluation by cardiac CT has been validated favorably. 3) Three or four chamber function evaluation techniques are developed and equipped in available image-processing workstations. 4) In cardiac CT with retrospective ECG-gating, multi-chamber function evaluation supports comprehensive cardiac evaluation.

ABSTRACT

By evaluating the adjacent cardiac chambers, more reliable information about single chamber function and inter-related compensatory functional mechanism may be acquired. Based on cardiac CT data with multi-phase reconstruction, morphological image markers are useful for evaluating the levels of the preload, inotropy, and afterload in each cardiac chamber as well as the global multi-chamber cardiac function. In the clinical practice, the inotropic function and the afterload of left ventricle are major concerns. The left ventricular ejection fraction and the cardiac output are good markers for the inotropy. The left ventricular endsystolic volume, the peripheral vascular resistance, and the aortic distensibility are useful markers for the afterload of left ventricle. The second major concern may be the afterload of right ventricle, which can be evaluated by the right ventricular end-systolic volume, the pulmonary vascular resistance, and the structural deformations. As we have been aware through multinational cohort studies, the left ventricular function and volume with cardiac CT improves risk stratification and identification of patients at risk for incident morality. The left ventricular function has been recognized a representative cardiac function in academic and practical fields. However, the global cardiac function should depend on four cardiac chambers' function and their interactions. For example, in a case with systemic hypertension, left ventricular concentric remodeling with accentuated left atrial late contraction and normal right ventricular function can be depicted in cardiac CT function study. This case suggests an early-stage hypertensive heart disease with compensated global cardiac function during resting state by left atrial inotropy. If the information about the cardiac function and the chamber volume could be acquired additionally on the CT coronary angiography in cases with retrospective ECGgaiting, it may be useful for clinical management of diverse cardiac diseases including ischemic heart disease, essential or secondary cardiomyopathies, and heart failure. In this lecture, we will discuss about background concept of multi-chamber cardiac functions, image-based parameters for the comprehensive cardiac function, and clinical application of this methodology.

Active Handout: Jongmin John Lee

http://abstract.rsna.org/uploads/2019/19001633/Active SPIS61R.pdf





SST01

Breast Imaging (Interventional and Pathological Correlation)

Friday, Dec. 6 10:30AM - 12:00PM Room: E450A

BR

AMA PRA Category 1 Credits ™: 1.50 ARRT Category A+ Credit: 1.75

FDA Discussions may include off-label uses.

Participants

Colleen H. Neal, MD, Ann Arbor, MI (*Moderator*) Nothing to Disclose Hiroyuki Abe, MD, Chicago, IL (*Moderator*) Nothing to Disclose

Sub-Events

SST01-01 Accuracy of MRI Biopsy in Diagnosing a Breast Cancer Pathologic Complete Response Following Neoadjuvant Chemotherapy

Friday, Dec. 6 10:30AM - 10:40AM Room: E450A

Participants

Elizabeth J. Sutton, MD, New York, NY (*Presenter*) Nothing to Disclose Mahmoud A. El-Tamer, MD, New York, NY (*Abstract Co-Author*) Nothing to Disclose Lior Braunstein, MD, Boston, MA (*Abstract Co-Author*) Nothing to Disclose Edi Brogi, MD, New York, NY (*Abstract Co-Author*) Nothing to Disclose Virgilio Sacchini, MD, New York, NY (*Abstract Co-Author*) Nothing to Disclose Elizabeth A. Morris, MD, New York, NY (*Abstract Co-Author*) Nothing to Disclose Marinela Capanu, New York, NY (*Abstract Co-Author*) Nothing to Disclose Pedram A. Razavi, MD, New York, NY (*Abstract Co-Author*) Institutional Grant, GRAIL Inc; Institutional Grant, Illumina; Consultant, Novartis AG; Advisory Board, Novartis AG Mary C. Hughes, MD, New York, NY (*Abstract Co-Author*) Nothing to Disclose

For information about this presentation, contact:

suttone@mskcc.org

PURPOSE

Neoadjuvant chemotherapy (NAC) has changed the management of breast cancer. The best outcome post-NAC is a pathologic complete response (pCR). There remains no minimally-invasive approach with sufficient accuracy to diagnose a pCR so surgery remains the standard of care. The purpose of this proof-of-concept clinical trial is to evaluate the accuracy of MRI-biopsy in diagnosing a pCR post NAC compared to reference-standard breast surgery specimen.

METHOD AND MATERIALS

Between 2017-2019, our IRB approved this pilot study that accrued 15 women with biopsy-proven operable invasive breast cancer who met the following inclusion criteria: (a) standard-of-care NAC, (b) pre- and post-NAC MRI, (c) imaging complete response defined as no residual enhancement on post-NAC MRI and (d) planned definitive surgery at our institution. A post-NAC standard of care MRI-guided biopsy was performed of the 15 treated tumor beds without intravenous contrast. The primary endpoint is to estimate the negative predictive value (NPV) of MRI biopsy to reference-standard breast surgery specimen. In this context, NPV is defined as the number of true pCR (biopsy negative, i.e. no disease found on the percutaneous biopsy and pCR at surgery) divided by the number of all biopsy negatives. The positive predicitve value (PPV), sensitivity, and specificity of the biopsy were also calculated.

RESULTS

15 patients with an MR imaging complete response post-NAC underwent MRI biopsy. Reference standard surgical pathology demonstrated a pCR in 10/15 (67%) and no-pCR in 5/15 (33%). The accuracy of MRI biopsy was 14/15 (93%). MRI biopsy was false in 1/15 (7%). In this false negative case surgical pathology identified 0.2mm of invasive disease, a true positive (no-pCR). All no-pCR tumor beds demonstrated very small volume residual disease with the largest invasive cancer measuring 3mm. The statistical measurements of MRI-guided biopsy in diagnosing a pCR compared with the reference standard surgical pathology are: NPV 91%, PPV 100%, Sensitivity 80% and Specificity 100%.

CONCLUSION

The accuracy of MRI-guided biopsy in diagnosing a pCR post-NAC in this pilot study is very high when compared to reference standard surgical pathology, which supports the need for a larger study.

CLINICAL RELEVANCE/APPLICATION

MRI-guided biopsy is a promising minimally-invasive approach with accuracy in diagnosing a pCR post-NAC to potentially obviate surgery in this subset of patients.

Participants Shruthi Ram, MD, Providence, RI (*Presenter*) Nothing to Disclose Helaina Regen-Tuero, Providence, RI (*Abstract Co-Author*) Nothing to Disclose Grayson L. Baird, PhD, Providence, RI (*Abstract Co-Author*) Nothing to Disclose Ana P. Lourenco, MD, Foxboro, MA (*Abstract Co-Author*) Nothing to Disclose

PURPOSE

To evaluate the utility and compliance of 6 month follow up MRI following benign concordant MRI guided breast biopsy and investigate potential causes for noncompliance.

METHOD AND MATERIALS

IRB approved retrospective review of all benign concordant MRI biopsies from 1/1/2013 to 1/1/2018. Biopsy results with high risk lesions or malignancy were excluded. For each benign concordant MRI biopsy, the following was collected from the electronic medical record: patient age, pathology from MRI biopsy, any recommendation for 6 month follow up MRI, any documented communication to thereferring physician, available follow up imaging, repeat biopsies, subsequent malignancies, insurance type, and referring physician's institution and specialty.

RESULTS

There were 139 benign concordant MRI biopsies in 127 patients during the study period. Mean patient age was 47.6 years (range 25 to 73). Follow-up MRI was performed at 6 months in 31.5% (40/127) and at 12 months in 18.1% (23/127) (Table 1). A 6 month follow up MRI was recommended in 63/127 (49.6%). Of these, 33/63 (52.4%) had a 6 month follow up MRI. Communication of the 6 month follow up recommendation was documented in only 6/63 (9.5%). Most patients without subsequent MRI in our system (n=50) had follow-up benign mammography at a mean of 0.9 years following MRI biopsy (range 0.2 to 2.2 years). There were no repeat biopsies or subsequent malignancies at the site of benign MRI biopsy. No correlation was observed between likelihood of 6 month follow up MRI and patient insurance type, ordering provider specialty or institution.

CONCLUSION

When 6 month follow-up MRI was recommended following a benign concordant biopsy, compliance was 52.4%. Lack of communication of the recommendation between the radiologist and referring physician may at least partially explain the low compliance. There were no false negative biopsies identified in this study, raising questions about the utility and cost-effectiveness of routine 6 month follow-up MRI following benign concordant MRI biopsy.

CLINICAL RELEVANCE/APPLICATION

Careful assessment of each benign concordant MRI biopsy may be more appropriate than routine 6 month follow-up MRI recommendation.

SST01-03 The Feasibility of Breast Conservation Therapy in Multifocal/Multicentric Breast Cancer Using Multiple Radioactive Seeds: A Paradigm Shift

Friday, Dec. 6 10:50AM - 11:00AM Room: E450A

Participants

Mary S. Guirguis, MD, Houston, TX (*Presenter*) Nothing to Disclose Beatriz E. Adrada, MD, Houston, TX (*Abstract Co-Author*) Nothing to Disclose Mark J. Dryden, MD, Houston, TX (*Abstract Co-Author*) Nothing to Disclose H. Carisa Le-Petross, MD, FRCPC, Houston, TX (*Abstract Co-Author*) Nothing to Disclose Jia Sun, Houston, TX (*Abstract Co-Author*) Nothing to Disclose Gaiane M. Rauch, MD, PhD, Houston, TX (*Abstract Co-Author*) Nothing to Disclose Cristina M. Checka, MD, Houston, TX (*Abstract Co-Author*) Nothing to Disclose Gary J. Whitman, MD, Houston, TX (*Abstract Co-Author*) Nothing to Disclose Tanya W. Moseley, MD, Houston, TX (*Abstract Co-Author*) Consultant, Hologic, Inc

For information about this presentation, contact:

mguirguis@mdanderson.org

PURPOSE

Our study aims to validate breast conservation therapy in multifocal/multicentric (MF/MC) breast cancer (BC) using multiple radioactive seeds for localization.

METHOD AND MATERIALS

We retrospectively reviewed all radioactive-seed-localized segmentectomies at our institution between January 1, 2014 and April 26, 2017, where two or more radioactive seeds were used in the same breast. Patients with benign breast disease, unifocal BC and noncontinguous multicentric BC were excluded. Patient's age, demographics, pathology, and imaging were reviewed. Pre-operative diagrams were provided denoting the number and location of radioactive seeds, which were then examined intraoperatively using handheld gamma probes prior to segmentectomy. Intraoperative margin assessment was performed for all cases, including whole specimen radiography and gross-sectioning. Positive or close margins were re-excised intraoperatively and examined by permanent pathology,

RESULTS

Ninety-two patients underwent breast conservation therapy for MF/MC BC, using two or more radioactive seeds for preoperative localization without technical problems. Mean patient age was 56.8 years (range 33-80), and 55% of patients received neoadjuvant chemotherapy. Forty-six percent of patients had invasive ductal carcinoma and ductal carcinoma in situ (DCIS), 30% invasive ductal carcinoma, 10% invasive lobular carcinoma, 9% DCIS, and 5% invasive mammary carcinoma. Forty-nine percent of patients underwent localization using three seeds, 45% with 2 seeds, and 6% with 4 or more seeds. The mean distance between seeds was 4.8 cm (range 1-10). Seventy-five percent (69/92) had negative final margins, 15% (14/92) close or 2 mm margins, and 10%

(9/92) positive margins. Of those with positive margins, 3 underwent margin re-excision, and 6 completion mastectomy. One patient with close margins underwent re-excision, while the remaining patients with close margins did not require repeat surgery and were treated with adjuvant radiation therapy.

CONCLUSION

Preoperative localization of MF/MC BC with multiple radioactive seeds can successfully achieve clear surgical margins in 75% of cases.

CLINICAL RELEVANCE/APPLICATION

Patients with MF/MC BC can achieve breast conserving surgery, instead of mastectomy, if meticulous preoperative localization is performed using multiple radioactive seeds.

SST01-05 Tomosynthesis-Guided Breast Biopsy versus Stereotactic Biopsy: What's So Different?

Friday, Dec. 6 11:10AM - 11:20AM Room: E450A

Participants Cleo Rochat, Providence, RI (*Presenter*) Nothing to Disclose Grayson L. Baird, PhD, Providence, RI (*Abstract Co-Author*) Nothing to Disclose Ana P. Lourenco, MD, Foxboro, MA (*Abstract Co-Author*) Nothing to Disclose

For information about this presentation, contact:

alourenco@lifespan.org

PURPOSE

To compare biopsy outcomes from two years preceding and following implementation of digital breast tomosynthesis (DBT)-guided biopsy.

METHOD AND MATERIALS

IRB-approved, HIPAA compliant retrospective review of all vacuum-assisted core breast biopsy procedures using 2D stereotactic guidance from 2013-2015 and DBT-guided biopsy from 2015-2017. All screening and diagnostic mammography was performed with DBT during the study period. Patient demographics, biopsy target type, pathology from 9G vacuum assisted core biopsy, surgical excision pathology when available, breast density, and imaging follow-up results were recorded. Biopsy targets and radiology-pathology discordance rate were compared between the two groups. Generalized mixed modeling was used to examine pre/post DBT biopsy results using SAS 9.4.

RESULTS

There were 1405 breast biopsy procedures in 1313 patients; 643 using 2D stereotactic guidance (2013-2015) (median age 56) and 762 using 3D DBT guidance (2015-2017) (median age 58). Of the 2D group, 55.6% had dense breast tissue as compared with 57.5% in the DBT group. Calcifications were the most common biopsy target for both groups constituting 89.9% (578/643) of 2D biopsies and 71.1% (542/762) of DBT biopsies (p<.0001). For 2D biopsies, architectural distortion (AD) was the least common biopsy target at 2.0% (13/643) but increased to 17.7% (135/762) for the DBT group (p<.0001). Overall radial scars identified increased from 1.7% [1.0, 3.1] to 8.3% [6.5, 10.5] (p<.0001). The discordance rate increased from 1.4% [1.0, 2.7] to 4.5% [3.2, 6.2] following the implementation of DBT-guided biopsy (p=.0021). Of the 34 discordant DBT-guided biopsies, 30 of the biopsy targets were architectural distortions.

CONCLUSION

With the transition from 2D stereotactic biopsy to DBT biopsy, there was a significant increase in the number of architectural distortions targeted for biopsy, the number of radial scars identified, and the radiology-pathology discordance rate.

CLINICAL RELEVANCE/APPLICATION

While DBT biopsy has enabled the targeting of very subtle lesions such as architectural distortion, radiologists should be cognizant of the potential for radiology-pathology discordance.

sst01-06 Radial Scars in the Era of Digital Breast Tomosynthesis: What is the Rate of Upgrade to Malignancy?

Friday, Dec. 6 11:20AM - 11:30AM Room: E450A

Participants

Pamela Yan, Providence, RI (*Presenter*) Nothing to Disclose Linda DeMello, MD, Warwick, RI (*Abstract Co-Author*) Nothing to Disclose Grayson L. Baird, PhD, Providence, RI (*Abstract Co-Author*) Nothing to Disclose Yihong Wang, MD, Providence, RI (*Abstract Co-Author*) Nothing to Disclose Ana P. Lourenco, MD, Foxboro, MA (*Abstract Co-Author*) Nothing to Disclose

For information about this presentation, contact:

alourenco@lifespan.org

PURPOSE

To determine the rate of upgrade for radial scars (RS) diagnosed at core needle biopsy and to assess how the radiologist's recommendation for excision based on imaging features compares with excisional biopsy results.

METHOD AND MATERIALS

IRB approved, HIPAA compliant retrospective review of radiology and pathology databases at a tertiary breast center to identify all "radial scar" and "complex sclerosing lesions" between March 2012 and December 2017. During the study period, all mammography was performed with digital breast tomosynthesis. Patient demographics, initial imaging, needle and excisional biopsies, and follow-up imaging data were collected. Upgrade to malignancy was defined as discovery of DCIS or invasive carcinoma at the same site as the RS upon surgical excision. Initial imaging leading to the discovery of the radial scar was reviewed by a fellowship trained breast radiologist. Based on the imaging findings, this radiologist recommended excisional biopsy or imaging follow-up for each case.

RESULTS

There were 146 biopsy-proven radial scars in 142 patients. Median patient age was 57 (range 26-87). Presenting imaging findings on mammography were mass 49 (34%), architectural distortion 40 (27%), calcifications 37 (25%), asymmetry 4 (3%); 5 (3%) mass on ultrasound; on MRI 7 (5%) mass and 4 (3%) non-mass enhancement. 117 (80%) demonstrated radial scar as the most ominous histological finding at that biopsy site (no atypia or cancer). The remaining 29 cases had associated atypia (n=15) or cancer (n=14) and were excluded. Of the 117 RS without associated atypia, 1 (0.8%) was upgraded to invasive ductal carcinoma at excision. Of these 117 RS without atypia, 72 were excised, 19 underwent benign imaging follow-up for a median of 3 years (range 1 to 5.5 years) and 16 were lost to follow-up. Based on initial imaging review, the radiologist recommended excision in 87%. No malignancy would have been missed if the remaining cases had not been excised.

CONCLUSION

Radial scars without atypia had an upgrade rate of 0.8% in this study. Radiologist assessment of imaging findings and recommendation for excision vs imaging follow-up would not have missed the one malignancy in this study.

CLINICAL RELEVANCE/APPLICATION

The very low upgrade rate of RS without atypia supports imaging follow-up rather than excision, which could reduce the number of benign surgeries patients undergo.

SST01-07 Evaluation of Pathological Results of Tomosynthesis Guided Vacuum Assisted Breast Biopsy

Friday, Dec. 6 11:30AM - 11:40AM Room: E450A

Participants

Xiaoqin J. Wang, MD, Lexington, KY (*Presenter*) Nothing to Disclose Arzu Canon, MD, Dallas, TX (*Abstract Co-Author*) Nothing to Disclose Li Chen, PhD, Lexington, KY (*Abstract Co-Author*) Nothing to Disclose Richard D. Gibbs, MD, Nicholasville, KY (*Abstract Co-Author*) Nothing to Disclose Wendi A. Owen, MD, Saint Louis, MO (*Abstract Co-Author*) Nothing to Disclose Paul J. Spicer, MD, Lexington, KY (*Abstract Co-Author*) Nothing to Disclose Margaret M. Szabunio, MD, Nicholasville, KY (*Abstract Co-Author*) Nothing to Disclose

For information about this presentation, contact:

xwangf@uky.edu

PURPOSE

Digital breast tomosynthesis (DBT) guided vacuum assisted breast biopsy (TVAB) can target not only the calcified lesions detected on 2D mammogram but also non-calcified lesions only visualized on DBT. It is unknown if TVAB will result in more malignant or invasive cancer. In this study, we aimed to evaluate the pathological results of tomosynthesis guided vacuum assisted breast biopsy (TVAB) and compare to those of conventional stereotactic vacuum assisted biopsy (SVAB).

METHOD AND MATERIALS

All women who underwent TVAB (from May 2013 to April 2015) or SVAB (from June 2015 to May 2017) procedure were included in this retrospective study. Patients' demographics, lesion mammographic appearance, and biopsy pathologic results were compared between these two groups. The significance level was accepted as p<0.05.

RESULTS

389 patients with 410 lesions underwent SVAB and 540 patients with 579 lesions underwent TVAB. The mean ages in SVAB and TVAB groups are 55.9 ± 10.3 and 57.9 ± 10.5 , respectively. TVAB is found to have a higher biopsy rate of non-calcified lesions than SVAB (26% vs 16%, P < 0.05). No statistically significant differences were found between the two groups with respect to histological results of lesions such as breast tissue, benign changes, high risk lesions, or malignant lesions (p=0.161). Similar high-risk lesion upgraded rate was also observed. Among the malignant lesions, the rate of ductal carcinoma in situ (DCIS) is high in both SVAB group (88.6%) and TVAB group (77.9%), but no difference in the rate between these two groups is identified either (p=0.26).

CONCLUSION

TVAB group can biopsy more non-calcified lesions compared to conventional SVAB because it can target not only the calcified lesions detected on 2D mammogram but also non-calcified lesions only visualized on DBT. However, no significant histological differences (malignant vs benign or DCIS vs invasive cancer) in the biopsied lesions were found in these two groups.

CLINICAL RELEVANCE/APPLICATION

With increasing utilization of digital breast tomosynthesis and DBT guided vacuum-assisted biopsy (TVAB) in clinical practice, understanding this new technology and predicting biopsy results are important for the radiologist.

SST01-08 Digital Breast Tomosynthesis (DBT)-Guided Vacuum-Assisted Biopsy (VAB) with Integrated Real-Time Radiography System (IRRS): Initial Single-Center Experience

Friday, Dec. 6 11:40AM - 11:50AM Room: E450A

Participants

Catherine Depretto, Milano, Italy (*Presenter*) Nothing to Disclose Rubina Manuela Trimboli, San Donato Milanese, Italy (*Abstract Co-Author*) Nothing to Disclose Cristian G. Monaco, MD, Milan, Italy (*Abstract Co-Author*) Nothing to Disclose Giulia F. Boffelli, MD, Pavia, Italy (*Abstract Co-Author*) Nothing to Disclose Alessandro Liguori, MD, Milano, Italy (*Abstract Co-Author*) Nothing to Disclose

For information about this presentation, contact:

catherine.depretto@istitutotumori.mi.it

PURPOSE

We reviewed our experience with a DBT-guided VAB with IRRS to evaluate technical success, time for completing the procedure and added value of real-time specimen radiographs.

METHOD AND MATERIALS

The institutional review board approved this retrospective study and informed consent was waived. From January 2018 to October 2018 consecutive patients with suspicious mammographic calcifications (BI-RADS >=4) were referred to DBT-guided VAB with an IRRS (Brevera®, Hologic, Bedford, Mass). A 9-gauge VAB device was used and 12 specimens were always acquired in a clockwise manner; real time specimen radiography was measured for all biopsied lesions. 95% confidence interval (CI) and chi-squared statistics were used.

RESULTS

A total of 74 patients with median age of 51 years (range 38-82) with 74 suspicious lesions underwent DBT-guided VAB. Technical success was achieved in 74 of 74 lesions (100%, 95% CI 95%, 100%). The time to complete the procedure was 15.54 ± 8.47 min (mean \pm standard deviation) including identification, targeting, sampling, and real-time specimen radiography. No major complications were observed. Pathology of specimens resulted into: 45 B2, 5 B3 and 24 B5 lesions. Only one B2 lesion was upgraded to high-grade DCIS at final pathology. While of 471 specimens with calcifications, 105 (22%) were found with cancer and 361 (78%) were cancer-free, of 417 specimens without calcifications 56 (13%) were found with cancer and 361 (87%) were cancer-free (P < 0.001).

CONCLUSION

DBT-guided VAB with IRRS using a 9-gauge needle allowed for a safe, rapid, and adequate sampling of lesions with mammographic suspicious calcifications. Even though a significant difference in cancer prevalence was observed between specimens with (22%) or without calcifications (13%), a strategy for reducing the number of samples based the IRRS result (presence or absence of calcifications) is not feasible due to the too overall high probability of non-cancer specimens (727/888, 82%, 95% CI 79%, 84%).

CLINICAL RELEVANCE/APPLICATION

The IRRS makes the operator more confident that the sample is adequate and may allow for sparing subsequent control mammogram after the procedure, with a better patient compliance. Nevertheless, an earlier completion of the procedure, reducing the number of samples, does not seem to be feasible.

SST01-09 Results of a Phase I, Prospective, Non-Randomized Study Evaluating a Magnetic Occult Lesion Localization Instrument (MOLLI) for Excision of Non-Palpable Breast Lesions

Friday, Dec. 6 11:50AM - 12:00PM Room: E450A

Participants

Ananth Ravi, PhD, Toronto, ON (*Presenter*) Research Consultant, MOLLI Surgical Inc Frances Wright, MD, MEd, Toronto, ON (*Abstract Co-Author*) Nothing to Disclose Mia Skarpathiotakis, MD, Toronto, ON (*Abstract Co-Author*) Nothing to Disclose Mark Semple, Toronto, ON (*Abstract Co-Author*) Nothing to Disclose Alexandru Nicolae, Torotno, ON (*Abstract Co-Author*) Nothing to Disclose Nicole Look Hong, MD, MSc, Toronto, ON (*Abstract Co-Author*) Nothing to Disclose

PURPOSE

The purpose of this first-in-human study was to evaluate the clinical feasibility of using a Magnetic Occult Lesion Localization Instrument (MOLLI) for localizing non-palpable breast lesions.

METHOD AND MATERIALS

A pilot study of 20 women with non-palpable lesions visualized under ultrasound received a lumpectomy using the MOLLI guidance system at a single institution. Patients were co-localized with magnetic and radioactive markers up to 3 days before excision under ultrasound guidance by a dedicated breast radiologist . Both markers were localized intraoperatively using dedicated hand-held probes. The primary outcome was successful excision of the magnetic maker, confirmed both radiographically and pathologically. Demographic data, margin positivity, and re-excision rates are reported. Surgical oncologists, radiologists and pathology staff were surveyed for user satisfaction using 5-point Likert scale questionnaires.

RESULTS

Demographic data can be found in Table 1. *Post-Radiological Analysis*: Post-implant mammograms verified that 17/20 markers were placed directly in the lesion center and 20/20 had minimal to no migration. Radiologists reported that all marker implantations procedures were 'easy' or 'very easy' following a single training session. *Post-Surgical Analysis*: All MOLLI markers were removed with the specimen during surgical excision; no cases required final verification using the radioactive marker. Measurement of the distance of the MOLLI marker from anterior, posterior, superior, inferior, medial and lateral aspects of the excised tissue specimen agreed with radiological imaging estimates to within 2 mm. In all cases, surgeons ranked the MOLLI guidance system as 'very easy' for lesion localization. *Pathologic Analysis*: All patients had negative margins and did not require re-excision. All Anatomic Pathology staff ranked the MOLLI system as 'very easy' to use and localize markers.

CONCLUSION

The MOLLI guidance system is a reliable, accurate, and non-radioactive method for localization and excision of non-palpable breast lesions. Further clinical evaluation of the MOLLI system in comparative studies against current standards of care are required to demonstrate efficacy and patient-reported outcomes.

CLINICAL RELEVANCE/APPLICATION

MOLLI guided lumpectomy results in similar re-excision and margin positivity rates are radioactive-seed localization.







SST02

Chest (Artificial Intelligence - Machine Learning)

Friday, Dec. 6 10:30AM - 12:00PM Room: E451A



AMA PRA Category 1 Credits ™: 1.50 ARRT Category A+ Credit: 1.75

FDA Discussions may include off-label uses.

Participants

Bram van Ginneken, PhD, Nijmegen, Netherlands (*Moderator*) Stockholder, Thirona; Co-founder, Thirona; Royalties, Thirona; Research Grant, Varian Medical Systems, Inc; Royalties, Varian Medical Systems, Inc; Research Grant, Canon Medical Systems Corporation; Royalties, Canon Medical Systems Corporation; Research Grant, Siemens AG; Michael T, Lu, MD, Boston, MA (*Moderator*) Grant, NVIDIA Corporation; Institutional Research Grant, Kowa Company, Ltd.

Michael T. Lu, MD, Boston, MA (*Moderator*) Grant, NVIDIA Corporation; Institutional Research Grant, Kowa Company, Ltd ; Institutional Research Grant, AstraZeneca PLC

Sub-Events

SST02-01 Combining Effects of Advanced Image Processing for Automatic Disease Classification on Chest X-Rays by Ensembling and Deep Learning

Friday, Dec. 6 10:30AM - 10:40AM Room: E451A

Participants

Ivo Matteo Baltruschat, Hamburg, Germany (*Abstract Co-Author*) Nothing to Disclose Leonhard A. Steinmeister, MD, Hamburg, Germany (*Presenter*) Nothing to Disclose Harald Ittrich, MD, Hamburg, Germany (*Abstract Co-Author*) Nothing to Disclose Gerhard B. Adam, MD, Hamburg, Germany (*Abstract Co-Author*) Nothing to Disclose Axel Saalbach, PHD, Aachen, Germany (*Abstract Co-Author*) Employee, Koninklijke Philips NV Michael Grass, PhD, Hamburg, Germany (*Abstract Co-Author*) Employee, Koninklijke Philips NV Hannes Nickisch, Hamburg, Germany (*Abstract Co-Author*) Koninklijke Philips NV Jens von Berg, Hamburg, Germany (*Abstract Co-Author*) Employee, Koninklijke Philips NV Tobias Knopp, DIPLENG, Hamburg, Germany (*Abstract Co-Author*) Nothing to Disclose

For information about this presentation, contact:

l.steinmeister@uke.de

PURPOSE

This study investigates the effect of combining two different advanced image processing (AIP) techniques, initially developed for chest X-ray reading by radiologists, on the disease classification accuracy of a Convolutional Neural Network (CNN): Bone Suppression (BS) and Lung Field Cropping (LFC).

METHOD AND MATERIALS

Following early work in this domain, BS and LFC have a positive effect on chest disease classification by CNNs. In this study, we propose ensembling to combine the effects of multiple CNNs optimized for different image inputs - i.e. normal, BS, LFC and the combination of BS and LFC. Like a radiologist, the information of multiple input sources is combined in this way. We pretrain our CNN, optimized for X-ray analysis, on a large publicly available X-ray dataset (ChestX-ray14) and fine-tuned it afterwards on a new dataset. For evaluation and testing, two radiologists annotated the Indiana dataset (3125 DICOM images) with eight different classes: pleural effusion, infiltrate, congestion, atelectasis, pneumothorax, cardiomegaly, mass and foreign object.

RESULTS

In a five-fold cross-validation, we use ROC statistics to evaluate the effect of ensembling. To have a fair comparison, we compare our AIP ensemble against an ensemble build with four CNNs trained on normal images. Overall the AIP ensemble increased the average AUC significantly by 1.56 % (from 0.898±0.013 to 0.912±0.011). Furthermore, for selected classes - i.e. mass - a total of 0.068 (8.84 %) AUC increase was achieved.

CONCLUSION

We have presented a novel ensemble of advanced image processings to train a CNN. It outperforms a standard ensemble in 6 out of 8 classes and increased the average AUC. Leveraging the information of different advanced processed images help to increase the AUC significantly.

CLINICAL RELEVANCE/APPLICATION

Automatic disease classification on chest X-rays can be improved by applying different methods of advanced image preprocessing and not focusing on a single input source.

SST02-02 Performance of the Unsupervised Anomaly Detection with Generative Adversarial Networks in Disease Detection on Chest Radiograph

Participants Hye-Young Choi, Seoul, Korea, Republic Of (*Presenter*) Nothing to Disclose Sang Min Lee, MD, Seoul, Korea, Republic Of (*Abstract Co-Author*) Nothing to Disclose Joon Beom Seo, MD, PhD, Seoul, Korea, Republic Of (*Abstract Co-Author*) Nothing to Disclose Namkug Kim, PhD, Seoul, Korea, Republic Of (*Abstract Co-Author*) Stockholder, Coreline Soft, Co Ltd; Stockholder, Anymedi, Inc Hyun-Jin Bae, PhD, Seoul, Korea, Republic Of (*Abstract Co-Author*) Co-founder, Promedius Inc: CEO, Promedius Inc

Hyun-Jin Bae, PhD, Seoul, Korea, Republic Of (*Abstract Co-Author*) Co-founder, Promedius Inc; CEO, Promedius Inc Yongwon Cho, Seoul, Korea, Republic Of (*Abstract Co-Author*) Nothing to Disclose Minjee Kim, Seoul, Korea, Republic Of (*Abstract Co-Author*) Nothing to Disclose

PURPOSE

To compare the performance of disease detection on chest radiographs with that of unsupervised anomaly detection with generative adversarial networks (AnoGAN) model and that of preexisting supervised anomaly detection with convolutional neural net (CNN) model.

METHOD AND MATERIALS

Total of 100 chest radiographs were obtained from one hospital to validate the model. The 100 examinations were composed of 12 classes as follows: nodule (n=8), calcification (n=9), consolidation (n=6), interstitial opacity (n=9), atelectasis (n=9), mediastinal widening (n=6), pleural effusion (n=8), pneumothorax (n=9), rib fracture (n=10), pneumomediastinum (n=10), subcutaneous emphysema (n=6), and pneumoperitoneum (n=10). AnoGAN model and 6-class CNN system (6-class: normal, nodule, consolidation, interstitial opacity, pleural effusion, and pneumothorax) were used for disease detection of the images. For these 100 query images, AnoGAN model generated normal fake image most similar to that image and then detected disease by subtraction of two images. After the test set, one board certified cardiothoracic radiologist reviewed the images to evaluate the model performance.

RESULTS

Of 100 chest radiographs, 90 diseases were detected using AnoGAN model as follows: Nodule 100.0% (8/8), calcification 100.0% (9/9), consolidation 100.0% (6/6), interstitial opacity 100% (9/9), atelectasis 88.9% (8/9), mediastinal widening 83.3% (5/6), pleural effusion 87.5% (7/8), pneumothorax 100.0% (8/9), rib fracture 80.0% (8/10), pneumomediastinum 60.0% (6/10), subcutaneous emphysema 83.3% (5/6), and pneumoperitoneum 100.0% (10/10). The 6-class CAD system detected 37 of 40 diseases for trained classes (92.5%) whereas that detected only 14 of 60 disease for untrained classes (23.3%). Overall detection rate was higher in AnoGAN model than that of 6-class CAD system (90.0% vs. 51.0%, p < 0.001).

CONCLUSION

AnoGAN model can detect diseases on chest radiograph without training for each disease. We propose that AnoGAN model can overcome the limitation of current CAD system.

CLINICAL RELEVANCE/APPLICATION

Using AnoGAN model, disease detection of chest radiographs can be helpful for evaluation of chest radiograph.

SST02-03 Deep Learning-Based Automatic Classification of the Normal, Active Tuberculosis and Other Abnormal Patterns on Chest Radiographs

Friday, Dec. 6 10:50AM - 11:00AM Room: E451A

Participants

Hye Jeon Hwang, MD,PhD, Anyang, Korea, Republic Of (*Presenter*) Nothing to Disclose Joon Beom Seo, MD, PhD, Seoul, Korea, Republic Of (*Abstract Co-Author*) Nothing to Disclose Yongwon Cho, Seoul, Korea, Republic Of (*Abstract Co-Author*) Nothing to Disclose Namkug Kim, PhD, Seoul, Korea, Republic Of (*Abstract Co-Author*) Stockholder, Coreline Soft, Co Ltd; Stockholder, Anymedi, Inc Sang Min Lee, MD, Seoul, Korea, Republic Of (*Abstract Co-Author*) Nothing to Disclose Kyung-Wook Jo, Seoul, Korea, Republic Of (*Abstract Co-Author*) Nothing to Disclose

For information about this presentation, contact:

seojb@amc.seoul.kr

PURPOSE

To develop a deep learning-based automatic algorithm for classifying active pulmonary tuberculosis (TB) from other pulmonary abnormalities and normal looking lung with chest radiographs (CR).

METHOD AND MATERIALS

We collected a total of 3804 CRs comprising 2414 normal CRs and 1390 abnormal CRs with active TB (n = 590) and other five abnormal patterns including nodule, consolidation, pleural effusion, pneumothorax, interstitial opacity (n = 800). All CRs were randomly split into three datasets; training dataset (n = 2027; 1000 normal and 1027 abnormal CRs), validation dataset (n = 352; 200 normal and 152 abnormal CRs), and test dataset (n = 1425; 1214 normal and 211 abnormal CRs). The algorithm was designed using densenet201, convolutional neural network (CNN) for classifying normal and abnormal CRs, and then using YOLOv2-densenet201 model deeply fine-tuned for the differentiation of active TB, other abnormal patterns and normal CRs from the classified abnormal CRs. Diagnostic performance including sensitivity, specificity and accuracy of the algorithm was investigated per-CR classification and for per-region of interest (ROI) detection. All CRs were annotated by 5 - 10 years experienced thoracic radiologists.

RESULTS

In the test dataset, the algorithm showed 98.18% accuracy in the classification of normal and abnormal CR. For differentiation of classified abnormal CRs to active TB, other abnormal patterns and normal CRs, the diagnostic

accuracies were 78.5% for per-CR and 82.7% for per-ROI. The overall accuracy of the algorithm was 95.61% for per-CR and 93.29% for per-ROI. Sensitivity and specificity of the algorithm for active TB were 79.73% and 96.96% for per-CR and 77.83% and 95.38 for per-ROI.

CONCLUSION

Deep learning with CNN demonstrated high diagnostic performance in the classifying normal, active TB and other abnormal patterns CRs.

CLINICAL RELEVANCE/APPLICATION

Deep learning with CNN can be useful in the screening of the active TB with CR, thereby improving diagnostic-flow efficacy.

SST02-04 Deep Neural Network to Determine the Activity of Pulmonary Tuberculosis on Chest Radiograph

Friday, Dec. 6 11:00AM - 11:10AM Room: E451A

Participants

Seowoo Lee, Seoul, Korea, Republic Of (*Presenter*) Nothing to Disclose Soon Ho Yoon, MD, Seoul, Korea, Republic Of (*Abstract Co-Author*) Nothing to Disclose Young Ae Kang, Seoul, Korea, Republic Of (*Abstract Co-Author*) Nothing to Disclose Ju Sang Kim, Seoul, Korea, Republic Of (*Abstract Co-Author*) Nothing to Disclose Yeon Joo Lee, Seongnam, Korea, Republic Of (*Abstract Co-Author*) Nothing to Disclose Jung-ku Lee, Seoul, Korea, Republic Of (*Abstract Co-Author*) Nothing to Disclose Jae-Joon Yim, Seoul, Korea, Republic Of (*Abstract Co-Author*) Nothing to Disclose Doo Soo Jeon, MD, Masan, Korea, Republic Of (*Abstract Co-Author*) Nothing to Disclose Jin Mo Goo, MD, PhD, Seoul, Korea, Republic Of (*Abstract Co-Author*) Nothing to Disclose Jin Mo Grant, DONGKOOK Pharmaceutical Co, Ltd;

For information about this presentation, contact:

seowoo.md@gmail.com

PURPOSE

Determining the activity of pulmonary tuberculosis on chest radiograph is difficult even for tuberculosis experts. We aimed to develop a deep neural network for determining the activity of pulmonary tuberculosis on chest radiographs.

METHOD AND MATERIALS

From January 2011 through December 2017, we retrospectively collected a total of 6,647 baseline and post-treatment chest radiographs in 2,052 adult patients with sputum smear- or culture-proven tuberculosis who were successfully treated from five tertiary or secondary hospitals. Baseline and post-treatment chest radiographs were labeled as active and inactive tuberculosis, respectively. A deep neural network was trained with those radiographs to output the percentage score regarding the activity of tuberculosis. The validation dataset consisted of a series of 619 monthly radiographs during the treatment from 46 patients with the same inclusion criteria in 2018. Baseline and post-treatment radiographs in the validation dataset were read by the network and by a pulmonologist and thoracic radiologist with 20 and 10 years of dedicated experience to tuberculosis regarding the activity of tuberculosis regarding the performance. One-sample t test and linear regression analysis were used to analyze a tendency of tuberculosis activity score during anti-tuberculosis treatment.

RESULTS

The preliminary results showed that the AUROC of deep neural network was 0.80 (95% confidence interval [CI]: $0.71 \sim 0.89$), which was comparable with thoracic radiologist (0.71 (95% CI: $0.60 \sim 0.82$)) and pulmonologist (0.74 (95% CI: $0.64 \sim 0.84$)). During the period of anti-tuberculosis treatment, Log odds of Tb activity score gradually decreased with mean decrease of 2.82 (95% CI: 1.55 - 4.09) at 2 months (P<.001) and 5.10 (95% CI: 2.28 - 7.91) at 6 months (P=.001).

CONCLUSION

The deep neural network could accurately determine the activity of tuberculosis on chest radiograph, and the network was comparable to tuberculosis experts.

CLINICAL RELEVANCE/APPLICATION

The deep neural network can be used to determine the activity of tuberculosis in settings with limited tuberculosis experts and to monitor the response of anti-tuberculosis treatment, potentially in patients with drug-resistant tuberculosis.

SST02-05 Development of a Deep Learning-Based Algorithm for Independent Detection of Chest Abnormalities on Chest Radiographs

Friday, Dec. 6 11:10AM - 11:20AM Room: E451A

Participants

Minchul Kim, MS, Seoul, Korea, Republic Of (*Presenter*) Employee, Lunit Inc Jongchan Park, Seoul, Korea, Republic Of (*Abstract Co-Author*) Employee, Lunit Inc Ki Hwan Kim, MD,PhD, Seoul, Korea, Republic Of (*Abstract Co-Author*) Employee, Lunit Inc Eui Jin Hwang, Seoul, Korea, Republic Of (*Abstract Co-Author*) Nothing to Disclose Chang Min Park, MD, PhD, Seoul, Korea, Republic Of (*Abstract Co-Author*) Research funded, Lunit Inc Sunggyun Park, Seoul, Korea, Republic Of (*Abstract Co-Author*) Employee, Lunit Inc

sgpark@lunit.io

PURPOSE

To independently detect 10 abnormal radiologic findings commonly found in chest radiographs (Atelectasis, Calcification, Cardiomegaly, Consolidation, Fibrosis, Nodule, Mediastinal Widening, Pleural Effusion, Pneumoperitoneum, and Pneumothorax), we developed a deep learning based automatic detection (DLAD) algorithm and evaluated its performance with large-scale chest radiographs (CRs).

METHOD AND MATERIALS

We collected a total of 151228 CRs comprised of 79113 cases with abnormal findings (M:F=0.51:0.49; mean age=56.19±16.55). The dataset was made up of 12173 atelectasis, 1617 calcification, 4059 cardiomegaly, 7915 consolidation, 2473 fibrosis, 14422 nodule, 264 mediastinal widening, 11412 pleural effusion, 5304 pneumoperitoneum, 8286 pneumothorax, and 72115 normal cases. The dataset was randomly split into training (70353 normal, 73753 abnormal), validation (881 normal, 2680 abnormal) and test (881 normal, 2680 abnormal) sets. We developed a deep convolutional neural network with 34 layers and 16 residual connections, and it generates 10 separate 2D maps which indicate the location of each abnormality. The dataset was labeled by 18 radiologists and 16194 cases were further annotated to specify the locations of the findings. Each case in the test set has been annotated by 5 radiologists. The annotations used for the test set were taken by a majority vote. We verified the network's performance by measuring the area under the ROC curve (AUC) and jackknife alternative free-response receiver operating characteristics (JAFROC). AUC measures classification performance and JAFROC measures localization performance.

RESULTS

Our network's performance for combined abnormalities was calculated to be AUC: 0.958, JAFROC: 0.912. For the settings comparing each abnormality to the normal cases, the AUC and JAFROC were 0.983, 0.965 for atelectasis, 0.981, 0.966 for consolidation, 0.985, 0.954 for calcification, 0.984, 0.984 for cardiomegaly, 0.995, 0.988 for fibrosis, 0.971, 0.918 for nodule, 0.981, 0.978 for mediastinal widening, 0.997, 0.994 for pleural effusion, 0.999, 0.998 for pneumoperitoneum, and 0.997, 0.994 for pneumothorax.

CONCLUSION

DLAD can accurately detect and localize 10 abnormal findings in the CRs.

CLINICAL RELEVANCE/APPLICATION

Since DLAD can detect abnormal findings commonly found in CRs, it can help radiologists accurately interpret various abnormalities and may also be used to distinguish between normal and abnormal CRs.

SST02-06 Too-Sensitive Error Caused by Label Noises for Training Classification Network with Deep Convolutional Neural Net in Chest PA X-ray

Friday, Dec. 6 11:20AM - 11:30AM Room: E451A

Participants

Ryoungwoo Jang, Seoul, Korea, Republic Of (*Presenter*) Nothing to Disclose

Yongwon Cho, Seoul, Korea, Republic Of (Abstract Co-Author) Nothing to Disclose

Namkug Kim, PhD, Seoul, Korea, Republic Of (*Abstract Co-Author*) Stockholder, Coreline Soft, Co Ltd; Stockholder, Anymedi, Inc

Joon Beom Seo, MD, PhD, Seoul, Korea, Republic Of (Abstract Co-Author) Nothing to Disclose

Sang Min Lee, MD, Seoul, Korea, Republic Of (*Abstract Co-Author*) Nothing to Disclose

PURPOSE

Clean labels are considered as a vital condition in deep learning based classification. However, since labels of many large public dataset are preprocessed by natural language processing, they contain inaccurate, noisy labels to some extent. To evaluate robustness of classification network with deep-learning based chest X-ray(CXR) we measured deep convolutional neural network model by making labels inaccurate intentionally.

METHOD AND MATERIALS

CXR collected from two hospitals, which consisted of 10137 healthy subjects and 3244 patients and 1035 healthy subjects and 4404 patients with various kinds of diseases including nodule(ND), consolidation(CS), interstitial opacity(IO), pleural effusion(PE), and pneumothorax(PT), respectively. Every abnormal lesion was confirmed with its corresponding computed tomography(CT) image by expert thoracic radiologists with more than 10 years experiences. We split this dataset into two groups including normal and abnormal. Fine-tuned resnet-50 architecture for this classification with labels changed randomly at 0%, 1%, 2%, 4%, 8%, 16%, 32% rates were evaluated. Every training was done by 20 epochs and test set performances for every epoch were recorded. To assess the accuracies, we compared it with Receiver Operating Characteristic(ROC) curve and Area Under the Curve(AUC).

RESULTS

CXR classification model with noisy labels was not robust to any noise levels. Accuracies fall continuously when noises were given. ROCs were 0.94, 0.91, 0.90, 0.88, 0.86, 0.81, 0.78 at 0%, 1%, 2%, 4%, 8%, 16%, 32% rate, respectively which dropped linearly when semi-log scale plot was drawn.

CONCLUSION

As every CXR was confirmed with CT image by expert radiologists, our dataset was regarded as nearly absolute clean labels. In this study, the classification network was very sensitive to any degree of label noise rate. This implies that labels are needed as accurate as we can achieve.

CLINICAL RELEVANCE/APPLICATION

Developing algorithms for Computer-Aided Detection(CAD) of CXR diseases is challenging problem. Many newly

developed algorithms are based on large public datasets, which contain inaccurate labels. This study indicates algorithms based on noisy dataset cannot be valid models regardless of noise levels. Therefore CAD developers should contemplate using clean label datasets for lung nodule detection as well as other various diseases.

SST02-07 Deep Learning for Pulmonary Nodule Diagnosis on Computed Tomography: Comparison with 126 Physicians

Friday, Dec. 6 11:30AM - 11:40AM Room: E451A

Participants

Wen Hui Lv, Nanjing, China (*Presenter*) Nothing to Disclose Changsheng Zhou, Nanjing, China (*Abstract Co-Author*) Nothing to Disclose Qirui Zhang, Nanjing, China (*Abstract Co-Author*) Nothing to Disclose Yizhou Yu, Beijing, China (*Abstract Co-Author*) Research Scientist, Deepwise Healthcare Zhen Zhou, Beijing, China (*Abstract Co-Author*) Nothing to Disclose Xiuli Li, Beijing, China (*Abstract Co-Author*) Nothing to Disclose Haoliang Lin, MSc,MSc, Beijing, China (*Abstract Co-Author*) Nothing to Disclose Haoliang Lin, MSc,MSc, Beijing, China (*Abstract Co-Author*) Researcher, Healthcare AI Company Chuxi Huang, Nanjing, China (*Abstract Co-Author*) Nothing to Disclose Xinyu Li, Nanjing , China (*Abstract Co-Author*) Nothing to Disclose Long Jiang Zhang, MD, PhD, Nanjing, China (*Abstract Co-Author*) Nothing to Disclose Lu Guangming, MD, Nanjing, China (*Abstract Co-Author*) Nothing to Disclose

For information about this presentation, contact:

lvwh1993@163.com

PURPOSE

To compare the diagnostic performance of a deep learning algorithm with a large panel of physicians for pulmonary nodules diagnosis at unenhanced CT.

METHOD AND MATERIALS

The deep learning algorithm was developed using 1186 pathologically confirmed pulmonary nodules found in local hospital between 2009 and 2018 and 620 nodules from National Lung Cancer Screening Trial (NLST). Internal (local set, n = 100, NLST set, n = 200) and external validation (multi-center set, n = 242) of the algorithm were performed. The performance of the algorithm was evaluated by using the area under the receiver operating characteristic curve (AUC), sensitivity and specificity. An observer performance test involving 126 board-certified physicians was conducted using local set. All physicians individually reviewed the nodules and scored them from 1-4. Spearman's correlation coefficient was used to calculate the consistency between the scores ranked by physicians and the algorithm. The nodules in the local set were further divided into easy-to-diagnose and hard-to-diagnose group according to the proportion of physicians who diagnosed it correctly. The performance of algorithm in the two groups was compared with that of the physicians.

RESULTS

The AUC of the algorithm was 0.968 and 0.855 on internal and external validation set, respectively. The mean AUC of results from 126 physicians (0.759 \pm 0.080, p < 0.001) was outperformed by the algorithm (0.927) on local set. The scores rated by physicians were highly related with the algorithm (r = 0.663, p < 0.001). Taken an arbitrary of 80% as the threshold, the AUC of the algorithm were higher than that of the physicians both in the easy-to-diagnose group (0.9921 vs. 0.9108 \pm 0.0854, p < 0.001) and hard-to-diagnose group (0.8541 vs. 0.6203 \pm 0.0860, p < 0.001), respectively.

CONCLUSION

This deep learning-based diagnostic algorithm exhibited strong performance on internal and external validation and outperformed a large panel of physicians in pulmonary nodule classification.

CLINICAL RELEVANCE/APPLICATION

Deep learning exhibits great cognitive consistency with physicians in pulmonary nodule diagnosis and may have the potential for clinical applications.

SST02-08 Evaluation of Deep Learning-Based Automatic Classification of Pneumothorax on Frontal Chest X-Ray Images

Friday, Dec. 6 11:40AM - 11:50AM Room: E451A

Participants

Karl N. Yaeger, MD, Coopersburg, PA (*Presenter*) Nothing to Disclose Robert S. Fournier, MD, Bethlehem, PA (*Abstract Co-Author*) Nothing to Disclose Rachael Callcut, MD,MPH, San Francisco, CA (*Abstract Co-Author*) License agreement General Electric Company; Grant, General Electric Company; Grant, SERVIER; Grant, Merck KGaA; Grant, Haemonetics Corporation Tianhao Zhang, PhD, Waukesha, WI (*Abstract Co-Author*) Employee, General Electric Company Pal Tegzes, PhD, Budapest, Hungary (*Abstract Co-Author*) Employee, General Electric Company Min Zhang, San Ramon, CA (*Abstract Co-Author*) Employee, General Electric Company Zita Herczeg, MD, Szeged, Hungary (*Abstract Co-Author*) Employee, General Electric Company Katelyn Nye, Waukesha, WI (*Abstract Co-Author*) Employee, General Electric Company Alec Baenen, Waukesha, WI (*Abstract Co-Author*) Employee, General Electric Company John M. Sabol, PhD, Waukesha, WI (*Abstract Co-Author*) Employee, General Electric Company Gireesha Rao, BEng, Waukesha, WI (*Abstract Co-Author*) Employee, General Electric Company Gopal B. Avinash, PHD, Waukesha, WI (*Abstract Co-Author*) Employee, General Electric Company

For information about this presentation, contact:

PURPOSE

To evaluate the performance of AI algorithms to automatically detect the presence of pneumothorax (PTX) on frontal chest x-ray images.

METHOD AND MATERIALS

A dataset of 808 adult frontal chest x-ray images was formed from an American (51%) and a Canadian hospital (49%) comprising of AP view/portable system (62%) and PA view / fixed system (38%). Images were generated systems manufactured by GE (67%), Phillips (32%), and Agfa (1%). Initially, ground truth for the presence, laterality, and size of a PTX was determined by two blinded radiologists, with a subsequent blinded arbitrator in cases of disagreement. Inferencing was then performed by two deep learning-based AI algorithms that were developed from independent datasets of over 44,000 images; a frontal chest x-ray classifier and a PTX classification algorithm - detecting the presence or absence of a PTX.

RESULTS

Radiologist's deemed PTX present as ground truth in 47% of the data set, with laterality of right for 53%, left for 44%, and bilateral for 3%. PTX size was determined to be small for 56%, large for 43%, and small + large for 1% in bilateral cases. The frontal chest x-ray classifier correctly identified 99.5% of the images as frontal chest, only the 804 images correctly identified as frontal chest were then subsequently inferenced by the PTX classifier. The PTX classifier had an AUC of 0.96 (0.95, 0.97) with AUC of 0.96 (0.95, 0.98) for AP and 0.96 (0.94, 0.98) for PA images. Balanced accuracy was achieved with overall sensitivity and specificity of 89% (82% sensitivity for small and 97% for large). Alternative ROC operating points offer high overall sensitivity performance of 94%, specificity of 80% (sensitivity of small and large PTX of 90% and 99% respectively), or high specificity with overall sensitivity of 84%, specificity of 93% (sensitivity of small and large PTX of 75% and 96% respectively).

CONCLUSION

Deep learning-based algorithms can effectively detect PTX in frontal x-ray images with high accuracy.

CLINICAL RELEVANCE/APPLICATION

A deep learning-based PTX algorithm could be an effective triaging tool for identifying exams that need a prioritized review, contributing towards improved workflow efficiency and patient outcomes.

SST02-09 Is the Juice Worth the Squeeze? Learning Curve of a Chest Radiograph Semantic Labeling DCNN versus Training Time

Friday, Dec. 6 11:50AM - 12:00PM Room: E451A

Participants

Paul H. Yi, MD, Baltimore, MD (*Presenter*) Nothing to Disclose
Joshua Garza, Baltimore, MD (*Abstract Co-Author*) Nothing to Disclose
Jonathan Wang, Baltimore, MD (*Abstract Co-Author*) Nothing to Disclose
Jinchi Wei, Baltimore, MD (*Abstract Co-Author*) Nothing to Disclose
Ferdinand K. Hui, MD, Richmond, VA (*Abstract Co-Author*) Speakers Bureau, Terumo Corporation Speakers Bureau,
Penumbra, Inc Stockholder, Blockade Medical Inc
Cheng Ting Lin, MD, Baltimore, MD (*Abstract Co-Author*) Nothing to Disclose
Gregory D. Hager, PhD, MSc, Baltimore, MD (*Abstract Co-Author*) Co-founder, Clear Guide Medical LLC CEO, Clear Guide

Haris I. Sair, MD, Baltimore, MD (Abstract Co-Author) Research Grant, Tocagen

For information about this presentation, contact:

pyi10@jhmi.edu

PURPOSE

The purpose of this study was to determine the learning and training time curves of a DCNN trained to classify frontal chest radiographs (CXRs) into AP or PA views based on increasing dataset sizes.

METHOD AND MATERIALS

We obtained 112,120 CXRs from the NIH ChestX-ray14 database which contained 44,810 (40%) AP and 67,420 PA (60%) CXRs. We created datasets based on random selection, each balanced to have 50% AP and 50% PA CXRs which would gradually increase by a factor of 2; accordingly, the largest dataset we used was 89,620 CXRs with 11 other smaller datasets (Table 1). Each dataset was randomly split into training (70%), validation (10%), and test (20%) sets, which were used to train, validate, and test the ResNet-50 DCNN pretrained on ImageNet. During each training epoch, each image was augmented by a random rotation between -5 and 5 degrees, random cropping, and horizontal flipping. All DCNN development and testing was performed using PyTorch on a 2.5 GHz Intel Haswell dual socket (12-core processors) with 128 GB of RAM and 2 NVIDIA K80 GPUs. Receiver operating characteristic (ROC) curves with area under the curve (AUC) and total training time was plotted to dataset size with regression analysis performed.

RESULTS

DCNNs trained to classify AP vs. PA CXRs achieved high AUC of 0.88 with the smallest utilized sample size of 44 and reached a consistent plateau of AUC of 1 with 350 CXRs, with no improvement in performance thereafter (Table 1). Interestingly, there was a linear increase in training time required as dataset size increased; in fact, there was a linear relationship defined by the equation, y = 1.1x - 286 (R2=0.999).

CONCLUSION

Semantic labeling of radiographs only require small datasets on the scale of hundreds to train a diagnostically-perfect DCNN. Accordingly, curating large datasets for these purposes is not worthwhile, especially given the increased training

time required for larger datasets. For the development of CXR-classification DCNNs, we propose that 350 CXRs is a reasonable starting point.

CLINICAL RELEVANCE/APPLICATION

Semantic labeling of radiographs only require small datasets on the scale of hundreds to train a diagnostically-perfect DCNN. Accordingly, curating large datasets for these purposes is not worthwhile, especially given the increased training time required for larger datasets.

Printed on: 10/29/20







SST03

Gastrointestinal (Advanced Ultrasound Techniques)

Friday, Dec. 6 10:30AM - 12:00PM Room: E352



AMA PRA Category 1 Credits ™: 1.50 ARRT Category A+ Credit: 1.75

FDA Discussions may include off-label uses.

Participants

Mark E. Lockhart, MD, Birmingham, AL (*Moderator*) Author, Oxford University Press; Author, Reed Elsevier; Editor, John Wiley & Sons, Inc; Deputy Editor, Journal of Ultrasound in Medicine Venkateswar R. Surabhi, MD, Sugar Land, TX (*Moderator*) Nothing to Disclose

Lauren M. Burke, MD, Chapel Hill, NC (Moderator) Nothing to Disclose

Sub-Events

SST03-01 Non-Enhanced Magnetic Resonance Imaging versus Ultrasonography for Surveillance of Hepatocellular Carcinoma: Intraindividual Comparison in a Prospective Cohort

Friday, Dec. 6 10:30AM - 10:40AM Room: E352

Participants

Dong Wook Kim, MD, Seoul, Korea, Republic Of (*Presenter*) Nothing to Disclose Hyo Jung Park, MD, Seoul, Korea, Republic Of (*Abstract Co-Author*) Nothing to Disclose So Yeon Kim, MD, Seoul, Korea, Republic Of (*Abstract Co-Author*) Nothing to Disclose Hye Young Jang, Daejon, Korea, Republic Of (*Abstract Co-Author*) Nothing to Disclose Sang Hyun Choi, Seoul, Korea, Republic Of (*Abstract Co-Author*) Nothing to Disclose Jae Ho Byun, MD, Seoul, Korea, Republic Of (*Abstract Co-Author*) Nothing to Disclose Seung Soo Lee, MD, Seoul, Korea, Republic Of (*Abstract Co-Author*) Nothing to Disclose Soung-Suk Lim, Seoul, Korea, Republic Of (*Abstract Co-Author*) Nothing to Disclose So Jung Lee, Seoul, Korea, Republic Of (*Abstract Co-Author*) Nothing to Disclose Hyung Jin Won, MD, Seoul, Korea, Republic Of (*Abstract Co-Author*) Nothing to Disclose Jihyun An, Seoul, Korea, Republic Of (*Abstract Co-Author*) Nothing to Disclose

For information about this presentation, contact:

sykim.radiology@gmail.com

PURPOSE

We aimed to compare the performance of non-enhanced MRI and US as a surveillance tool for hepatocellular carcinoma (HCC) by making intraindividual comparisons in a prospective cohort at high risk of HCC.

METHOD AND MATERIALS

This prospective cohort included 382 patients with an estimated annual HCC risk > 5% who underwent paired gadoxetic acidenhanced MRI and US between 2011 and 2013. Non-enhanced MRI consisted of diffusion-weighted images (DWI) (b = 0, 50, and 500 s/mm2) and T2-weighted images (T2WI), and was considered positive when a lesion >= 1 cm showed diffusion restriction or mild-moderate T2 hyperintensity on a retrospective analysis. On US, a discrete mass >= 1 cm or a suspicious tumor thrombus was regarded as positive. HCC was diagnosed pathologically and/or radiologically. Sensitivity and positive predictive value (PPV) obtained on a per-lesion and per-patient basis, and specificity and negative predictive value (NPV) obtained on a per-patient basis, were compared between modalities using generalized estimating equations, McNemar tests, and Fisher's exact tests, as appropriate.

RESULTS

Thirty-two HCCs were diagnosed in 28 patients. The per-lesion and per-patient sensitivities of non-enhanced MRI were 84.5% (27/32) and 85.7% (24/28), respectively, and were higher than those of US (34.6% [11/32] and 39.3% [11/28], respectively, P <= 0.001). PPVs were higher on non-enhanced MRI (65.9% [27/41] per-lesion and 64.9% [24/37] per-patient) than on US (32.4% [11/34] and 35.5% [11/31], P <= 0.028), while the specificity of non-enhanced MRI was not significantly different from that of US (96.3% [341/354] for non-enhanced MRI vs. 94.4% [334/354] for US, P = 0.377). The NPV of non-enhanced MRI (98.8% [341/345]) was higher than that of US (95.2% [334/351], P = 0.006).

CONCLUSION

Non-enhanced MRI consisting of DWI and T2WI showed better sensitivity, PPV, and NPV than US. Non-enhanced MRI is a promising option for HCC surveillance.

CLINICAL RELEVANCE/APPLICATION

In patients at high risk of HCC, non-enhanced MRI consisting of DWI and T2WI can be considered an alternative surveillance tool to US.

Biopsy as Reference for Diagnosis of Chronic Liver Disease

Friday, Dec. 6 10:40AM - 10:50AM Room: E352

Participants

Ilias Gatos, MSc, PhD, Rion, Greece (Abstract Co-Author) Institutional Research Grant, Shenzhen Mindray Bio-Medical Electronics Co, Ltd

Petros Drazinos, PhD,MSc, Kifissia, Greece (Abstract Co-Author) Institutional Research Grant, Shenzhen Mindray Bio-Medical Electronics Co, Ltd

Spyros D. Yarmenitis, MD, Athens, Greece (Abstract Co-Author) Institutional Research Grant, Shenzhen Mindray Bio-Medical

Electronics Co, Ltd

Ioannis Theotokas, Athens, Greece (*Abstract Co-Author*) Institutional Research Grant, Shenzhen Mindray Bio-Medical Electronics Co, Ltd

Eleni Panteleakou, Athens, Greece (Abstract Co-Author) Institutional Research Grant, Shenzhen Mindray Bio-Medical Electronics Co, Ltd

Ioannis Koskinas, Athens, Greece (Abstract Co-Author) Nothing to Disclose

Pavlos Zoumpoulis, MD, PhD, Kifissia, Greece (*Presenter*) Institutional Research Grant, Shenzhen Mindray Bio-Medical Electronics Co, Ltd

For information about this presentation, contact:

p.drazinos@echomed.gr

PURPOSE

Chronic Liver Disease (CLD) is currently one of the major causes of death and the major cause of Hepatocellular Carcinoma development. Therefore, accurate diagnosis regarding CLD progress is very important. Although Liver Biopsy (LB) is considered as 'Gold Standard' for diagnosis, several non-invasive methods exist in order to avoid LB complications. Sound Touch Elastography (STE) that is available in Resona 7 Ultrasound (US) device and is similar to Shear Wave Elastography (SWE), seems promising but needs to be validated. The aim of this study is to compare the diagnostic performance between the STE and SWE for CLD assessment, using LB as "Gold Standard".

METHOD AND MATERIALS

290 subjects, 68 normal (F0) and 222 with CLD (F1-F4), were included in the study. a B-Mode and Elastographic examination was performed on each patient with Resona 7 and Aixplorer US devices. The STE (Resona 7) and SWE (Aixplorer) measurements were performed on the Right Lobe (RL) of each patient and were compared to LB results according to the Metavir Classification System (F0-F4). Receiver Operating Characteristic (ROC) analysis was then performed for each of the two methods to obtain best cut-off stiffness values.

RESULTS

ROC analysis showed AUCSTE=0.9741 and AUCSWE=0.9854 for F=F4 Cirrhosis, AUCSTE=0.9723 and AUCSWE=0.9755 for F>=F3 Fibrosis Stage, AUCSTE=0.9675 and AUCSWE=0.9662 for F>=F2 Fibrosis Stage, AUCSTE=0.8889 and AUCSWE=0.9288 for F>=F1 Fibrosis Stage. Best cut-off stiffness values were calculated for each method (STE/SWE) compared to Metavir fibrosis stages: F=F4: 12.2/13.5 kPa, F>=F3: 9.5/8.7 kPa, F>=F2: 9.15/8.55 kPa, F>=F1: 6.5/6.05 kPa respectively.

CONCLUSION

Both STE and SWE can differentiate between the 5 Metavir fibrosis stages. SWE seems more reliable in differentiating normal subjects from subjects with CLD (F >= F1) and Cirrhotic patients (F = F4) but less accurate in diagnosing intermediate stages (F >= F2, F >= F3).

CLINICAL RELEVANCE/APPLICATION

Many Elastography technologies emerged with liver in focus. Comparison between them is useful in order to make Elastography reliably applicable to patients regardless of the underlying technology.

SST03-03 ACR US LI-RADS: Outcomes of Category US-2 Observations

Friday, Dec. 6 10:50AM - 11:00AM Room: E352

Participants

John D. Millet, MD, Ann Arbor, MI (*Presenter*) Nothing to Disclose Ashish P. Wasnik, MD, Ann Arbor, MI (*Abstract Co-Author*) Nothing to Disclose William Masch, MD, Ann Arbor, MI (*Abstract Co-Author*) Nothing to Disclose Mishal Mendiratta-Lala, MD, Ann Arbor, MI (*Abstract Co-Author*) Nothing to Disclose Katherine E. Maturen, MD, Ann Arbor, MI (*Abstract Co-Author*) Royalties, Reed Elsevier; Royalties, Wolters Kluwer nv; ;

PURPOSE

To evaluate the outcomes of ACR US LI-RADS Category 2 (US-2) observations detected at ultrasound performed for hepatocellular carcinoma (HCC) screening and surveillance.

METHOD AND MATERIALS

In this retrospective, single center study, 138 patients at high risk for HCC (77 men and 61 women; mean age 58.7 years) underwent screening liver ultrasound between January 2017 and December 2018 and were assigned US-2 observations on a prospective clinical basis. Results of follow-up imaging studies and/or histopathology were recorded. Statistical analysis was performed.

RESULTS

The most common indications for HCC screening were cirrhosis (111/138, 80%), chronic hepatitis B virus without cirrhosis (15/138, 11%), and chronic hepatitis C virus without cirrhosis (7/138, 5%). Reasons for US-2 observations were a measureable mass (116/138, 84%; mean size 0.7 ± 0.2 cm; range 0.3-0.9 cm) and a subcentimeter area of parenchymal heterogeneity (22/138,

16%). 72% (99/138) of patients had imaging follow-up and management was discordant with US LI-RADS recommendations in 56% (55/99) of these patients. Confirmatory tests including multiphase contrast-enhanced CT or MRI (61/80), histopathology (6/80), or negative ultrasound follow-up for at least 1 year (13/80) were available for 59% (80/138) of patients. Etiologies of US-2 observations in the subset of 67 patients with CT, MRI, or histopathology included no mass/benign tissue (48/67, 72%), hemangioma (5/67, 7.5%), regenerative nodule (5/67, 7.5%), cyst (3/67, 4%), HCC (2/67, 3%), granuloma (2/67, 3%), LR-3 observation (1/67, 1.5%), and focal steatosis (1/67, 1.5%). Positive predictive value of a US-2 observation for HCC was 2.5%.

CONCLUSION

The positive predictive value of a US-2 (subcentimeter) observation for the detection of HCC is very low. As per US LI-RADS guidelines, US-2 observations can be safely followed with ultrasound rather than escalating workup to contrast-enhanced imaging.

CLINICAL RELEVANCE/APPLICATION

The vast majority of US LI-RADS Category 2 (US-2) observations are benign and can be safely followed with ultrasound.

SST03-04 Subharmonic Aided Pressure Estimation (SHAPE) for Long-Term Follow up of Patients with Portal Hypertension

Friday, Dec. 6 11:00AM - 11:10AM Room: E352

Participants

Ipshita Gupta, MS, Philadelphia, PA (*Abstract Co-Author*) Nothing to Disclose Flemming Forsberg, PhD, Philadelphia, PA (*Presenter*) Research Grant, Canon Medical Systems Corporation Research Grant, General Electric Company Research Grant, Siemens AG Research Grant, Lantheus Medical Imaging, Inc Jonathan M. Fenkel, Philadelphia, PA (*Abstract Co-Author*) Nothing to Disclose Maria Stanczak, MS, Lafayette Hill, PA (*Abstract Co-Author*) Nothing to Disclose Priscilla Machado, MD, Philadelphia, PA (*Abstract Co-Author*) Nothing to Disclose Colette Shaw, MBBCh, Philadelphia, PA (*Abstract Co-Author*) Nothing to Disclose Susan S. Noori, Philadelphia, PA (*Abstract Co-Author*) Nothing to Disclose Michael C. Soulen, MD, Lafayette Hill, PA (*Abstract Co-Author*) Nothing to Disclose Susan M. Schultz, Philadelphia, PA (*Abstract Co-Author*) Nothing to Disclose Kirk Wallace, PhD, Niskayuna, NY (*Abstract Co-Author*) Nothing to Disclose Kirk Wallace, PhD, Niskayuna, NY (*Abstract Co-Author*) Employee, General Electric Company John R. Eisenbrey, PhD, Philadelphia, PA (*Abstract Co-Author*) Employee, General Electric Company Support, Lantheus Medical Imaging, Inc

For information about this presentation, contact:

ipshitagupta89@gmail.com

PURPOSE

To verify if noninvasive contrast-enhanced ultrasound (US) in the form of subharmonic aided pressure estimation (SHAPE) can accurately monitor disease progression or treatment response in patients identified with portal hypertension.

METHOD AND MATERIALS

SHAPE is based on the inverse relationship between the subharmonic amplitude of US contrast microbubbles and ambient pressure. A modified Logiq 9 scanner with a 4C curvi-linear probe (GE, Waukesha, WI) was used to acquire SHAPE data (transmitting/receiving at 2.5/1.25MHz) using Sonazoid (GE Healthcare, Oslo, Norway; IND 124,465). This IRB approved study has enrolled 177 subjects undergoing a transjugular liver biopsy, 22 patients have been identified with clinically significant portal hypertension (median age 59 yrs; 13 Males) based on their HVPG results. These subjects had follow-up clinic visits or CT/MRI scans every 6 months and at those times a repeat SHAPE examination was performed collecting data from the portal and hepatic vein in triplicate. The SHAPE gradient was calculated as the difference between subharmonic signals in the two vessels. Liver function tests (albumin, bilirubin and coagulation panel), MELD scores and presence of ascites and varices were used to establish clinical treatment response.

RESULTS

Of the 22 portal hypertensive cases, 1 patient has had four follow up scans, 1 has had three follow up scans, 3 have had two follow up scans, 7 have had one follow up, 7 have not had any follow up yet and 3 were lost due to death or refusal to follow up. There was a significantly higher signal reduction in the group who were classified as responders according to the SHAPE study compared to the SHAPE non-responders (p < 0.001). The mean change in the SHAPE gradient for the responders (n = 9) was -4.70 ±3.27 dB vs 1.77±0.55 dB in the SHAPE non-responders (n = 3). Results matched the corresponding clinical outcomes of improved MELD scores, improvement in underlying cause of portal hypertension, decreased bilirubin and reduced ascites indicating a reduction in portal hypertension amongst responders.

CONCLUSION

SHAPE can noninvasively monitor disease progression in portal hypertensive patients and hence, may help clinicians in patient management.

CLINICAL RELEVANCE/APPLICATION

Serial SHAPE can be a cost-effective and noninvasive technique to differentiate between portal hypertension treatment responders and non-responders and reduce the need for repeat catheterizations.

SST03-05 Inter-System Agreement and Repeatability of Two-Dimensional Shear Wave Elastography Measurements in Elastic Phantoms and In Vivo Human Livers Across Six Commercially-Available Ultrasound Systems

Friday, Dec. 6 11:10AM - 11:20AM Room: E352

Andrew T. Trout, MD, Cincinnati, OH (*Abstract Co-Author*) Author, Reed Elsevier; Author, Wolters Kluwer nv; Research Grant, Canon Medical Systems Corporation; Board Member, Joint Review Committee on Educational Programs in Nuclear Medicine Technology; Speakers Bureau, Reed Elsevier; Speakers Bureau, iiCME

Paula Bennett, Cincinnati, OH (Abstract Co-Author) Nothing to Disclose

Jonathan R. Dillman, MD, MSc, Cincinnati, OH (*Abstract Co-Author*) Research Grant, Siemens AG; Research Grant, Guerbet SA; Travel support, Koninklijke Philips NV; Research Grant, Canon Medical Systems Corporation; Research Grant, Bracco Group

For information about this presentation, contact:

leah.gilligan@cchmc.org

PURPOSE

To determine inter-system agreement and repeatability of two-dimensional (2D) shear wave elastography (SWE) shear wave speed (SWS) measurements in elastic phantoms and in vivo human livers across six ultrasound systems.

METHOD AND MATERIALS

This HIPAA-compliant study was institutional review board-approved; informed consent was obtained. Serial 2D SWE exams were performed using six commercially-available ultrasound systems (Aplio i800, Canon Medical Systems; LOGIQ E10, GE Healthcare; Resona 7, Mindray North America; EPIQ Elite, Philips Healthcare; ACUSON Sequoia, Siemens Medical Solutions; Aixplorer MACH 30, SuperSonic Imagine). Exams were performed on four elastic phantoms (Model 039, Shear Wave Liver Fibrosis Phantoms; CIRS, Inc., SWS range:0.82-3.51 m/s) by two operators (20 measurements/operator, 1 cm circular region-of-interest [ROI], 4 cm depth) and on 24 fasting adults (14 healthy volunteers, 10 with known liver stiffening) by one operator/system (2 non-sequential exams/system, 10 measurements/creater). Intra-class correlation coefficients (ICC) were calculated to assess inter-system and test-retest agreement. Interquartile range (IQR)/median and coefficient of variation (COV) values were used to assess patient-level variance.

RESULTS

ICCs for overall inter-system agreement of SWS were 0.99 (95% CI:0.96-1.0) in phantoms and 0.66 (95% CI:0.47-0.81) in humans (Figure). Pairwise ICCs for inter-system agreement in participants across two systems ranged from 0.41 to 0.91. Average patient level variance (IQR/median SWS) across all 288 examinations (24 participants, 12 exams/participant) was 0.07 (mean inter-system range:0.045-0.09), with an average COV of 6.0% (mean inter-system range:4.0-7.5%). Test-retest repeatability in humans was excellent for all systems, with ICCs of: 0.87-0.97.

CONCLUSION

There is good to excellent inter-system agreement of measured SWS in elastic phantoms and in vivo human livers across six 2D SWE ultrasound systems. Test-retest agreement for all systems is excellent. Average patient-level variance of SWS measurements is minimal.

CLINICAL RELEVANCE/APPLICATION

Commercially-available 2D ultrasound shear wave elastography systems exhibit satisfactory inter-system agreement and test-retest repeatability in phantoms and in vivo human livers.

sst03-06 Is There a Role for Ultrasound in the Evaluation of Transplant Graft Small Bowel?

Friday, Dec. 6 11:20AM - 11:30AM Room: E352

Participants

Katy Hickman, MBBS, London, United Kingdom (*Presenter*) Nothing to Disclose Janette Smith, MBBChir, Cambridge, United Kingdom (*Abstract Co-Author*) Nothing to Disclose David Hulse, BMBS, Cambo, United Kingdom (*Abstract Co-Author*) Nothing to Disclose Lisa Sharkey, Cambridge, United Kingdom (*Abstract Co-Author*) Nothing to Disclose Edmund M. Godfrey, MBBCh, FRCR, Cambridge, United Kingdom (*Abstract Co-Author*) Nothing to Disclose Andrew Butler, Cambridge, United Kingdom (*Abstract Co-Author*) Nothing to Disclose Sara S. Upponi, MBBS, Saffron Walden , United Kingdom (*Abstract Co-Author*) Nothing to Disclose

For information about this presentation, contact:

katy.hickman@addenbrookes.nhs.uk

PURPOSE

Intestinal graft recipients are subjected to significant doses of radiation. MRI studies may not be feasible acutely. Endoscopic examination of the intestine is usually limited to small sections of the graft. Ultrasound (US) is an established technique in the evaluation of disease extent in patients with small bowel Crohn's, therefore we have utilized US for several years to evaluate the graft small bowel and retrospectively reviewed our findings.

METHOD AND MATERIALS

This is a retrospective review of small bowel US studies performed post operatively for our cohort of 97 patients receiving an intestine-containing transplant (IT) between 2007 and 2019. Imaging interpretation was based of grey-scale images and Doppler imaging. US images were reviewed with subsequent clinical, imaging, endoscopy and histology findings.

RESULTS

97 patients received an IT between 2007 and 2019. There were 45 US studies undertaken in 27 patients. The majority of studies (23 studies in 9 patients) were undertaken in those with biopsy-proven acute cellular rejection (ACR). Imaging findings of mural thickening, loss of mural stratification, reduced peristalsis and mesenteric hypervascularity were observed in 7 patients with ACR. 2 patients with a history of ACR had normal US appearances at follow up, which correlated with endoscopic findings of recovery. Of the US performed for ACR, concurrent endoscopy (within 1 week) occurred in 11 US studies. 8 endoscopies demonstrated features related to rejection confirmed at histology. 3 demonstrated recovery. 5 patients underwent US immediately post-surgery with normal findings consistent with concurrent CT or endoscopy findings. 11 studies in 6 patients demonstrated minimal mural thickening but no further features to suggest rejection, 4 were followed with endoscopy with no features of rejection. The remainder were

followed clinically and radiologically.

CONCLUSION

Small bowel US is a useful technique in establishing normal appearances of the bowel. When interpreted in conjunction with clinical and endoscopic findings in patients with ACR it could have a role in surveillance.

CLINICAL RELEVANCE/APPLICATION

Ultrasound (US) is established in imaging of Crohn's disease. Rejection in intestinal transplantation is evaluated with endoscopic surveillance. We hypothesize that US may be use as an adjunct.

SST03-07 Spleen Elastography as a Predictor of Esophageal Varices

Friday, Dec. 6 11:30AM - 11:40AM Room: E352

Participants

Monica P. Cueva, MD, Quito, Ecuador (*Presenter*) Nothing to Disclose Jorge R. Aldean, MEd, Quito, Ecuador (*Abstract Co-Author*) Nothing to Disclose Xavier S. Herdoiza, MD, Quito, Ecuador (*Abstract Co-Author*) Nothing to Disclose Cristian Armijos, Quito, Ecuador (*Abstract Co-Author*) Nothing to Disclose Ricardo Chong, Quito, Ecuador (*Abstract Co-Author*) Nothing to Disclose Maria J. Andrade, Quito, Ecuador (*Abstract Co-Author*) Nothing to Disclose

PURPOSE

To evaluate the diagnostic performance of splenic elastography and other non-invasive methods to detect high-risk esophageal varices in patients with cirrhosis. The verification of the existence of varices was performed with upper digestive endoscopy, which is the gold standard.

METHOD AND MATERIALS

A prospective study was performed with 100 patients with a recent diagnosis of cirrhosis who were evaluated with upper abdomen ultrasound, hepatic Doppler, liver elastography, upper digestive endoscopy and that complied with the following criteria: no history of digestive bleeding, no treatment with beta-blockers, no thrombosis of the holder. Splenic elastography was performed by a radiologist with training in elastography using shear wave point elastography with a 5-7MHz convex probe. After the imaging studies, upper digestive endoscopy was performed by two hepatologists who were blinded to the information and the diagnosis of esophageal varices was obtained as well as the classification of patients into three groups: those who had no varices, low-risk varices and high-risk varices. A cross-sectional, unicentric study was carried out from April 2017 until December 2018. The data was organized in frequency tables. The comparison with the gold standard included the use of Chi square and ROC curves were obtained to present sensitivity and specificity data.

RESULTS

Spleen elastography proved to be a good predictive study of the presence of esophageal varices (AUC 0.84, CI 95%: 0.71-0.97), followed by the diameter of the spleen (AUC 0.81, 95% CI: 0.66-0.96), while the congestivity index (AUC 0.46, 95% CI: 0.27 - 0.64) and liver elastography (AUC 0.39, 95% CI: 0.21 - 0.58) proved to be the parameters with less precision. The cut-off point of 3.8m/s in the splenic elastography was able to identify high risk varices with a sensitivity of 90.9%.

CONCLUSION

Splenic elastography demonstrated sensitivity and specificity values similar to the ones published in international studies with adequate correlation with endoscopy for diagnosing high-risk esophageal varices.

CLINICAL RELEVANCE/APPLICATION

Bleeding is the most common and dangerous complication of esophageal varices. With early detection of high-risk varices using a non-invasive technique such as spleen elastogrpahy, patients can start prophylaxis with beta-blockers.

SST03-08 A Diagnostic Role of US-Guided Percutaneous Biopsy in Patients at Risk for Hepatocellular Carcinoma: Comparison with Noninvasive Diagnostic Approaches

Friday, Dec. 6 11:40AM - 11:50AM Room: E352

Participants

Dong Wook Kim, MD, Seoul, Korea, Republic Of (*Presenter*) Nothing to Disclose So Yeon Kim, MD, Seoul, Korea, Republic Of (*Abstract Co-Author*) Nothing to Disclose Jihun Kang, Seoul, Korea, Republic Of (*Abstract Co-Author*) Nothing to Disclose Sang Hyun Choi, Seoul, Korea, Republic Of (*Abstract Co-Author*) Nothing to Disclose Yong Moon Shin, Seoul, Korea, Republic Of (*Abstract Co-Author*) Nothing to Disclose Seung Soo Lee, MD, Seoul, Korea, Republic Of (*Abstract Co-Author*) Nothing to Disclose Jae Ho Byun, MD, Seoul, Korea, Republic Of (*Abstract Co-Author*) Nothing to Disclose

PURPOSE

To explore a diagnostic role of US-guided percutaneous biopsy for suspicious focal hepatic lesions in patients at risk for hepatocellular carcinoma (HCC) and to compare the results with noninvasive diagnostic approaches using the Liver Imaging Reporting and Data System (LI-RADS) classification

METHOD AND MATERIALS

We retrospectively included 169 lesions in 160 patients at risk for HCC who underwent US-guided percutaneous biopsy for newly developed suspicious hepatic malignancy in 2016. Each target lesion on biopsy was evaluated on CT and/or MRI and was assigned to the LI-RADS v2018 categories. We compared the biopsy results with the LI-RADS categories and evaluated the agreement by using percent agreement and Cohen's kappa statistic after recategorization of the LI-RADS into three groups: (a) favoring HCC (including LR-4, 5, and TIV without targetoid mass) (b) favoring non-HCC malignancy (including LR-M and TIV with targetoid mass)

(c) indeterminate (LR-3). In 30 patients subsequently undergoing surgical excision, agreements with surgical pathology were compared between biopsy results and CT/MRI LIRADS categories by using percent agreement.

RESULTS

US-guided biopsy achieved successful diagnostic results in 81.7% (138/169) without difference across the LI-RADS categories (CT, p = 0.35; MRI, p = 0.86). Among these 138 lesions, 73 lesions were evaluated both on CT and MRI, whereas 65 were solely assessed by using either CT or MRI. Biopsy showed fair-to-good agreement with noninvasive categorization by CT and MRI (κ =0.61 for each) with substantial percent disagreement (CT, 24%; MRI, 23%). Three of LR-3 lesions each on CT (20%) and MRI (27%) were diagnosed with malignancy on biopsy; 3 (7%) on CT and 3 (7%) on MRI favoring HCC were benign on biopsy; 4 (11%) on CT and 3 (7%) on MRI favoring HCC were non-HCC malignancy on biopsy. Biopsy showed higher percent agreement (90%) with surgical pathology than the diagnostic categories on CT (75%) and MRI (70%).

CONCLUSION

Despite its substantial non-diagnostic results, US-guided percutaneous biopsy showed superior diagnostic performance for focal hepatic lesions than noninvasive imaging diagnosis using the LI-RADS classification.

CLINICAL RELEVANCE/APPLICATION

If diagnostically adequate samples are obtained, US-guided percutaneous biopsy poses an important role for classifying hepatic nodules which even show the typical HCC hallmarks on imaging in patients at risk for HCC.

SST03-09 Diagnostic Benefit of Oral Contrast Administration (Small Intestine Contrast-Enhanced Ultrasonography [SICUS]) over Conventional Enteric US in Crohn's Disease

Friday, Dec. 6 11:50AM - 12:00PM Room: E352

Participants

Gauraang Bhatnagar, FRCR, MBBS, London, United Kingdom (*Presenter*) Nothing to Disclose Laura Quinn, Birmingham, United Kingdom (*Abstract Co-Author*) Nothing to Disclose Anthony Higginson, Portsmouth, United Kingdom (*Abstract Co-Author*) Nothing to Disclose Arun Gupta, MBChB, Wembly, United Kingdom (*Abstract Co-Author*) Nothing to Disclose Richard A. Beable, MBChB, Portsmouth, United Kingdom (*Abstract Co-Author*) Nothing to Disclose Steve Halligan, MD, Herts, United Kingdom (*Abstract Co-Author*) Nothing to Disclose Steve Halligan, MD, MedSc, London, United Kingdom (*Abstract Co-Author*) Nothing to Disclose Uday B. Patel, MBBS, BSc, Sutton, United Kingdom (*Abstract Co-Author*) Nothing to Disclose Andrew Plumb, MBBCh, MRCP, Stockport, United Kingdom (*Abstract Co-Author*) Nothing to Disclose Sue Mallett, DIPLPHYS,MS, Birmingham, United Kingdom (*Abstract Co-Author*) Nothing to Disclose Stuart A. Taylor, MBBS, Great Missenden, United Kingdom (*Abstract Co-Author*) Research Consultant, Robarts Clinical Trials, Inc; Shareholder, Motilent

For information about this presentation, contact:

g.bhatnagar@nhs.net

PURPOSE

Enteric ultrasound (US) following an oral contrast agent (SICUS) may facilitate better visualisation of the bowel wall compared to unprepared US. The purpose of this study was to compare the diagnostic accuracy of unprepared US and SICUS for detecting small bowel Crohns disease (CD).

METHOD AND MATERIALS

The study utilised patients recruited to a prospective trial comparing the diagnostic accuracy of MRE and US for CD (either newly diagnosed or with relapsing disease) recruited across 8 hospitals. A construct reference standard (multidisciplinary panel diagnosis) was used in the trial, incorporating 6 months of patient follow up. 64 patients underwent standard US followed by SICUS (using 11 of hyperosmolar luminal contrast), performed by the same practitioner, blinded to all clinical data. Practitioners recorded findings on the presence of small bowel/colonic CD after each US examination. Sensitivity and specificity for small bowel disease extent (i.e. presence and correct segmental location) was compared to the trial construct reference standard using bivariate multilevel patient specific random effects models, from paired data using meqrlogit in STATA 14.2.

RESULTS

Sensitivity and specificity for small bowel disease extent was identical between SICUS and unprepared US (71% [58-81] and 86% [49-97] respectively). SICUS specificity for colonic disease was 92%[80-97] and 82%[68-91] for unprepared US, a non-significant difference of 10% (95% CI -2 to 22), p=0.125. Both US and SCIUS detected 9/14 (64%) of segments deemed to be stenosed and causing obstruction by the consensus reference standard. There were numerically fewer false positive diagnoses of obstructing stenosis on SICUS compared to US (7 vs. 11 respectively).

CONCLUSION

We found no evidence that SICUS increases diagnosed accuracy for small bowel disease extent compared to conventional US. Stenosis detection was not improved by SICUS but false positive diagnoses may be reduced.

CLINICAL RELEVANCE/APPLICATION

SICUS offers no significant advantage over standard US for detecting small bowel CD. Given the patient symptom burden induced by ingesting hyperosmolar fluid, first line SICUS cannot be recommended.

Printed on: 10/29/20





SST04

Genitourinary (Urographic Imaging)

Friday, Dec. 6 10:30AM - 12:00PM Room: E350

GU

AMA PRA Category 1 Credits ™: 1.50 ARRT Category A+ Credit: 1.75

FDA Discussions may include off-label uses.

Participants

Dean A. Nakamoto, MD, Beachwood, OH (*Moderator*) Research agreement, Canon Medical Systems Corporation; Research agreement, General Electric Company

John R. Leyendecker, MD, Dallas, TX (*Moderator*) Nothing to Disclose Geoffrey E. Wile, MD, Nashville, TN (*Moderator*) Nothing to Disclose

Sub-Events

SST04-01 Evaluation of Asymptomatic Microscopic Hematuria by Renal Ultrasound to Detect Upper Tract Malignancy: A 20-Year Experience in a Community Hospital

Friday, Dec. 6 10:30AM - 10:40AM Room: E350

Participants

Matthew Smith, MD,PhD, la Crosse, WI (*Presenter*) Nothing to Disclose Keaton Read, la Crosse, WI (*Abstract Co-Author*) Nothing to Disclose Matthew Stegman, MD, la Crosse, WI (*Abstract Co-Author*) Nothing to Disclose Neil J. Kroll, MD, la Crosse, WI (*Abstract Co-Author*) Nothing to Disclose Marvin van Every, MD, La Crosse, WI (*Abstract Co-Author*) Nothing to Disclose

For information about this presentation, contact:

mattsmith4@gmail.com

PURPOSE

Asymptomatic microscopic hematuria (AMH) can be a sign of upper tract (UT) malignancy and requires evaluation. However, the preferred imaging modality of the UT is controversial. Our healthcare system is an integrated medical center with 30 regional clinics serving 21 counties over a tri-state region has routinely used renal ultrasound (RUS) for the initial evaluation of the UT in patients with AMH because of cost and performance. The purpose of this study was to evaluate the sensitivity of RUS for detecting UT malignancy in patients with AMH.

METHOD AND MATERIALS

An IRB approved, retrospective study was performed of all patients who received a renal ultrasound in our health system from January 1, 1997 to July 1, 2015. Patients were excluded if they had <3 years of follow-up, <18 years old, history of prior UT genitourinary cancer, catheter, inpatient status, pregnant status, gross hematuria (GH) or spotting, or if the health record did not contain sufficient detail to rule out GH. The initial RUS was considered positive if findings led to a diagnosis of UT malignancy. Regardless of the RUS results, health records were then reviewed to determine whether any UT cancer was subsequently diagnosed to assess for false negatives.

RESULTS

Of the 4871 patients who underwent a RUS during the study period, 2124 met eligibility criteria. The average follow-up was 11.6 years (range: 3-21.6, stdev: 4.9). Twelve (0.6%) patients were diagnosed with UT malignancy (9 renal cell carcinoma and 3 urothelial carcinomas) during their initial evaluation, all of whom had an initial RUS positive for malignancy for an overall sensitivity of 100% and negative predictive value of 100%. Four patients were diagnosed with UT malignancy >3 years after an initially negative RUS.

CONCLUSION

We have demonstrated that the sensitivity of RUS is adequate for detection of UT malignancy in patients with AMH, a low-risk population. This study represents a general population from a community outpatient setting with reliable long-term follow-up. Patients whose RUS and cystoscopy findings are negative for signs of malignancy can safely be advised to return for further evaluation if they develop GH, flank pain, or irritative voiding symptoms.

CLINICAL RELEVANCE/APPLICATION

Renal ultrasound is highly sensitive for detection of upper tract malignancies and can be used for initial screening in low-risk patients with asymptomatic microhematuria.

SST04-02 The Diagnostic Yield of CT Urography in the Workup of Hematuria with Negative Cystoscopy

Friday, Dec. 6 10:40AM - 10:50AM Room: E350

For information about this presentation, contact:

jessica.common@medportal.ca

PURPOSE

Current American Urological Association (AUA) guidelines recommend risk-stratified cystoscopy in the workup of hematuria. However, due to insufficient evidence for risk-stratified upper urinary tract imaging, the AUA recommends multiphasic computed tomography urography (CTU) for all patients. The aims of this study are to determine the diagnostic yield of CTU in patients evaluated for hematuria with negative cystoscopy, and to identify those at highest risk of urinary tract malignancy, who would benefit most from upper urinary tract imaging.

METHOD AND MATERIALS

A retrospective study was conducted of patients who underwent CTU within 12 months of negative cystoscopy for workup of hematuria at our institution between January 2017-December 2017. Patients were grouped according to etiology of hematuria. Clinical diagnoses were correlated with patient characteristics, including age, sex, smoking history, and type of hematuria, as well as renal ultrasound (US) and CTU results. Diagnostic concordance of renal US and CTU was compared.

RESULTS

258 patients met the inclusion criteria. Of these, only 1 patient was diagnosed with an upper urinary tract malignancy. 6 other malignancies were diagnosed including 3 renal cell carcinomas (RCC), 2 prostate adenocarcinomas, and 1 metastatic gynecologic malignancy. All malignancies were diagnosed in patients over 50 years of age. 60 patients were diagnosed with urolithiasis, and 56 were diagnosed with benign prostatic hyperplasia (BPH). There was no etiology identified in 109 patients, including 21 of 30 patients age 50 years and under. Renal US was performed in 93 patients. Renal US was diagnostic and concordant with CTU in 56 patients. Renal US failed to detect the diagnosis identified on CTU in 18 cases, including 1 RCC, 7 urolithiasis, 7 BPH, and 3 other benign findings. Both renal US and CTU were non-diagnostic in 11 patients in whom the etiology of hematuria was identified on cystoscopy.

CONCLUSION

Renal US with or without computed tomography of the kidneys, ureters, and bladder (CT KUB) should be considered as an alternative to multiphasic CTU in the workup of hematuria in patients with negative cystoscopy.

CLINICAL RELEVANCE/APPLICATION

Risk-stratified upper tract imaging in the workup of hematuria may reduce radiation exposure with no significant effect on detection of upper urinary tract malignancy or other significant findings.

SST04-03 Multi-Vendor Performance for Determination of Renal Stone Composition: Comparison with Six Dual-Energy CT Scanners

Friday, Dec. 6 10:50AM - 11:00AM Room: E350

Participants

Ali Pourvaziri, MD, MPH, Boston, MA (Presenter) Nothing to Disclose

Anushri Parakh, MBBS, MD, Boston, MA (Abstract Co-Author) Nothing to Disclose

Jinjin Cao, MD, Boston, MA (Abstract Co-Author) Nothing to Disclose

Cristy Savage, RT, Boston, MA (Abstract Co-Author) Nothing to Disclose

Adrian A. Negreros-Osuna, MD, Boston, MA (Abstract Co-Author) Nothing to Disclose

Dushyant Sahani, MD, Boston, MA (Abstract Co-Author) Research support, General Electric Company Medical Advisory Board, Allena Pharmaceuticals, Inc

Avinash R. Kambadakone, MD, Boston, MA (*Abstract Co-Author*) Research Grant, General Electric Company; Research Grant, Koninklijke Philips NV

For information about this presentation, contact:

apourvaziri@mgh.harvard.edu

PURPOSE

The aim of this in-vitro study was to compare the performance of six dual-energy CT (DECT) scanners in determination of stone composition

METHOD AND MATERIALS

A total of 71 urinary stones (size: 2 mm - 16 mm) of known chemical composition (51calcium, 4 struvite, 4 cystine and 12 urate) were placed in a custom-made cylindrical phantom. Consecutive scans with manufacturer-recommended protocols were performed on second-generation dsDECT (S1: SOMATOM Definition Flash, Siemens;100/Sn140kVp), third-generation dsDECT (S2: Force,Siemens;100/Sn150kVp), sfDECT (S3: Edge, Siemens;AuSn120kVp), first-generation rsDECT (S4: Discovery750HD, GE; 80/140kVp), second-generation rsDECT (S5: Revolution, GE; 80/140kVp) and dlDECT (S6: IQon, Philips; 120kVp). Data sets were analysed using effective atomic number (Zeff) and dual-energy ratio indices (DEI) of maximally available spectra (40/190keV for dsDECT and sfDECT, 40/140 keV for rsDECT and 40/200keV for dlDECT) and comparable spectra (40 keV/140 keV) all S1-S6 were computed. Agreement of Zeff and DEI among the scanners was assessed with inter-class coefficient test.

RESULTS

Both Zeff and DEI could differentiate between non-urate and urate stones. For all stone compositions, Zeff showed excellent agreement between scanners (ICC:0.90, 95% CI : 0.86- 0.93). DEI showed lower agreement compared to Zeff. Both, DEI computed by maximally separated spectra (40/140-200keV) and similar spectra (40/140keV for all) showed comparable agreement (ICC:0.63, 95 % CI:0.49-0.75 vs. ICC:0.62, 95 % CI:0.47-74).

CONCLUSION

Overall cross-vendor measurements for determination of stone composition were comparable with all DECT techniques. Zeff is a better quantitative measure than DEI for stone characterization.

CLINICAL RELEVANCE/APPLICATION

In a busy practice with multivendor setting it is important to cross validate the performance for stone composition to provide consistent results since patients can be scanned at different scanners.

SST04-04 Automated Radiomic Analysis of Ureteral Stones Using ER Renal Stone CT Images Predicts Likelihood of Spontaneous Passage

Friday, Dec. 6 11:00AM - 11:10AM Room: E350

Participants

Payam Mohammadinejad, MD, Rochester, MN (*Presenter*) Nothing to Disclose David J. Bartlett, MD, Rochester, MN (*Abstract Co-Author*) Nothing to Disclose Ashish R. Khandelwal, MD, Rochester, MN (*Abstract Co-Author*) Nothing to Disclose Andrea Ferrero, PhD, Rochester, MN (*Abstract Co-Author*) Nothing to Disclose Taylor Moen, Rochester, MN (*Abstract Co-Author*) Nothing to Disclose Roy Marcus, MD, Rochester, MN (*Abstract Co-Author*) Nothing to Disclose Kristin Mara, Rochester, MN (*Abstract Co-Author*) Nothing to Disclose Felicity Enders, Rochester, MN (*Abstract Co-Author*) Nothing to Disclose John C. Lieske, MD, Rochester, MN (*Abstract Co-Author*) Nothing to Disclose Cynthia H. McCollough, PhD, Rochester, MN (*Abstract Co-Author*) Research Grant, Siemens AG Joel G. Fletcher, MD, Rochester, MN (*Abstract Co-Author*) Grant, Siemens AG; Consultant, Medtronic plc; Consultant, Takeda Pharmaceutical Company Limited; Grant, Takeda Pharmaceutical Company Limited; ;

For information about this presentation, contact:

fletcher.joel@mayo.edu

PURPOSE

To quantify the ability of automated radiomic analysis of CT images to predict the likelihood of spontaneous passage of symptomatic renal stones, and to compare the results with the performance of manual measurements.

METHOD AND MATERIALS

This IRB-approved, HIPAA-compliant, retrospective study included symptomatic patients undergoing emergency renal stone CT who had one stone in the kidney or ureters; patients with bladder stones were excluded. Spontaneous passage (or not) was documented based on review of clinical records, patient report, follow-up CT scans, or the need for stone extraction during 6 months of follow-up. Radiologists-in-training manually measured axial and coronal stone dimensions. Automated quantitative stone analysis software computed stone length, width, height, maximum dimension, volume, and CT number, as well as morphologic parameters related to stone heterogeneity and roughness. Univariate logistic regression was used to define odds ratios (OR) of spontaneous passage and ROC analysis was used to assess the ability to predict stone passage. Independent variables identified using multivariable logistic regression were used to create models that incorporated parameters such as patient age and sex, stone volume and dimensions, and morphological features.

RESULTS

Of 195 patients, spontaneous passage was documented in 58% (114/195). Univariate analysis demonstrated numerous significant stone parameters (from the CT data) associated with stone passage (p<0.001), including OR (95% CI) of 10.1 (5.11, 19.9) for axial dimension < 4.6 mm and 9.40 (4.84, 18.2) for coronal dimension < 4.9 mm (manual measurements), and 11.14 (5.21, 23.8) for volume < 81 mm3 and 10.58 (5.37, 20.8) for mean curvature < -0.14 (automated measurements). Area under the ROC curve was 0.83 for manual measurements and increased to 0.88 when patient and morphological stone features were included.

CONCLUSION

Automated radiomic analysis quickly and reproducibly predicted stone passage better than manual radiologist measurements. Prospective clinical validation of the developed model is needed.

CLINICAL RELEVANCE/APPLICATION

Automated radiomic analysis of CT data can quickly provide reproducible objective data for guiding management of patients with acute ureterolithiasis.

SST04-05 Dose Independent Characterization of Renal Stones by Means of Spectral Detector Computed Tomography and Machine Learning

Friday, Dec. 6 11:10AM - 11:20AM Room: E350

Participants

Nils Grosse Hokamp, MD, Koln, Germany (*Presenter*) Speakers Bureau, Koninklijke Philips NV Simon Lennartz, MD, Cologne, Germany (*Abstract Co-Author*) Institutional Research Grant, Koninklijke Philips NV Johannes Salem, Cologne, Germany (*Abstract Co-Author*) Nothing to Disclose David C. Maintz, MD, Koln, Germany (*Abstract Co-Author*) Nothing to Disclose Stefan Haneder, MD, Cologne, Germany (*Abstract Co-Author*) Nothing to Disclose

For information about this presentation, contact:

nils.grosse-hokamp@uk-koeln.de

PURPOSE

To predict the main component of both, pure and compound kidney stones using dual energy computed tomography and machine

learning.

METHOD AND MATERIALS

200 kidney stones with a known composition as determined by infrared spectroscopy were examined using a non-anthropomorphic phantom on a spectral detector computed tomography scanner. Stones were of either pure (monocrystalline, n=116) or compound (dicrystalline, n=84) composition. Image acquisition was repeated twice using both, normal and low-dose protocols, respectively (ND/LD). Conventional images and low and high keV virtual monoenergetic images were reconstructed. Stones were semi-automatically segmented. Further analysis was conducted on a per-voxel basis. using a shallow neural network (SNN). ND data was imported in the SNN and split in training (70%), testing (15%) and validation-datasets (15%). LD data then was analyzed by the same network. Accuracy on a per-voxel and a per-stone basis was calculated.

RESULTS

Main components were: Whewellite (n=80), weddellite (n=21), Ca-phosphate (n=39), cysteine (n=20), struvite (n=13), uric acid (n=18) and xanthine stones (n=9). Stone size ranged from 3 - 18 mm. Overall diagnostic accuracy attained with test/training dataset for determining stone composition was 91.1%. On independently tested LD-acquisitions accuracy was 87.1-90.4%.

CONCLUSION

Even in compound stones, the main component can be reliably determined using dual energy CT and machine learning, irrespective of dose protocol.

CLINICAL RELEVANCE/APPLICATION

After transfer to patients, spectral detector CT and machine learning may enable a detailed analysis of renal stone composition and therefore a targeted therapy of different types.

SST04-06 Estimating Differential Renal Function in Patients with Upper Urinary Tract Stones Using Non-Enhanced Computed Tomography

Friday, Dec. 6 11:20AM - 11:30AM Room: E350

Participants

Jiali Li, Wuhan, China (*Presenter*) Nothing to Disclose Daoyu Hu, Wuhan, China (*Abstract Co-Author*) Nothing to Disclose Zhen Li, MD, PhD, Wuhan, China (*Abstract Co-Author*) Nothing to Disclose

PURPOSE

For chronic urinary tract stones patients, differential renal function (DRF) is a key indicator for assisting urologists in selecting treatment options (lithotripsy versus nephrectomy). The wide popularity and short acquisition time of unenhanced computed tomography (CT) make it a first-line examination method for imaging patients with ureteral stonesTherefore, this study aimed to determine whether Unenhanced CTimaging can estimate DRF in patients with chronic unilateral obstructive upper urinary tract stones.

METHOD AND MATERIALS

This was a retrospective study of 76 patients, and all patients underwent nonenhanced CT and nuclear renography (RG) at an interval of 4 to 6 weeks due to chronic unilateral obstructive urinary stones. Renal CT measurements (RCMs), consisting of residual parenchymal volume (RPV) and volumetric CT texture analysis parameters, were obtained using a semiautomated method. The percent RCM were calculated using the general format '100*(Left RCM/[Left RCM+Right RCM])'. Then percent RCMs were evaluated for theircorrelation power to DRFderived from RG.

RESULTS

The strongest Pearson coefficient between percent RCM and DRF was reflected by RPV (r=0.957, P<0.001). Combinations of RPV and other parameters did not significantly improve the correlation compared with RPV alone (Pearson's r=0.957 versus r=0.957, 0.957, 0.887, 0.815, and 0.956, for combinations of Hounsfield unit, parenchymal voxel, skewness, kurtosis, and entropy, respectively; all P<0.001). Percent RPV was subsequently introduced into linear regression, and the equation y = -2.66+1.07*x (P < 0.001) was derived to calculate predicted DRF. No statistically difference was found between predicted DRF using the equation and observed DRF according to RG (P=0.959).

CONCLUSION

Unenhanced CT imaging can estimate DRF and may reduce unnecessary use of RG for most patients with chronic unilateral obstructive upper urinary tract stones.

CLINICAL RELEVANCE/APPLICATION

Unenhanced CT can be used as a convenient tool to predict DRF and RPV should be considered as part of routine CT reporting in patients with chronic unilateral obstructive upper urinary tract stones.

SST04-07 Computed Tomography Findings of Upper-Urinary-Tract Lesions in Immunoglobulin G4-Related Disease: Comparison with Urothelial Carcinoma

Friday, Dec. 6 11:30AM - 11:40AM Room: E350

Participants

Minobu Kamo, MD, PhD, Hamburg, Germany (*Presenter*) Nothing to Disclose Taiki Nozaki, MD, Tokyo, Japan (*Abstract Co-Author*) Nothing to Disclose Natsuka Muraishi, MD, Tokyo, Japan (*Abstract Co-Author*) Nothing to Disclose Jin Yamamura, MD, Hamburg, Germany (*Abstract Co-Author*) Nothing to Disclose

PURPOSE

Immunoglobulin G4-related disease (IgG4-RD) can sometimes involve the upper urinary tract and mimic urothelial carcinoma

clinically. There have been indeed quite a few reports mentioning that unnecessary radical nephroureterectomy was performed to those patients. The purpose of this study was to investigate computed tomography (CT) findings of IgG4-RD lesions involving the upper urinary tract and to compare them with those of urothelial carcinomas.

METHOD AND MATERIALS

Pretreatment CT images of 13 consecutive patients of IgG4-RD with urinary tract lesions and 80 consecutive patients with urothelial carcinoma were retrospectively evaluated by two board-certified radiologists. Clinical information of each group was obtained by chart review.

RESULTS

Upper-urinary-tract findings between two groups is summarized in the table. Bilaterality (P < 0.0001), symmetry (P < 0.0001), extramural growth pattern (P < 0.0001), longer lesions(P = 0.04) and gradual dynamic enhancement pattern (P < 0.001) were statistically more frequent in IgG4-RD patients compared to urothelial carcinoma patients. Concerning extra-urinary-tract findings, following findings were significantly common among IgG4-RD patients; paraaortic fat stranding (P = 0.03), presacral fat stranding (P < 0.001), and fat stranding of pelvic walls (P < 0.001). Aortic lesions were significantly more frequent in IgG4-RD patients (P < 0.001), on the other hand kidney lesions was seen in only one patient of IgG4-RD and patients with urothelial carcinoma tended to present with direct tumoral invasion to renal parenchyma, although there was no significant difference. There was no significant difference on frequency of hydronephrosis and coexisting pancreatic lesions between each group.

CONCLUSION

Compared to urothelial carcinoma, bilateral, symmetric, and longer involvement, extramural growth pattern, ill-defined margin, gradual enhancement pattern in dynamic CT are suggestive findings of IgG4-RD urinary tract lesions. IgG4-RD can also manifest as ipsilateral asymmetric lesion, which could overlap with those of urothelial carcinoma. Extra-urinary-tract findings such as fat stranding in paraaorta, presacral or pelvic wall area are also useful findings in differentiating IgG4-RD lesions from urothelial carcinoma.

CLINICAL RELEVANCE/APPLICATION

CT is useful in differentiating urinary tract lesions of IgG4-RD from urothelial carcinoma and can prevent unnecessary ureteronephrectomy.

SST04-08 The Feasibility of Compressed Sensing With and Without Breath-Holding on Magnetic Resonance Urography: A Comparison with Conventional 3D Magnetic Resonance Urography Looking at Acquisition Time, Image Quality, and Diagnostic Performance

Friday, Dec. 6 11:40AM - 11:50AM Room: E350

Participants

Xiaoge Liu, Zhengzhou, China (*Presenter*) Nothing to Disclose Jinxia Zhu, Beijing, China (*Abstract Co-Author*) Nothing to Disclose Bernd Kuehn, PhD, Erlangen, Germany (*Abstract Co-Author*) Employee, Siemens AG Elisabeth Weiland, Erlangen, Germany (*Abstract Co-Author*) Nothing to Disclose Xiangtian Zhao, MD, Shanghai, China (*Abstract Co-Author*) Nothing to Disclose Yanan Ren, Zhengzhou , China (*Abstract Co-Author*) Nothing to Disclose Man Xu, Zhengzhou, China (*Abstract Co-Author*) Nothing to Disclose Jingliang Cheng, MD,PhD, Zhengzhou, China (*Abstract Co-Author*) Nothing to Disclose

For information about this presentation, contact:

wumingjubo@hotmail.com

PURPOSE

To investigate the feasibility of prototypical 3D magnetic resonance urography (MRU) with a compressed sensing (CS) technique for patients with or without breath-holding (BH) capabilities.

METHOD AND MATERIALS

MRU was performed in 66 patients on a 3T system, including BH with CS, navigator-triggered (NT) CS, and conventional NT (cNT) protocols. The patients were divided into two groups, Group1 (the BH group, n = 56) and Group II (the compromised BH group, n = 10), according to the image quality of a BH-T1-weighted protocol. The quality of urinary tract sharpness and background suppression were scored with a scale of 1 to 5 (poor to good). Urinary tract lesions were detected on reconstructed maximum intensity projections, multiplanar reconstructions, and source images, and graded with the same scale. Comparative analyses of acquisition time and image quality were performed. Receiver operating characteristic (ROC) curve analysis was performed, and sensitivity, specificity, and the area under the ROC curve (AUC) were calculated to determine diagnostic performances.

RESULTS

BH-CS MRU showed reductions of 88.1% and 96.7% in acquisition times compared with NT-CS MRU and cNT MRU in Group1. The acquisition time was reduced by 71.2% for NT-CS MRU compared with cNT MRU in Group II. BH-CS MRU had the best urinary tract sharpness in Group 1, and NT-CS MRU had the least background signal in both groups (both P < 0.05). BH-CS MRU presented superior urinary tract sharpness and background suppression in Group1 than Group II (both P < 0.05). Group II had better urinary tract sharpness with NT-CS MRU and less background suppression with cNT MRU than Group1 (both P < 0.05). Diagnostic efficiencies of all protocols were comparable in Group1 (all P > 0.05), while the diagnostic efficiency of BH-CS MRU was significantly lower than the other two protocols in Group II (both P < 0.05).

CONCLUSION

BH-CS MRU showed great potential for urinary tract imaging with the shortest acquisition times and excellent image qualities in patients that can hold their breath. For patients that cannot hold their breath, NT-CS MRU would be helpful.

CLINICAL RELEVANCE/APPLICATION

Compressed sensing magnetic resonance urography (MRU) can shorten MR acquisition time with better image quality compared with

conventional MRU.

SST04-09 Validation of Vesical-Imaging Reporting and Data System (VI-RADS): A Single-Centre Retrospective Evaluation of Interobserver Agreement and Diagnostic Accuracy of Multiparametric MRI (mpMRI) in the Setting of Bladder Cancer

Friday, Dec. 6 11:50AM - 12:00PM Room: E350

Participants

Martina Pecoraro, MD, Roma , Italy (*Abstract Co-Author*) Nothing to Disclose Riccardo Campa, MD, Roma , Italy (*Presenter*) Nothing to Disclose Stefano Cipollari, Rome, Italy (*Abstract Co-Author*) Nothing to Disclose Giovanni Barchetti, MD, Roma, Italy (*Abstract Co-Author*) Nothing to Disclose Carlo Catalano, MD, Rome, Italy (*Abstract Co-Author*) Nothing to Disclose Valeria Panebianco, MD, Rome, Italy (*Abstract Co-Author*) Nothing to Disclose

For information about this presentation, contact:

pecoraro.martina1@gmail.com

PURPOSE

Vesical Imaging-Reporting and Data System (VI-RADS) has been developed to standardize multiparametric MRI (mpMRI) approach to bladder cancer (BC). The aim of this study was to evaluate interobserver agreement and diagnostic accuracy of mpMRI with the use of VI-RADS to discriminate between non-muscle invasive bladder cancer (NMIBC) and muscle-invasive bladder cancer (MIBC).

METHOD AND MATERIALS

Between September 2017 and March 2019, 138 patients referred for suspected bladder cancer underwentmultiparametric MRI of the bladder (mpMRI) prior to transurethral resection of bladder tumor (TURBT). All mpMRI were reviewed by two radiologists, who scored each lesion according to VI-RADS. Sensitivity, specificity, positive predictive value (PPV), and negative predictive value (NPV) were calculated for each VI-RADS cutoff. Receiver operating characteristics curves were used to evaluate the performance of mpMRI. The k statistics was used to estimate inter-readeragreement.

RESULTS

One hundred twenty-six patients were included in the final analysis, 88 with NMIBC and 38 with MIBC. Sensitivity and specificity were 93% and 91% for reader 1 and 86% and 85% for reader 2 respectively when the cutoff VI-RADS > 2 was used to define MIBC. At the same cutoff, PPV and NPV were 81% and 97% for reader 1 and 75% and 94% for reader 2. When the cutoff VI-RADS > 3 was used, sensitivity and specificity were 84% and 95% for reader 1 and 79% and 91% for reader 2. Corresponding PPV and NPV were 85% and 92% for reader 1 and 79% for reader 2. Area under curve was 0.918 and 0.886 for reader 1 and 2 respectively. Inter-reader agreement was good for the overall score (k =0.748).

CONCLUSION

VI-RADS is accurate in differentiating MIBC from NMIBC. The optimal cutoff is VI-RADS >2 to maximize sensitivity and NPV. Interreader agreement is overall good.

CLINICAL RELEVANCE/APPLICATION

Magnetic resonance imaging (MRI) scans for bladder cancer with the use of a standardized and validated score as the VI-RADS may help improve patient care.

Printed on: 10/29/20





SST05

Musculoskeletal (Spine)

Friday, Dec. 6 10:30AM - 12:00PM Room: E450B



AMA PRA Category 1 Credits ™: 1.50 ARRT Category A+ Credit: 1.75

FDA Discussions may include off-label uses.

Participants

Shlomit Goldberg-Stein, MD, Bronx, NY (Moderator) Nothing to Disclose

Jan Fritz, MD, Baltimore, MD (*Moderator*) Institutional research support, Siemens AG; Institutional research support, Johnson & Johnson; Institutional research support, Zimmer Biomet Holdings, Inc; Institutional research support, Microsoft Corporation; Institutional research support, BTG International Ltd; Scientific Advisor, Siemens AG; Scientific Advisor, General Electric Company; Scientific Advisor, BTG International Ltd; Speaker, Siemens AG; Patent agreement, Siemens AG

Sub-Events

SST05-02 Dose Optimization in Spinal Computed Tomography for Planning of Scoliosis Surgery

Friday, Dec. 6 10:40AM - 10:50AM Room: E450B

Participants

Yan Klosterkemper, Dusseldorf, Germany (*Presenter*) Nothing to Disclose Markus Konieczny, Dusseldorf, Germany (*Abstract Co-Author*) Nothing to Disclose Tobias Hesper, MD, Dusseldorf, Germany (*Abstract Co-Author*) Nothing to Disclose Joel Aissa, MD, Duesseldorf, Germany (*Abstract Co-Author*) Nothing to Disclose Christoph K. Thomas, MD, Dusseldorf, Germany (*Abstract Co-Author*) Nothing to Disclose Gerald Antoch, MD, Dusseldorf, Germany (*Abstract Co-Author*) Nothing to Disclose Johannes Boos, MD, Dusseldorf, Germany (*Abstract Co-Author*) Nothing to Disclose

For information about this presentation, contact:

yan.klosterkemper@med.uni-duesseldorf.de

PURPOSE

To assess the potential for dose optimization in patients undergoing spinal CT for planning of scoliosis surgery.

METHOD AND MATERIALS

Ten patients (3 male, 7 female, 18±11 years) were included in this prospective, IRB-approved study. CT examinations were performed with automated exposure control (mean CTDIvol 4.1 ± 0.9 mGy; DLP: 192 \pm 50mGyxcm). Dose reduction to 50%, 20 %, 10% and 5% was simulated using dedicated reconstruction software. Two spinal surgeons blinded to the dose level independently and randomly measured the length and the width of each pedicle for screw size selection. Additionally, the confidence in the measurements was assessed (5=very confident in the measurement, 1=measurement cannot be performed with any confidence). Two radiologists rated the image quality for the assessment of bone and soft tissue structures (5=excellent, 1=non-diagnostic). Bonferroni was used to correct for multiple testing (p<0.0125).

RESULTS

Pedicle length and width measurements were comparable between 100% and 50% reconstructions (36.4mm/4.1mm vs 36.6mm/4.1mm) whereas both measurements decreased with further dose reduction (20%: 36.1mm/4.1mm; 10%: 35.5mm/4.0mm; 5%: 34.6mm/3.9mm). Confidence in the measurements was excellent at 100% and 50% (all ratings of 5) and decreased with further dose reduction (20%: 4.7; 10%: 3.7; 5%: 2.5). Image quality decreased with decreasing dose (4.9 \pm 0.4 for 100 % to 1 \pm 0 for the 5% reconstructions; p<0.001, respectively). For bone assessment, image quality was comparable between 100% and 50% reconstructions (4.9 \pm 0.4 vs 4.7 \pm 0.5;).

CONCLUSION

Dose of preoperative spinal CT for planning of scoliosis surgery can be reduced to 50% without impairment of pedicle size measurements or surgeons' confidence in planning the operation.

CLINICAL RELEVANCE/APPLICATION

CT dose in preoperative spine CT can be reduced to 50% for patients undergoing scoliosis surgery.

SST05-03 Making Spine MR Reports More Clinically Appropriate: A Questionnaire-Based Survey of Sub-Specialty Spine Surgeons

Friday, Dec. 6 10:50AM - 11:00AM Room: E450B

Participants

Vidur Mahajan, MBBS, New Delhi, India (*Abstract Co-Author*) Researcher, CARING; Associate Director, Mahajan Imaging; Research collaboration, General Electric Company; Research collaboration, Koninklijke Philips NV; Research collaboration, Qure.ai; Research

collaboration, Predible Health; Research collaboration, Oxipit.ai; Research collaboration, Synapsica; Research collaboration, Quibim Sriram Rajan, MD, New Delhi, India (*Presenter*) Nothing to Disclose

Vasanthakumar Venugopal, MD, New Delhi, India (*Abstract Co-Author*) Consultant, CARING; Research collaboration, General Electric Company ; Research collaboration, Koninklijke Philips NV; Research collaboration, Qure.ai; Research collaboration, Predible Health; Research collaboration, Oxipit.ai; Research collaboration, Synapsica; Research collaboration, Quibim Harsh Mahajan, MD, MBBS, New Delhi, India (*Abstract Co-Author*) Director, Mahajan Imaging Pvt Ltd; Research collaboration, General Electric Company; Research collaboration, Koninklijke Philips NV; Research collaboration, Quibim

For information about this presentation, contact:

vidur@mahajanimaging.com

PURPOSE

Health

MR reports have been unchanged for a long time, and clinical relevance of MR findings are being challenged in literature. We assess the weightage that spine surgeons give to certain aspects of the MR report, their preference for report structure and towards different modalities.

METHOD AND MATERIALS

An anonymous online survey, created in consultation with 5 spine surgeons, which included questions related measurement of spinal canal dimensions, information about nerve root impingement, anomalies and take-off, annular fissures, Modic changes, scoliosis and listhesis, was circulated amongst sub-specialist spine surgeons. Preference for report format (every level reported, significant levels reported, pain chart diagram), and modality of investigation before surgery for lumbar degenerative disc disease was also recorded.

RESULTS

24 sub-specialist spine surgeons, with average 13.9 years' experience (range: 3 - 30 years) from 6 cities, completed the questionnaire. Responses were weighted towards surgically relevant details such as effective spinal canal measurement (79%), nerve root impingement (91%), obvious anomalies at the level of significant disc (61%), level of nerve root take-off (75%), only details of posterior annular fissures (50%), and 25% surgeons preferred "hyperintense zone terminology". Surprisingly, equal number of responses for Modic changes (62%), and for the possibility of inflammatory spondyloarthropathy (58%) or infection (67%) we obtained. On reporting formats, majority asked for only involved levels (71%) while 33% asked for every level. 33% asked for a diagrammatic pain chart. There was no consensus on reporting of scoliosis cases. Also, majority asked for information about cause of listhesis. As expected, for presurgical assessment for degenerative disc disease, MR (87%) with and X ray spine with flexion and extension (75%) was preferred while only 8.3% asked for plain CT and none asked for CT myelography.

CONCLUSION

These results highlight clinically relevant information that should be included on an MR report, including effective spinal canal dimensions, details of nerve root anomalies at the level of disc herniation, details of nerve root impingement. There was lack of consensus on Modic changes, format of report, and scoliosis assessment.

CLINICAL RELEVANCE/APPLICATION

Two-way communication between spine surgeons, and radiologists helps in generation of effective reports, that improve clinical outcomes.

SST05-04 Deep Learning-Based Reconstruction of Osseous Structures of the Cervical Spine Using Bone MRI: A Qualitative Analysis

Friday, Dec. 6 11:00AM - 11:10AM Room: E450B

Participants

Brigitta van der Kolk, MD, Zwolle , Netherlands (*Presenter*) Research Grant, MRIguidance D.J. (Jorik) Slotman, BSC, Zwolle, Netherlands (*Abstract Co-Author*) Nothing to Disclose Tess J. Snoeijink, BSC, Zwolle, Netherlands (*Abstract Co-Author*) Nothing to Disclose Jochen van Osch, Zwolle, Netherlands (*Abstract Co-Author*) Nothing to Disclose Ingrid M. Nijholt, Zwolle, Netherlands (*Abstract Co-Author*) Nothing to Disclose Martin Podlogar, MD,PhD, Zwolle, Netherlands (*Abstract Co-Author*) Nothing to Disclose Boudewijn A.A.M. van Hasselt, MD, Zwolle , Netherlands (*Abstract Co-Author*) Nothing to Disclose Henk J. Boelhouwers, MD, Zwolle, Netherlands (*Abstract Co-Author*) Nothing to Disclose Marijn van Stralen, MSc, PhD, Utrecht , Netherlands (*Abstract Co-Author*) Nothing to Disclose BV; CTO, MRIguidance BV Peter R. Seevinck, MSc,PhD, Utrecht, Netherlands (*Abstract Co-Author*) Nothing to Disclose Marijn F. Boomsma, MD, Zwolle, Netherlands (*Abstract Co-Author*) Nothing to Disclose

For information about this presentation, contact:

b.y.m.van.der.kolk@isala.nl

PURPOSE

To qualitatively assess deep learning-based synthetic CT (BoneMRI) derived from MRI scans of the cervical spine.

METHOD AND MATERIALS

Paired MRI and CT data were collected from 25 consecutive outpatients of 50 years or older presenting with cervical radiculopathy. Patients with osteosynthesis material in the cervical spine or known pathological bone disorders were excluded. The MRI exam (Ingenia 1.5T, Philips Healthcare, the Netherlands) included a T1 multiple gradient echo sequence for BoneMRI reconstruction (3 minutes, 53 seconds). The deep learning-based method (BoneMRI, MRIguidance, the Netherlands) was previously developed based on data from 25 patients from a similar cohort. In this study we qualitatively assessed BoneMRI on an independent cohort. BoneMRI images and conventional CT images were independently evaluated by a neurosurgeon, neuroradiologist and musculoskeletal radiologist. A four-point Likert scale (1=poor, 4=excellent) was used to assess image quality of various structures at two cervical levels (C3-C4 and C6-C7: cortical delineation, intervertebral joints, neural foramina, trabecular bone). Cut-off value for the qualitative assessment in BoneMRI imges was a score of 3 or higher in 80% of the assessed components.

RESULTS

A score of 3 or higher for BoneMRI was achieved for cortical delineation (C3-C4 100%, C6-C7 93.3%), intervertebral joints (both levels 100%) and neural foramina (both levels 100%). The cut-off value of 3 or higher was not met for visualization of the trabecular bone (C3-C4 65.3%, C6-C7 48%).

CONCLUSION

BoneMRI of the cervical spine is a promising tool for 3D morphological assessment of osseous structures without the need for ionizing radiation. Implementation of BoneMRI could facilitate an easier workflow, provide additional information for clinicians, reduce costs and lower patient burden by obviating the CT; and therefore contribute to value-based healthcare. Future work will prospectively investigate BoneMRI in an unrestricted population to further explore the performance of the method.

CLINICAL RELEVANCE/APPLICATION

BoneMRI of the cervical spine offers osseous visualization without the use of ionizing radiation and provides structural information regarding both soft and osseous tissues in a single examination.

SST05-05 Dixon Imaging of the Spine - Comparison of T1 VIBE and T2 TSE Derived Relative Fat Fraction

Friday, Dec. 6 11:10AM - 11:20AM Room: E450B

Participants

Ricardo Donners, MD, Basel, Switzerland (*Presenter*) Nothing to Disclose Anna Hirschmann, MD, Basel, Switzerland (*Abstract Co-Author*) Nothing to Disclose Dorothee Harder, Basel, Switzerland (*Abstract Co-Author*) Nothing to Disclose

For information about this presentation, contact:

ricardo.donners@usb.ch

PURPOSE

A comparison between the quantitative relative fat fraction (rFF) derived from T1 VIBE Dixon and T2 TSE two-point Dixon MRI of vertebral metastases and healthy vertebrae.

METHOD AND MATERIALS

MRI of the spine including T1 VIBE (10° flip angle) and T2 TSE (120° flip angle) two-point Dixon sequences with dedicated in- on opposed echo timing of 25 patients with vertebral metastases of known primary tumor and 25 healthy individuals without conspicuous vertebral lesions were retrospectively reviewed. MRIs were performed on the same 1.5T scanner. Patients with history of malignancy were excluded from the healthy cohort. rFF was calculated by dividing the fat-only through the water- plus fat-only images. Volumes of interest (VOIs) of one vertebral metastasis of each patient of the tumor group and one vertebra of each patient in the healthy cohort were generated. The VOI was created on the T1 VIBE Dixon rFF image and copied onto the T2 TSE rFF image. Mean rFF value and VOI volume were noted. Additionally a region of interest (ROIs) was drawn in the VOI and the subcutaneous gluteal fat and copied onto the T2 TSE rFF image. Mean rFF values were noted. Intraclass correlation coefficients testing for absolute agreement and t-tests were performed comparing rFF mean values in the healthy and malignant cohort. A p-value <0.05 was deemed statistically significant.

RESULTS

For malignant vertebrae VOI measurement based mean T1 VIBE rFF was 11%, mean T2 TSE rFF was 9% (p < 0.001). In healthy patients mean vertebral T1 VIBE rFF was 67% and T2 TSE rFF was 73% (p < 0.001). There was no significant difference in mean VOI size between the malignant and healthy cohort (p = 0.53). Mean T1 VIBE and T2 TSE rFF were significantly smaller in the malignant cohort (each p < 0.001). Mean T1 VIBE rFF of the subcutaneous fat was 93% and T2 TSE rFF was 91.5% (p = 0.02). There was moderate correlation between T1 VIBE and T2 TSE VOI, T1 VIBE VOI and ROI and T2 TSE VOI and ROI rFF measurements (each intraclass correlation coefficient > 0.67). Less correlation was found between subcutaneous T1 VIBE rFF and T2 TSE rFF (pearson correlation coefficient = 0.55).

CONCLUSION

There was significant difference between the T1 VIBE Dixon rFF and T2 TSE Dixon rFF in vertebral metastases as well as healthy vertebrae. While each technique allows approximatization of fat content absolute values are not comparable.

CLINICAL RELEVANCE/APPLICATION

While T1 VIBE and T2 TSE Dixon rFF each allow approximatization of the fat content and aid characterization of vertebral lesions, absolute rFF values cannot be compared between both sequences.

SST05-07 Machine Learning Classification of Spinal Lesions: Compared Accuracy of Texture Parameters Extracted with Different Software

Friday, Dec. 6 11:30AM - 11:40AM Room: E450B

Participants

Vito Chianca, MD, Milano, Italy (*Presenter*) Nothing to Disclose Domenico Albano, Palermo, Italy (*Abstract Co-Author*) Nothing to Disclose Renato Cuocolo, MD, Naples, Italy (*Abstract Co-Author*) Nothing to Disclose Carmelo Messina, MD, Milano, Italy (*Abstract Co-Author*) Nothing to Disclose Salvatore Gitto, MD, Milano, Italy (*Abstract Co-Author*) Nothing to Disclose Angelo Corazza, MD, Genova, Italy (*Abstract Co-Author*) Nothing to Disclose Luca Maria Sconfienza, MD, PhD, Milano, Italy (*Abstract Co-Author*) Travel support, Bracco Group; Travel support, Esaote SpA; Travel support, ABIOGEN PHARMA SpA; Speakers Bureau, Fidia Pharma Group SpA

For information about this presentation, contact:

vitochianca@gmail.com

PURPOSE

To compare the accuracy of machine learning (ML) algorithms for classification of spinal lesions based on texture analysis (TA) parameters extracted by different software from unenhanced Magnetic Resonance images (MRI).

METHOD AND MATERIALS

We retrospectively enrolled 146 patients with 146 spinal lesions (49 benign, 57 metastatic and 40 primary malignant lesions) imaged using MRI. Of them, 117 were histopathologically confirmed after surgery while 29 benign lesions were confirmed by follow-up. Patients were randomly divided in training (n=100) and test groups (n=46), respectively for classification model development and testing. Lesions were manually segmented on T1-weighted and T2-weighted images by drawing a bi-dimensional polygonal region of interest. These were used for first order and texture feature extraction on two software, 3D-Slicer heterogeneity CAD module (hCAD) and Pyradiomics. For each of them, different data subsets, obtained by four feature selection methods were analyzed by 9 ML classification algorithms to evaluate their accuracy in identifying benign vs. malignant lesions and benign vs. primary malignant vs. metastatic lesions.

RESULTS

In the test group, a random forest algorithm correctly classified 89% of lesions as benign or malignant, based on hCAD TA, while a Support Vector Machine could achieve an accuracy of 87% from Pyradiomics TA. For the classification of benign, primary malignant and metastatic lesions, RF models accurately classified 70% of lesions for both TA software.

CONCLUSION

ML algorithms show good accuracy in spinal lesion classification based on non-contrast MRI exams. Furthermore, feature extraction performed using different software has shown consistent results at subsequent ML analysis.

CLINICAL RELEVANCE/APPLICATION

This is the first study that compares the accuracy of different softwares for texture analysis in msk field.

SST05-08 Automatic Spine Segmentation for Detection of Abnormal Vertebra and Differentiation of Benign and Malignant Fracture on CT Using Deep Learning

Friday, Dec. 6 11:40AM - 11:50AM Room: E450B

Participants

Ning Lang, MD, Beijing, China (*Presenter*) Nothing to Disclose Yang Zhang, Irvine, CA (*Abstract Co-Author*) Nothing to Disclose Xiaoying Xing, MD, Beijing, China (*Abstract Co-Author*) Nothing to Disclose Yongye Chen, Beijing, China (*Abstract Co-Author*) Nothing to Disclose Qizheng Wang, Beijing, China (*Abstract Co-Author*) Nothing to Disclose Peter Chang, MD, San Francisco, CA (*Abstract Co-Author*) Nothing to Disclose Daniel S. Chow, MD, Orange, CA (*Abstract Co-Author*) Nothing to Disclose Huishu Yuan, Beijing, China (*Abstract Co-Author*) Nothing to Disclose Min-Ying Su, PhD, Irvine, CA (*Abstract Co-Author*) Nothing to Disclose

PURPOSE

To evaluate the performance in detection of abnormal vertebra and differentiation of benign and malignant vertebral fracture on CT using deep learning.

METHOD AND MATERIALS

A dataset of 296 patients with malignant and 137 patients with benign fracture was generated from our spinal CT database. The CT was acquired using a GE Discovery CT 750HD scanner with 120 kV, 137~543 mAs, and 3 mm thickness. The acquired images were reformatted to Sagittal view for further analysis. An experienced radiologist performed reading by evaluating eight features. A subset of 69 benign and 76 malignant patients with a clearly distinguishable abnormality involving only one spinal segment were selected for deep learning analysis. An ROI was placed, and the smallest square bounding box containing the entire affected vertebra was used as input in ResNet50. The diagnostic performance was tested using 10-fold cross-validation. After obtaining the malignancy probability for all slices of one patient, the highest probability was assigned to that patient, and the prediction of benign or malignancy was done by using the threshold of 0.5. In order to develop an automatic detection scheme, the spine was segmented first, and then ResNet50 was applied to detect the abnormal vertebra. The labeled vertebral fractures and randomly selected normal vertebral bodies were used for training.

RESULTS

The entire dataset of 433 patients were randomly presented to a radiologist for reading, and the accuracy was very high at 99%. The soft tissue mass and bone destruction were highly suggesting malignancy; the presence of transverse fracture line and trauma history were highly suggesting benign. In per-slice diagnosis using ResNet50, sensitivity=0.90, specificity=0.79, and accuracy=0.85. In per-patient diagnosis, sensitivity=0.95, specificity=0.80, and accuracy=0.88. In differentiation of normal vs. abnormal segments, the accuracy was much worse.

CONCLUSION

When the abnormal area was identified as inputs, differentiation of benign and malignant fracture on CT using deep learning achieved a high diagnostic accuracy. When the entire spine was evaluated, the automatic detection of abnormality was challenging.

CLINICAL RELEVANCE/APPLICATION

Deep learning using ResNet yields a high accuracy to distinguish benign from malignant fracture on CT, but more research is needed to develop automatic detection methods to identify abnormal segments.

SST05-09 Clinical-Radiomics Nomograms for Preoperative Prediction of Tumor Type of Sacrum Based on Computed Tomography and Multiparametric Magnetic Resonance Imaging

Friday, Dec. 6 11:50AM - 12:00PM Room: E450B

Participants Ping Yin, Beijing, China (*Presenter*) Nothing to Disclose Nan Hong, MD, Beijing, China (*Abstract Co-Author*) Nothing to Disclose

For information about this presentation, contact:

yinping915@pku.edu.cn

PURPOSE

To develop and validate clinical-radiomics nomograms based on 3D computed tomography (CT) and multiparametric magnetic resonance imaging (mpMRI) for preoperative differentiation of sacral chordoma (SC) and sacral giant cell tumor (SGCT).

METHOD AND MATERIALS

A total of 83 SC and 54 SGCT patients diagnosed through surgical pathology were retrospectively analyzed and divided into a training set and validating set by the ratio of 7:3. We built six models based on CT, CT enhancement (CTE), T1-weighted, T2-weighted, diffusion weighted imaging (DWI), and contrast-enhanced T1-weighted features, two radiomics nomograms and two clinical-radiomics nomograms combined radiomics mixed features with clinical data. The area under the receiver operating characteristic curve (AUC) and accuracy (ACC) analysis were used to assess the performance of the models.

RESULTS

SC and SGCT presented significant differences in terms of age, sex, and tumor location (tage = 9.00, X2sex = 10.86, X2location = 26.20; P < 0.01). For individual scan, the radiomics model based on DWI features yielded the highest AUC of 0.889 and ACC of 0.885, followed by CT (AUC=0.857; ACC=0.846) and CTE (AUC=0.833; ACC=0.769). For the combined features, the radiomics model based on mixed CT features exhibited a better AUC of 0.942 and ACC of 0.880, whereas mixed MRI features achieved a lower performance than the individual scan. The clinical-radiomics nomogram based on combined CT features achieved the highest AUC of 0.948 and ACC of 0.920.

CONCLUSION

The radiomics model based on CT and mpMRI present a certain predictive value in distinguishing SC and SGCT, which can be used for auxiliary diagnosis before operation. The clinical-radiomics nomograms performed better than radiomics nomograms.

CLINICAL RELEVANCE/APPLICATION

Clinical-radiomics nomograms based on CT and mpMRI features can be used for preoperative differentiation of SC and SGCT.

Printed on: 10/29/20





SST06

Nuclear Medicine (Thoracic Oncology Nuclear Medicine and PET)

Friday, Dec. 6 10:30AM - 12:00PM Room: E353B



AMA PRA Category 1 Credits ™: 1.50 ARRT Category A+ Credit: 1.75

Participants

Robert R. Flavell, MD, PhD, San Francisco, CA (*Moderator*) Nothing to Disclose Andrew C. Homb, MD, Rochester, MN (*Moderator*) Nothing to Disclose

Sub-Events

SST06-01 TNM Sub-Stage Does Not Predict Survival in Surgical Patients with Both Clinical and Pathological Stage I Non-Small Cell Lung Cancer

Friday, Dec. 6 10:30AM - 10:40AM Room: E353B

Participants

Jingmian Zhang, MD, Shijiazhuang, China (*Abstract Co-Author*) Nothing to Disclose Bill C. Penney, PhD, Chicago, IL (*Abstract Co-Author*) Nothing to Disclose Daniel E. Appelbaum, MD, Chicago, IL (*Abstract Co-Author*) Nothing to Disclose Yonglin Pu, MD, PhD, Chicago, IL (*Presenter*) Nothing to Disclose

PURPOSE

To determine if TNM sub-stage (IA1-IB) and PET tumor measurements are predictive of survival in surgical patients with both clinical and pathological stage I non-small cell lung cancer (NSCLC).

METHOD AND MATERIALS

This study reviewed surgical patients with clinical and pathological stage I NSCLC and a baseline FDG PET/CT between Feb 2004 and Dec 2014. The pathological staging was based on the prevailing staging system at the time of the surgery. The clinical stage (8th edition) was determined retrospectively by radiologists based on FDG PET/CT and contrast CT. The metabolic tumor volume (MTV), total lesion glycolysis (TLG), and SUVmax from PET/CT were measured. The primary endpoint was overall survival (OS). Kaplan-Meier and Cox survival analyses were performed.

RESULTS

172 surgical patients with pathological stage I also had clinical stage I (9 with IA1, 63 with IA2, 63 with IA3 and 37 with IB) (111 females and 61 males), with 44.8% who expired during follow-up, median OS was 69.1 months; and the 1-year, 2-year, and 5-year OS rates were 96.0%, 88.3% and 71.7 %, respectively. The median follow-up among survivors was 79.2 months. Univariate analysis showed that age [hazard ratio (HR) of age for every year= 1.04, p=0.001] and ECOG performance status (p=0.027) were associated with OS. Clinical TNM sub-stage (p=0.702), gender (p=0.405), smoking status (0.171), histology (p=0.111), ln(MTV) (p=0.120), ln(TLG) (p=0.147) and ln(SUVmax) (p=0.316) were not significantly associated with OS. The statistically significant association of age (HR= 1.04, p=0.002) and ECOG performance status (p=0.027) with OS persisted in multivariate Cox regression analyses after adjusting for clinical TNM sub-stage and ln(MTV). However, there was no significant association of clinical TNM sub-stage and ln(MTV). However, there was no significant association of clinical TNM sub-stage and ln(MTV). However, there was no significant association of clinical TNM sub-stage and ln(MTV). However, there was no significant association of Clinical TNM sub-stage (p=0.451) and ln(MTV) (p=0.08) with OS. Kaplan-Meier survival analysis showed statistically significant association of MTV (>=3.5 ml vs <3.5ml, p=0.049), age (p=0.001) and ECOG performance status (p=0.02) with OS.

CONCLUSION

Clinical TNM sub-stage is not associated with OS in the surgical patients with both clinical and pathological stage I NSCLC. Age, MTV (>=3.5 ml vs <3.5ml) and ECOG performance status are significantly associated with OS in such patients.

CLINICAL RELEVANCE/APPLICATION

Patients with clinical stage 1 as determined with CT and PET, and pathologic stage 1 do well after surgery. Clinical TNM sub-stages add little prognostic information in this group.

SST06-02 Mediastinal Lymph Nodal Staging by 18 F FDG PET CT in Patients with Co-Existent Carcinoma Lung and Tuberculosis: A Tertiary Care Centre Experience

Friday, Dec. 6 10:40AM - 10:50AM Room: E353B

Participants

Ritu Verma, New Delhi, India (*Abstract Co-Author*) Nothing to Disclose Ram K. E, New Delhi, India (*Abstract Co-Author*) Nothing to Disclose Amit Dhamija, New Delhi, India (*Abstract Co-Author*) Nothing to Disclose Ankur Pruthi, New Delhi, India (*Abstract Co-Author*) Nothing to Disclose Ethel S. Belho, New Delhi, India (*Abstract Co-Author*) Nothing to Disclose Dharmender Malik, New Delhi, India (*Abstract Co-Author*) Nothing to Disclose Nikhil Seniaray, New Delhi, India (*Abstract Co-Author*) Nothing to Disclose Vanshika Gupta, New Delhi, India (*Abstract Co-Author*) Nothing to Disclose

Nitin Gupta, New Delhi, India (Abstract Co-Author) Nothing to Disclose

Harsh Mahajan, MD,MBBS, New Delhi, India (*Presenter*) Director, Mahajan Imaging Pvt Ltd; Research collaboration, General Electric Company; Research collaboration, Koninklijke Philips NV; Research collaboration, Qure.ai; Research collaboration, Predible Health Vidur Mahajan, MBBS, New Delhi, India (*Abstract Co-Author*) Researcher, CARING; Associate Director, Mahajan Imaging; Research collaboration, General Electric Company; Research collaboration, Koninklijke Philips NV; Research collaboration, Qure.ai; Research collaboration, Predible Health; Research collaboration, Oxipit.ai; Research collaboration, Synapsica; Research collaboration, Quibim

For information about this presentation, contact:

drrituverma29@gmail.com

PURPOSE

The aim of this study is to evaluate the imaging characteristics of metastatic and benign (Tubercular) lymph nodes on 18 F FDG PET/CT, in patients with co-existent Carcinoma lung and Tuberculosis, and correlation with histopathological analysis.

METHOD AND MATERIALS

A retrospective analysis of 25 patients (19 males, 6 females; mean age 62.4+/- 10.08 years) with co-existent Carcinoma lung and Tuberculosis was done. All the subjects underwent F-18 FDG PET/CT scanning and subsequently the mediastinal lymph nodes were biopsied. SUV Max-Tumour, SUV Max-Lymph node and SUV Max-Ratio (SUV Max Lymph node / SUV Max Tumour) for each lymph node station on 18F-FDG PET/CT was determined and then each station was classified into one of the three groups based on SUV Max -Tumour (low, medium and high SUV Max -Tumour groups). Diagnostic performance was assessed based on receiver operating characteristic (ROC) curve analysis, and the optimal cut-off values that would best discriminate metastatic from benign lymph nodes were determined for each method.

RESULTS

A total of 115 lymph node stations with a mean of 4.6 lymph node station per patient and total of 540 lymph nodes with a mean of 21.6 lymph nodes per patient were resected and biopsied. 79 nodes were reported positive for metastasis and 27 nodes were reported as granulomatous. On pre-treatment 18F-FDG PET/CT scan, the mean SUV Max-Tumour of squamous cell carcinoma was significantly higher than that of adenocarcinoma (9.9 ± 3.97 vs. 5.76 ± 3.48 , P<0.001). The mean SUVmax of malignant lymph nodes was significantly higher than that of tubercular lymph nodes (6.7 ± 0.94 vs. 2.7 ± 0.84 P<0.001). The mean SUV Max-Ratio in patients with malignant lymph nodes was significantly higher than in those with tubercular lymph nodes (0.91 ± 0.36 vs. 0.41 ± 0.28 , P<0.001).

CONCLUSION

The overall diagnostic accuracy of 18 F FDG PET CT in mediastinal lymph nodal staging in patients with co-existent Tuberculosis and Carcinoma lung carcinoma is 67.4 %, if SUV Max of 2.5 is taken as the cut off criteria, however if SUV Max-Ratio is taken into consideration, the overall diagnostic accuracy increases to 74.8%, thus helping in the accurate staging of patients

CLINICAL RELEVANCE/APPLICATION

Carcinoma lung with co-existing Tuberculosis results in false positive mediastinal lymph nodes and fallacies in pre-operative staging.

SST06-03 Improving Accuracy of FDG PET/CT to Diagnose Mediastinal Nodal Involvement in Non Small Cell Lung Cancer (NSCLC): Utility of Using various Predictive Models

Friday, Dec. 6 10:50AM - 11:00AM Room: E353B

Participants Boon Mathew, MD, Mumbai, India (*Presenter*) Nothing to Disclose Nilendu C. Purandare, DMRD, Mumbai, India (*Abstract Co-Author*) Nothing to Disclose Ameya D. Puranik, MBBS, Mumbai, India (*Abstract Co-Author*) Nothing to Disclose Sneha A. Shah, Mumbai, India (*Abstract Co-Author*) Nothing to Disclose Archi Agrawal, MBBS, Mumbai, India (*Abstract Co-Author*) Nothing to Disclose C S Pramesh, Mumbai, India (*Abstract Co-Author*) Nothing to Disclose Venkatesh Rangarajan, MBBS, Mumbai, India (*Abstract Co-Author*) Nothing to Disclose

For information about this presentation, contact:

drboonmathew@gmail.com

PURPOSE

Accurate nodal staging is crucial in deciding the therapy for NSCLC patients. PET using FDG as well as CECT scan have not been proven to be sufficiently accurate in predicting mediastinal nodal disease, particular in infection endemic regions of the world. The purpose of the study was to determine a predictive model that could improve the accuracy for identifying mediastinal (N2) nodal metastases based on both PET and CT findings seen on baseline FDG PET/CT.

METHOD AND MATERIALS

This retrospective study includes 339 patients with NSCLC who underwent FDG PET/CT within 6 weeks prior to surgery. PET parameters obtained were 1) number of visual PET positive N2 nodes (FDG uptake more than mediastinal blood pool), 2) maximum standardized uptake value (SUVmax) of nodes and 3) ratio of node to aorta (N/A) SUVmax. CT parameters obtained were 1) short axis diameter and 2) Hounsfield units (HU) of PET positive nodes. Cutoff value of N/A ratio and HU for predicting metastases were obtained from ROC curve analysis. PET and CT parameters were correlated with nodal histopathology alone and in combination to find out the sensitivity, specificity, PPV and NPV. 3 different predictive models (PM) were devised and the incremental improvement in accuracy was determined.

RESULTS

PET positive N2 nodes were seen in 139 patients. Pathologically proven N2 disease was seen in 54 patients. 285 patients were negative for N2 nodal metastases. Predictive model (PM1) based on visual PET positivity showed sensitivity, specificity, PPV, NPV and accuracy of 70.3, 64.6, 27.3, 92 and 65.5 respectively. Predictive model (PM2) which combined visual PET positivity and N/A ratio >= 2 showed sensitivity, specificity, PPV, NPV and accuracy of 57.4, 92.2, 55.4, 91.9 and 85.8 respectively. Predictive model

(PM3) which combined visual PET positivity, N/A ratio >= 2 and HU < 75 showed sensitivity, specificity, PPV, NPV and accuracy of 55.5, 96.5, 75, 92 and 90 respectively.

CONCLUSION

Predictive model (PM3) which combined visual PET positivity, N/A ratio ≥ 2 and HU < 75 showed much improved accuracy in the preoperative diagnosis of mediastinal nodal metastases.

CLINICAL RELEVANCE/APPLICATION

Predictive model combining PET and CT parameters can identify N2 nodal involvement with high accuracy than either alone. The specificity and NPV appears excellent. However the sensitivity and PPV is only modest, demanding invasive nodal sampling especially in infectious endemic areas

SST06-05 FDG-PET/MRI versus Whole-Body MRI versus FDG-PET/CT versus Conventional Radiological Examination: Diagnostic and Prediction Capabilities for Postoperative Recurrence in Non-Small Cell Lung Cancer Patients

Friday, Dec. 6 11:10AM - 11:20AM Room: E353B

Participants

Yoshiharu Ohno, MD, PhD, Toyoake, Japan (*Presenter*) Research Grant, Canon Medical Systems Corporation; Research Grant, DAIICHI SANKYO Group; ;

Shinichiro Seki, Kobe, Japan (*Abstract Co-Author*) Research Grant, Canon Medical Systems Corporation Yuji Kishida, MD,PhD, Kobe, Japan (*Abstract Co-Author*) Nothing to Disclose Kota Aoyagi, Otawara, Japan (*Abstract Co-Author*) Employee, Canon Medical Systems Corporation Masao Yui, Otawara, Japan (*Abstract Co-Author*) Employee, Canon Medical Systems Corporation Takeshi Yoshikawa, MD, Kobe, Japan (*Abstract Co-Author*) Research Grant, Canon Medical Systems Corporation

For information about this presentation, contact:

yohno@fujita-hu.ac.jp

PURPOSE

To compare the utilities of diagnostis and prediction for postoperative recurrence among FDG-PET/MRI, whole-body MRI, FDG-PET/CT and conventional radiological method in non-small lung cancer (NSCLC) patients.

METHOD AND MATERIALS

484 consecutive postoperative NSCLC patients (289 men, 195 women; mean age 69 years) prospectively underwent whole-body MRI, integrated PET/CTs and conventional radiological method as well as follow-up and pathological examinations. Then, all patients were divided into recurrence (n=42) and non-recurrence (n=484) groups based on pathological and follow-up examination results. All co-registered PET/MRIs were generated by means of our proprietary software. Then, probability postoperative recurrence in each patient was visually assessed on all methods by means of 5-point visual scoring system. To compare diagnostic performance among all methods, receiver operating characteristic analyses were performed. Then, diagnostic accuracy of postoperative recurrence was statistically compared each other by using McNemar's test. Finally, multivariate analysis was performed to determine predictors for postoperative recurrence.

RESULTS

Area under the curves (Azs) of PET/MRI (Az=0.99) was significantly larger than that of MRI (Az=0.97, p<0.05), PET/CT (Az=0.97, p<0.05) and conventional radiological examination (Az=0.94, p<0.05). When applied feasible threshold values, accuracy of PET/MRI (97.7%) was significantly higher than that of others (MRI: 96.3%, p=0.004; PET/CT: 94.8%, p=0.0001; conventional radiological method: 90.0%, p<0.0001). Accuracy of MRI was also significantly higher than that of PET/CT (p=0.02) and conventional radiological method (p<0.0001). Moreover, accuracy of PET/CT was significantly higher than that of conventional radiological method (p<0.0001). As the results of multivariate analysis for prediction of postoperative recurrence, histological subtype (p=0.005), tumor marker (p<0.0001), PET/MRI result (p=0.001) and conventional radiological method result (p=0.002) were determined as significant predictors.

CONCLUSION

FDG-PET/MRI has better potential for diagnosis of postoperative recurrence than others and considered as one of the predictors in postoperative NSCLC patients.

CLINICAL RELEVANCE/APPLICATION

FDG-PET/MRI has better potential for diagnosis of postoperative recurrence than others and considered as one of the predictors in postoperative NSCLC patients.

SST06-06 Radiomics Features of Lung Adenocarcinoma Based on 18F-FDG PET/CT for Predicting the Mutation Status of EGFR and Its Correlation Analysis with Prognosis

Friday, Dec. 6 11:20AM - 11:30AM Room: E353B

Participants

Bin Yang, MD, Dali, China (*Presenter*) Nothing to Disclose Guangming Lu, Nanjing, China (*Abstract Co-Author*) Nothing to Disclose Ying Qian Ge, Philomont, China (*Abstract Co-Author*) Nothing to Disclose

For information about this presentation, contact:

yangbinapple@163.com

PURPOSE

To investigate whether the radiomics features of 18F-FDG PET-CT in lung adenocarcinoma combining with relevant clinical

characteristics can predict the EGFR mutation status, and to explore the association with the prognosis of patients with different mutation status.

METHOD AND MATERIALS

A total of 174 patients with lung adenocarcinoma who received PET/CT scan and EGFR gene test were retrospectively analyzed. 1672 Radiomics features were extracted from PET/CT images using a Radiomics prototype (Frontier, VB10, Siemens Healthineers). The clinical and pathological datas were retrospectively analyzed and a combination of radiomics signature with clinical factors model was constructed using the Randon Forest (RF) method to identify EGFR mutants from wild types. The mutant/wild model was trained on a set of 149 patients and validated on an independent test group (n=35) using the AUC. A subset of 99 patients with EGFR mutation were further analyzed. The second model was built with RF classifier to predict 19/21 mutation site. The performance of training group (n=79) and test group (n=20) were evaluated by AUC. And then, and the COX proportional hazard model of multivariate analysis was established.

RESULTS

56.9% (99/174) of patients showed EGFR mutation. EGFR mutation of exon 21wa the most common mutation type (57/99). We identified a combined radiomics signature and clinical factor model to discrimated between EGFR mutant and wild type in the training group (AUC=0.77) and the validation group (AUC=0.71). (Figure1)The performance of the second model for the identification of 19/21 mutation site reached an AUC of 0.82 and 0.73 in the training group and validation group, respectively. (Figure2) The average survival time of the mutant and wild-type patients was 54.653 months (95% CI:44.940 - 64.366) and 35.993 months (95% CI: 29.377 - 42.608)respectively; the median survival time was 46 months (95% CI: 39.216-52.784) and 28 months (95% CI : 18.842-37.158) respectively. (Table1,2)(Figure3)

CONCLUSION

Radiomics features based on the 18F-FDG PET/CT combining with clinical pathological data could have the potential to predict EGFR mutation type, moreover, associated with patients' prognosis, thus providing reference for individualized molecular targeted therapy.

CLINICAL RELEVANCE/APPLICATION

Radiomics features based on the 18F-FDG PET/CT could have the potential to predict EGFR mutation type.

SST06-07 18F-FDG PET-CT Can Predict the Major Pathologic Response to the Neo-Adjuvant PD-1 Blockade in Resectable Non-Small Cell Lung Cancer

Friday, Dec. 6 11:30AM - 11:40AM Room: E353B

Participants

Xiuli Tao, Beijing, China (*Presenter*) Nothing to Disclose Ning Wu, MD, Beijing, China (*Abstract Co-Author*) Nothing to Disclose Jie He, Beijing, China (*Abstract Co-Author*) Nothing to Disclose Shugeng Gao, Beijing, China (*Abstract Co-Author*) Nothing to Disclose Ning Li, Beijing, China (*Abstract Co-Author*) Nothing to Disclose Zhijie Wang, Beijing, China (*Abstract Co-Author*) Nothing to Disclose Jie Wang, Beijing, China (*Abstract Co-Author*) Nothing to Disclose Jianming Ying, Beijing, China (*Abstract Co-Author*) Nothing to Disclose Yun Ling, Beijing, China (*Abstract Co-Author*) Nothing to Disclose Wei Tang, Beijing, China (*Abstract Co-Author*) Nothing to Disclose

PURPOSE

To investigate if 18F-FDG PET-CT has the potential to predict the major pathologic response to the neoadjuvant PD-1 blockade in resectable NSCLC patients.

METHOD AND MATERIALS

From March 2018 to March 2019, 35 patients with resectable NSCLC (the largest diameter of the pulmonary mass was 2.0 cm or larger) who were eligible to the open-label, single-center, single-arm phase Ib clinical trial with PD-1 blockade (IBI308) as neoadjuvant therapy treatment were enrolled. All patients received two doses of intravenous PD-1 blockade (at a dose of 200mg) every 2 weeks. PET-CT scan was performed before neoadjuvant therapy (baseline) and 4 weeks after the first dose (before surgery). PET responses were classified using PET response criteria in solid tumors (PERCIST). Peak standardized uptake values normalized by lean body mass (SULpeak) were measured, and post-treatment percentage changes in SULpeak (ΔSULpeak%) were calculated. The above metabolic information on FDG-PET was correlated with the surgical pathology.

RESULTS

After 4 weeks of neoadjuvant PD-1 blockade treatment, all 35 patients were under surgery, and the major pathological response (MPR, defined as 10% or less residual viable tumor) occurred in 13 of 35 resected tumors (37%). 13 patients (37%) showed partial metabolic response (PMR), 21 (60%) had stable metabolic disease (SMD), and 1 (3%) had progressive metabolic disease (PMD). There was a significant correlation between the pathological response and the PET responses which were classified using PET response criteria in solid tumors (PERCIST). All (100%) the partial metabolic response (PMR, Δ SULpeak% < -30%) tumors showed the major pathological response (MPR, defined as 10% or less residual viable tumor). The patient who had progressive metabolic disease (PMD, Δ SULpeak% > 30%) was progressive confirmed by the biopsy of the pleural metastasis.

CONCLUSION

18F-FDG PET-CT can predict the major pathologic response to the neoadjuvant PD-1 blockade in resectable non-small cell lung cancer.

CLINICAL RELEVANCE/APPLICATION

Metabolic responses by 18F-FDG uptake which were classified using PET response criteria in solid tumors (PERCIST) are significant associated with therapeutic response at 4 weeks after PD-1 blockade treatment. Even if morphological changes on CT scans are investigated to evaluate the response to PD-1 blockade at an early phase, it is difficult to distinguish between responders and non-

responders. Thus, the uptake of 18F-FDG PET-CT appears to be a promising biomarker for sift patients who probably benefit form immunotherapy.

SST06-08 Relationship between the Expression of PD-L1 and F-FDG Uptake in Advanced Non-Small Cell Lung Cancer (NSCLC)

Friday, Dec. 6 11:40AM - 11:50AM Room: E353B

Participants Wang Huoqiang, MD, Shanghai, China (*Presenter*) Nothing to Disclose Zhao Long, MD, Shanghai, China (*Abstract Co-Author*) Nothing to Disclose

For information about this presentation, contact:

whq2216@sina.cn

PURPOSE

Programmed cell death-ligand 1 (PD-L1) have been identified as novel targets of immunotherapy of lung cancer. To our knowledge, all published studies of the relationship between the 18F-FDG uptake of lung cancer and PD-L1 expression were performed in patients undergoing surgical resection. However, majority of reports have demonstrated the superiority of PD-L1 inhibitors as a therapy for patients with advanced lung cancer. The purpose of this study is to investigate the predictive value of 18F-fluorodoxyglucose positron emission tomography/computed tomography (18F-FDG PET/CT) in evaluating PD-L1 expression in advanced non-small cell lung cancer (NSCLC).

METHOD AND MATERIALS

From January 2017 to December 2018, advanced NSCLCs were retrospectively identified in 154 consecutive patients who underwent 18F-FDG PET/CT scan and PD-L1 expression test. The histopathological results were confirmed by aspirated or biopsied samples. The maximum standardized uptake value (SUVmax) of 18F-FDG uptake were calculated for the primary lesion. Associations between quantitative continuous variables and PD-L1 expression were investigated by using the Mann-Whitney U test. This study was approved by the institutional review board of our hospital.

RESULTS

PD-L1 expression were identified in 77 patients (50%). PD-L1 expression of NSCLC occurred more frequently in larger lesions (p = 0.039), higher SUVmax value (p = 0.019), KRAS mutation-positive (p = 0.048). PD-L1 expression of adenocarcinoma (ADC) occurred more frequently in larger lesions (p = 0.022), higher SUVmax value (p = 0.043). The receiver operating characteristic (ROC) curve yielded area under the curve (AUC) values of 0.596 (95%CI, 0.506-0.686, p = 0.039) and 0.633 (95%CI, 0.509-0.756, p = 0.043) for NSCLC and ADC, respectively.

CONCLUSION

We demonstrated that higher 18F-FDG uptake may be helpful in predicting PD-L1 expression of advanced NSCLC, especially advanced ADC.

CLINICAL RELEVANCE/APPLICATION

For the first time, we demonstrated that PD-L1 expression were more frequent in advanced NSCLC with higher 18F-FDG uptake.

SST06-09 The Role of 18F-FDG SPECT/CT in Predicting Expression of PD-1/PD-L1 in Surgically Resected Non-Small Cell Lung Cancer (NSCLC)

Friday, Dec. 6 11:50AM - 12:00PM Room: E353B

Participants Wang Huoqiang, MD, Shanghai, China (*Presenter*) Nothing to Disclose Zhao Long, MD, Shanghai, China (*Abstract Co-Author*) Nothing to Disclose

For information about this presentation, contact:

whq2216@sina.cn

PURPOSE

Although 18F-fluorodoxyglucose positron emission tomography/computed tomography (18F-FDG PET/CT) has been widely used, there are still many hospitals performing 18F-FDG single photon emission computed tomography/computed tomography (18F-FDG SPECT/CT) scan. In previous studies, 18F-FDG SPECT/CT was a reliable tool in evaluation of malignant tumours, which were concordant with 18F-FDG PET/CT. At present, some studies have demonstrated a correlation between PD-1/PD-L1 expression and SUVmax in NSCLC, but the relationship between PD-1/PD-L1 expression and T/NT value are not clear. The purpose of this study is to investigate the value of 18F-FDG SPECT/CT predicting expression of PD-1/PD-L1 in NSCLC.

METHOD AND MATERIALS

From July 2014 to May 2016, NSCLCs were retrospectively identified in 229 consecutive patients who underwent 18F-FDG SPECT/CT scan and PD-1/PD-L1 expression test. The histopathological results were confirmed by resected samples. Tumor-to-normal tissue (T/NT) uptake ratios of 18F-FDG were calculated for the primary lesion.

RESULTS

PD-1 and PD-L1 expression were identified in 120 patients (52.4%) and 81 patients (35.4%), respectively. PD-L1 expression occurred more frequently in males (p = 0.013), larger lesions (p < 0.001), higher T/NT value (p < 0.001), T3/4 stage (p = 0.002), III stage (p = 0.002). In multivariate analysis, T/NT was significantly associated with PD-L1 expression. PD-1 expression occurred more frequently only in patients with higher T/NT value (p = 0.028). The receiver operating characteristic (ROC) curve yielded area under the curve (AUC) values of 0.685 (95%CI, 0.615-0.756, p < 0.001) and 0.568 (95%CI, 0.512-0.659, p = 0.025) for PD-L1 and PD-1 expression, respectively.

CONCLUSION

We demonstrated that T/NT value of FDG uptake may be helpful in predicting PD-1/PD-L1 expression, which is consistent with results of 18F-FDG PET/CT. In some countries, 18F-FDG SPECT/CT scan is covered by medical insurance, while 18F-FDG PET/CT is not, which enhances the clinical value of 18F-FDG SPECT/CT scan for cost reasons.

CLINICAL RELEVANCE/APPLICATION

For the first time, we demonstrated that PD-1/PD-L1 expression were more frequent in NSCLC with higher T/NT value.

Printed on: 10/29/20





SST07

Neuroradiology (Vascular and Interventions)



AMA PRA Category 1 Credits ™: 1.50 ARRT Category A+ Credit: 1.75

FDA Discussions may include off-label uses.

Participants

Adrien Guenego, MD, Montjoire, France (*Moderator*) Nothing to Disclose Benjamin Y. Huang, MD, MPH, Chapel Hill, NC (*Moderator*) Nothing to Disclose Jalal B. Andre, MD, Seattle, WA (*Moderator*) Research Grant, Koninklijke Philips NV Consultant, Hobbitview, Inc Research Grant, Toshiba Corporation

Sub-Events

SST07-01 National Trends in the Use of Initial Imaging for Carotid Stenosis in the Outpatient Setting

Friday, Dec. 6 10:30AM - 10:40AM Room: E353A

Participants Jina Pakpoor, MD, Baltimore, MD (*Presenter*) Nothing to Disclose Andrew Harris, BS, Baltimore, MD (*Abstract Co-Author*) Nothing to Disclose Joseph Canner, Baltimore, MD (*Abstract Co-Author*) Nothing to Disclose Caitilin Hicks, MD, Baltimore, MD (*Abstract Co-Author*) Nothing to Disclose

PURPOSE

The Society for Vascular Surgery currently recommends carotid artery duplex ultrasonography (DUS) as the first-line imaging modality for the diagnosis of carotid artery stenosis, and this is in keeping with Appropriateness criteria of the American College of Radiology. We sought to investigate compliance with these guidelines on a national level for the initial work-up of suspected carotid artery stenosis in the outpatient setting.

METHOD AND MATERIALS

Using a national commercial claims database, we identified patients between 18-65 years old who had an outpatient visit with an associated initial diagnosis of carotid stenosis (ICD-9 433.10; ICD-10 165.2) from 2011-2016. Use of imaging was identified by Current Procedural Terminology (codes for DUS, CTA, and MRA associated with the initial outpatient visit. Trends were assessed using logistic regression analyses. Patients with any of the relevant ICD codes or CPT codes for one year prior to the encounter were excluded.

RESULTS

Overall, 229,464 patients with a new diagnosis of carotid artery stenosis were included in the analysis (mean age 55 years, 51.2% male). The majority (95.8%) of patients received DUS as the initial imaging modality, 2.4% received CTA, 1.3% received MRA, and 0.5% had more than one study associated with the encounter. The proportion of patients receiving DUS as the only initial imaging modality decreased from 97% in 2011 to 94% in 2016 (p<0.001). The rate of patients receiving CTA as the initial imaging modality increased from 1.6% in 2011 to 4.7% in 2016 (p<0.001). Use of MRA relatively stable (1.2%-1.5%) over the course of the study period. Use of initial advanced imaging (MRA/CTA) was highest in the West region of the USA (5.5%) and lowest in the Northeast (2.0%), p<0.001.

CONCLUSION

Our findings demonstrate that while the majority of initial imaging studies for suspected carotid artery stenosis are compliant with current recommendations from the Society of Vascular Surgery, the use of CTA is significantly increasing with time (p<0.001). Compared to DUS, CTA is associated with radiation exposure to the patient and a significantly higher imaging cost.

CLINICAL RELEVANCE/APPLICATION

Further education of the outpatient provider is needed to shift the current trend of initial CTA use for carotid stenosis; in particular in the setting of increasing availability of CT technology.

SST07-02 Identification of Patients with Carotid Stenosis Using Natural Language Processing

Friday, Dec. 6 10:40AM - 10:50AM Room: E353A

Participants Xiao Wu, New Haven, CT (*Presenter*) Nothing to Disclose Yuzhe Zhao, PhD, New Haven, CT (*Abstract Co-Author*) Nothing to Disclose Seyedmehdi Payabvash, MD, San Francisco, CA (*Abstract Co-Author*) Nothing to Disclose Ajay Malhotra, MD, Stamford, CT (*Abstract Co-Author*) Nothing to Disclose

For information about this presentation, contact:

PURPOSE

This study aims to develop a natural language processing (NLP) model to retrospectively retrieve patients with presence, history and severity of carotid stenosis (CS) using their ultrasound reports.

METHOD AND MATERIALS

Ultrasound reports from our institution between January 2016 and December 2017. To process the texts, we developed a parser to divide the raw text into fields. For baseline method, we use bag of n-grams and term frequency inverse document frequency as the features and use linear classifiers. Logistic regression is performed as the baseline model. Convolution and recurrent neural networks (CNN; RNN) with attention mechanism are applied to the data set to improve the classification accuracy.

RESULTS

We had 1,220 ultrasound reports for training, and 307 for testing, totaling to 1,527 reports. For predicting history of CS, both CNN and RNN-Attention models have a significantly higher specificity than logistic regression. In addition, RNN-Attention also has a significantly higher F1 score and overall accuracy. For predicting presence, all models achieved above 93% accuracy. RNN-attention achieved a 95.4% overall accuracy, although the difference with logistic regression is not statistically significant with. RNN-Attention has a statistically significant higher specificity than logistic regression.

CONCLUSION

We have developed a parser to automatically segment the report text into different sections and predict history, presence and severity of CS. We have demonstrated NLP to be an efficient approach for large-scale retrospective patient identification, with wide applications in long-term follow-up of patients and further clinical research studies.

CLINICAL RELEVANCE/APPLICATION

NLP is shown to be an efficient approach for large-scale retrospective patient identification, with wide applications in long-term follow-up of patients and further clinical research studies.

SST07-04 3D-Arterial Analysis Software and CEUS in the Assessment of Severity and Vulnerability of Carotid Atherosclerotic Plaque in Comparison with CTA and Histology

Friday, Dec. 6 11:00AM - 11:10AM Room: E353A

Participants

Daniele Fresilli, Roma, Italy (*Presenter*) Nothing to Disclose Giuseppe Schillizzi, Roma, Italy (*Abstract Co-Author*) Nothing to Disclose Daniela Elia, Roma, Italy (*Abstract Co-Author*) Nothing to Disclose Carlo Catalano, MD, Rome, Italy (*Abstract Co-Author*) Nothing to Disclose Ferdinando D'Ambrosio, Rome, Italy (*Abstract Co-Author*) Nothing to Disclose Vito Cantisani, MD, Roma, Italy (*Abstract Co-Author*) Nothing to Disclose Vito Cantisani, MD, Roma, Italy (*Abstract Co-Author*) Speaker, Canon Medical Systems Corporation; Speaker, Bracco Group; Speaker, Samsung Electronics Co, Ltd; Giorgia Polti, Rome, Italy (*Abstract Co-Author*) Nothing to Disclose Patrizia Pacini, Rome, Italy (*Abstract Co-Author*) Nothing to Disclose Olga Guiban, Rome, Italy (*Abstract Co-Author*) Nothing to Disclose Eleonora Polito, Rome, Italy (*Abstract Co-Author*) Nothing to Disclose Yana Solskaya, MD, Riga, Latvia (*Abstract Co-Author*) Nothing to Disclose Eleonora Tassone, Rome, Italy (*Abstract Co-Author*) Nothing to Disclose Vincenzo Dolcetti, Rome, Italy (*Abstract Co-Author*) Nothing to Disclose

Nicola Di Leo, MD, Rome, Italy (Abstract Co-Author) Nothing to Disclose

PURPOSE

To evaluate the accuracy of ultrasonographic 3D-Arterial Analysis and CEUS in assessing severity and vulnerability of carotid plaques.

METHOD AND MATERIALS

134 patients were enrolled with the following criteria: (1) asymptomatic stenosis of carotid artery >70% but <100%; or (2) recent transient ischemic attack or ischemic stroke, and ipsilateral carotid stenosis >50%. All the patients underwent endarterectomy and gross and histology evaluation was performed to grade the plaque. 3D-Arterial Analysis provided a colour map to evaluate plaque vulnerability and a 3D volumetric stenosis evaluation. Its diagnostic performance has been compared to histological examination for plaque's vulnerability and to CEUS and CTA for stenosis' grading.

RESULTS

94 vulnerable plaques at histological examination were identified with at least one of the following criteria: fibrous cap < 200μ m, presence of lipid core, intra-plaque haemorrhage, leukocyte recruitment or angiogenesis. 3D-Arterial Analysis software, CEUS and CTA were able to detect 84, 82 and 82 of these 94 vulnerable plaques respectively, with 89%, 87% and 87% sensitivity and 100% specificity. CTA has identified 84 severe stenosis of which 83 were correctly evaluated by 3D-Arterial Analysis software and CEUS, with a sensitivity of 88% and specificity of 100%.

CONCLUSION

3D-Arterial Analysis software and CEUS seem effective tools to assess plaque's vulnerability and stenosis severity, providing useful information for surgery planning. Multicenter prospective evaluation is warranted to clarify the role of US multiparametric evaluation.

CLINICAL RELEVANCE/APPLICATION

Pre-operative evaluation of carotid plaque is crucial for prompt follow-up or treatment. New Ultrasound diagnostic tool may open new further prospects. Multicenter prospective evaluation is warranted to clarify the role of US multiparametric evaluation

sst07-05 Current Challenges and Accuracy of Carotid Plaque Neovascularization Grading with Contrast-

Enhanced Ultrasound Method

Friday, Dec. 6 11:10AM - 11:20AM Room: E353A

Participants Andrejs Lioznovs, Riga, Latvia (*Abstract Co-Author*) Nothing to Disclose Maija Radzina, MD,PhD, Riga, Latvia (*Presenter*) Speaker, Canon Medical Systems Corporation

For information about this presentation, contact:

mradzina@gmail.com

PURPOSE

One of the stroke risk factors is unstable carotid atherosclerotic plaque with ulceration, soft plaque with surface irregularity as well as presence of nevascularisation. Contrast ultrasound (CEUS) is a new noinvasive method, that can detect vasa vasorum within plaque. The purpose of the study was to analyze CEUS technique ability to confirm plaque instability in correlation with CT angiography (CTA) and histological findings and to determine methods accuracy and limitations.

METHOD AND MATERIALS

Within period of 2 years a prospective study enrolled 54 patients with unstable plaque signs on ultrasound (US), all patients received baseline Duplex scanning, microvascular imaging (SMI) and contrast enhanced US with sulfur hexafluoride 1 ml followed by saline flush. CTA and histology results were used as reference standart. 32 patients underwent endarterectomy surgery. Based on CEUS results 2 groups were identified: poor (Grade 1) neovascularization and well visible (Grade2) vasa vasorum. For determination of CEUS sensitivity and specificity and limitations - two groups were compared - extensive calcified vs. soft plaques.

RESULTS

The neovascularization was diagnosed in 27 (50%) patients by CEUS - in 12 cases (44.4%) plaques showed neovascularization grade 1 and in 15 cases (55.6%) grade 2 plaques were detected. Comparing CEUS method and results of histology statistically significant correlation was found (rs = 0,624; p = 0,002). Comparing 2 groups: soft plaques neovascularization by CEUS was diagnosed in 13 cases (48.1%) with sensitivity - 77.78%, specificity 60%, positive predictive value 77.78%, negative predictive value 60%, accuracy 76.3%; In a group with extensive calcified plaques - neovascularization was detected in 14 patients (51.9%), methods sensitivity 53.33%, specificity 37.5%, positive predictive value 61.54%, negative predictive value 30%, accuracy 47.83% regardless stenosis grade.

CONCLUSION

CEUS is accurate method for confirmation of unstable plaque neovascularization regardless of stenosis grade well corresponding to histological results, but it cannot be recommended in cases of extensive calcinosis

CLINICAL RELEVANCE/APPLICATION

CEUS is a new noninvasive method, that may facilitate early detection of unstable carotid plaque (neovascularization) and may change patient management regardless stenosis grade concept in high stroke risk. Prerequisite is informative, but inconclusive baseline Duplex US and/or CTA findings.

SST07-06 Carotid Plaque Ulceration on Contrast-Enhanced Ultrasound: Diagnostic Accuracy Compared to Angiography

Friday, Dec. 6 11:20AM - 11:30AM Room: E353A

Participants

Ji Eun Park, Seongnam, Korea, Republic Of (*Presenter*) Nothing to Disclose Yeo Koon Kim, Seongnam-si , Korea, Republic Of (*Abstract Co-Author*) Nothing to Disclose

PURPOSE

The plaque ulceration is one of the features of plaque vulnerability and related to the risk for embolic stroke. The purpose of this study was to define the diagnostic accuracy of contrast-enhanced ultrasound (CEUS) for the carotid plaque ulceration.

METHOD AND MATERIALS

This study is a retrospective case series study. Institutional review board approved the study and waived informed consent. Patients who had CEUS and carotid angiography for evaluation of carotid plaque from September 2015 to June 2018 in our institution were consecutively included in this study (184 patients, 142 males, 280 carotid arteries, age 72±8.5 years, age range 32-91 years). The time interval between angiography and CEUS was limited to within six months. Carotid arteries with prior intervention (endarterectomy and stent) were excluded. CEUS was performed in order of 1) Doppler ultrasound, 2) injection of ultrasound contrast agent (SonoVue, Bracco, Italy), and 3) CEUS. A radiologist who was blinded to clinical information reviewed the CEUS images for plaque ulceration and the degree of stenosis. A neuro-intervention radiologist reviewed the angiography images. The plaque ulceration was defined to plaque surface indentation deeper than 2mm on both CEUS and angiography. Sensitivity, specificity and diagnostic accuracy were calculated for the detection of plaque ulceration and the significant (>50%) stenosis.

RESULTS

The prevalence of plaque ulceration was 25% on angiography. The sensitivity of CEUS for detection of plaque ulceration was 85.7% (95% confidence interval [CI]: 75.3% to 93.9%), specificity was 96.2% (95% CI: 92.6% to 98.3%), positive predictive value was 88.2% (95% CI: 79% to 93.7%), negative predictive value was 95.2% (95% CI: 91.9% to 97.2%), and the diagnostic accuracy was 93.6% (95% CI: 90% to 96.1%). The reason of false-negative cases was mainly calcification shadow on CEUS, and the false-positive cases were due to plaque surface irregularity.

CONCLUSION

CEUS can accurately visualize carotid plaque ulceration.

The CEUS showed excellent diagnostic accuracy for carotid plaque surface evaluation.

SST07-07 Elevated Hemoglobin A1c is Associated with Intracranial Plaque Enhancement: Novel Findings from Magnetic Resonance Imaging Study in Stroke Patients

Friday, Dec. 6 11:30AM - 11:40AM Room: E353A

Participants

Xiao Li, Shanghai, China (*Presenter*) Nothing to Disclose Beibei Sun, Shanghai, China (*Abstract Co-Author*) Nothing to Disclose Xiaosheng Liu, Shanghai, China (*Abstract Co-Author*) Nothing to Disclose

PURPOSE

Few study reported the association between Hemoglobin A1c (HbA1c) level and intracranial plaque vulnerability by magnetic resonance imaging (MRI). The present study of MRI-identified intracranial atherosclerotic lesions in patients with ischemic symptom therefore sought to determine the association between HbA1c level and intracranial plaque morphological and compositional characteristics and cerebral infarction severity.

METHOD AND MATERIALS

108 patients with intracranial ischemia were recruited. All patients were stratified into high (>6.5%) and low (<6.5%) HbA1c groups and underwent both intracranial vessel wall MRI and brain MRI scans. Intracranial plaque features and intracranial ischemic lesions were assessed.

RESULTS

More intracranial plaques (2.38 ± 1.50 vs. 0.96 ± 0.75 , P=0.001), higher incidence rate of intracranial symptomatic plaque enhancement (88.24% vs. 45.95%, P=0.001), more acute cerebral infarct (50.00% vs. 25.67%, P=0.013) and more recurrent infarct (67.65% vs. 45.95%, P=0.036) were in the high as compared to the low HbA1c group. High HbA1c was the independent risk factor for the presence of intracranial symptomatic plaque enhancement [odds ratio (OR)=7.05].

CONCLUSION

Our study suggested that an elevated HbA1c might have an adverse effect on intracranial plaque enhancement, which might induce acute cerebral infarct.

CLINICAL RELEVANCE/APPLICATION

Our findings indicate that determination of HbA1c levels and characterization of intracranial atherosclerotic plaque by MR vessel wall imaging might be useful to better select proper treatment options of stroke subjects.

SST07-08 Digital Variance Angiography Allows 50% Contrast Medium Reduction in Carotid X-Ray Angiography

Friday, Dec. 6 11:40AM - 11:50AM Room: E353A

Participants

Viktor I. Orias, MD, Budapest, Hungary (*Presenter*) Clinical Research and Development Specialist, Kinepict Health Kft David Szollosi, MD, Budapest, Hungary (*Abstract Co-Author*) Nothing to Disclose Marcell Gyano, MD, Budapest, Hungary (*Abstract Co-Author*) Researcher, Kinepict Health Ltd. Sandor Nardai, MD,PhD, Budapest, Hungary (*Abstract Co-Author*) Nothing to Disclose Krisztian Szigeti, PhD, MSc, Budapest, Hungary (*Abstract Co-Author*) CEO, Kinepict Health Ltd Szabolcs Osvath, PhD, Budakeszi, Hungary (*Abstract Co-Author*) CEO, Kinepict Health Ltd Janos P. Kiss, MD,PhD, Budapest, Hungary (*Abstract Co-Author*) Officer, Kinepict Health Ltd Peter Sotonyi, MD,PhD, Budapest, Hungary (*Abstract Co-Author*) Nothing to Disclose Zoltan Ruzsa, MD,PhD, Budapest, Hungary (*Abstract Co-Author*) Nothing to Disclose

For information about this presentation, contact:

orias.viktor@gmail.com

PURPOSE

In previous clinical studies Digital Variance Angiography (DVA) provided higher SNR and better image quality than Digital Subtraction Angiography (DSA). The observed quality reserve might provide opportunity for the reduction of ICM in CXA. Our aim was to evaluate the potential of DVA to reduce iodinated contrast medium (ICM) in carotid X-ray angiography (CXA).

METHOD AND MATERIALS

Our prospective study enrolled 26 patients undergoing carotid percutaneous transluminal angioplasty between January and June 2018. Mean±SD age (years): 67.0±8.1, 23 males 67.3±8.1, 3 females 64.7±9.8. We compared the signal-to-noise ratio (SNR) of DSA and DVA image pairs obtained by a standard (100% ICM) or a low-dose (50% ICM) protocol. Visual evaluation of single DVA or DSA images was performed by specialists using a 5-grade rating scale. The quality of DSA and DVA videos was also compared. Interrater agreement was described by percent agreement and Fleiss' kappa.

RESULTS

DVA provided more than two-fold SNR, the median SNRDVA/SNRDSA ratio was 2.06 (100%) and 2.25 (50%). In the visual evaluation the DVA100% score (3.73 ± 0.06) was significantly higher than the DSA100% score (3.52 ± 0.07 , p<0.001), and the DVA50% score (3.64 ± 0.13) was also significantly higher than the DSA50% score (3.01 ± 0.17 , p < 0.01). There was no statistical difference between the DSA100% and DVA50% scores. Evaluators preferred DVA50% over DSA100% videos in 61 % of comparisons, the interrater agreement was 81% (Fleiss' kappa 0.35, p<0.001)

CONCLUSION

Our data show, that DVA allows a very substantial (50%) ICM reduction in CXA without affecting the quality and diagnostic value of angiograms.

CLINICAL RELEVANCE/APPLICATION

Digital Variance Angiography (DVA) is a novel medical image processing method that significantly improves the image quality of Xray angiograms compared to Digital Subtraction Angiography The quality reserve of DVA allows a substantial amount of iodinated contrast medium dose reduction in the carotid X-ray angiography setting without affecting the quality and diagnostic value of angiograms

SST07-09 Readmission after Treatment of Symptomatic Carotid Stenosis: A Nationwide Readmission Database Analysis

Friday, Dec. 6 11:50AM - 12:00PM Room: E353A

Awards

Trainee Research Prize - Fellow

Participants

Pouya Nazari, MD, Chicago, IL (*Presenter*) Nothing to Disclose Pedram Golnari, MD, Chicago, IL (*Abstract Co-Author*) Nothing to Disclose Roxanna M. Garcia, Chicago, IL (*Abstract Co-Author*) Nothing to Disclose Hannah K. Weiss, Chicago, IL (*Abstract Co-Author*) Nothing to Disclose Sameer A. Ansari, MD,PhD, Chicago, IL (*Abstract Co-Author*) Nothing to Disclose Ali Shaibani, MD, Chicago, IL (*Abstract Co-Author*) Nothing to Disclose Michael C. Hurley, MBBCh, Chicago, IL (*Abstract Co-Author*) Nothing to Disclose Matthew B. Potts, MD, Chicago, IL (*Abstract Co-Author*) Nothing to Disclose Babak S. Jahromi, MD,PhD, Chicago, IL (*Abstract Co-Author*) Nothing to Disclose

PURPOSE

Carotid endarterectomy (CEA) and stenting (CAS) are two well-described methods for treating symptomatic carotid artery stenosis. However, literature on readmission after CEA and CAS is limited. We therefore utilized the Nationwide Readmission Database (NRD) to characterize the rate and causes of 30 and 90-day unplanned readmissions after CEA and CAS for symptomatic stenosis.

METHOD AND MATERIALS

Data was extracted from the NRD spanning 2010 to 2015. The population consisted of adult patients who underwent CEA or CAS with a primary diagnosis of occlusion and/or stenosis of carotid artery with cerebral infarction or TIA. Non-elective readmission rates within 30 and 90 days for CEA vs CAS were compared. To calculate 30 and 90-day readmission rates, we included patients within the first 11 and 9 months of each year respectively. Poisson regression was performed using generalized estimating equations and adjusted risk ratio (aRR)s were obtained for factors associated with 30 and 90-day readmission. The adjusted model included terms for patient- and hospital-specific factors, comorbidity scores and disease severity.

RESULTS

Of 54,704 patients treated and discharged alive, 8.0% patients were readmitted within 30 days, and 13.6%) patients were readmitted within 90 days. The 30 and 90-day non-elective readmission rate for CEA vs CAS was 7.7% vs 9.1% (p<0.0001) and 12.8% vs 17.0% (p<0.0001), respectively (figure). Patients undergoing CAS had a higher adjusted risk of non-elective 30 and 90-day readmission than patients having CEA (aRR=1.16; 95%CI, 1.09-1.23; p<0.001 and aRR=1.04; 95%CI, 1.01-1.08; p=0.024, respectively). The most common primary diagnoses for non-elective readmission within 30 and 90 days, respectively, were cerebral artery occlusion with infarct, septicemia, TIA, myocardial infarction, pneumonia, carotid artery stenosis/occlusion without infarction, and acute kidney failure.

CONCLUSION

Common reasons for 30 and 90-day non-elective readmission after CEA or CAS for symptomatic stenosis were cerebral artery occlusion with infarct, septicemia and TIA. Adjusted risk and rates of non-elective readmission after 30 and 90 days were higher after CAS than CEA.

CLINICAL RELEVANCE/APPLICATION

Patients undergoing CAS had higher risk of readmission than those undergoing CEA at 30 and 90-day post-procedure.

SPECIAL NOTE

This paper has received the Kuo York Chynn Neuroradiology Research Award. This award is funded in perpetuity by the Chynn Family Foundation. Through the Chynn Family Foundation, Emil William Chynn, MD, FACS, MBA will guide future distributions to support research in radiology.

Printed on: 10/29/20







SST08

Science Session with Keynote: Pediatrics (Artificial Intelligence and Machine Learning)

Friday, Dec. 6 10:30AM - 12:00PM Room: E261



AMA PRA Category 1 Credits ™: 1.50 ARRT Category A+ Credit: 1.75

FDA Discussions may include off-label uses.

Participants

Michael M. Moore, MD, Hershey, PA (*Moderator*) Nothing to Disclose Raymond W. Sze, MD, Philadelphia, PA (*Moderator*) Nothing to Disclose Ramesh S. Iyer, MD, Issaquah, WA (*Moderator*) Nothing to Disclose

Sub-Events

SST08-01 Pediatrics Keynote Speaker: Emerging Machine Learning in Pediatric Radiology

Friday, Dec. 6 10:30AM - 10:40AM Room: E261

Participants Michael M. Moore, MD, Hershey, PA (*Presenter*) Nothing to Disclose

SST08-02 Children's Long Bones Acute Fracture Discrimination Using Multi-View Screening and Trained Deep Network

Friday, Dec. 6 10:40AM - 10:50AM Room: E261

Participants

Zbigniew Starosolski, PhD, Houston, TX (*Presenter*) Stockholder, Alzeca Biosciences, LLC Haithuy N. Nguyen, MD, Houston, TX (*Abstract Co-Author*) Nothing to Disclose Melissa C. Cano, RRA, Houston, TX (*Abstract Co-Author*) Nothing to Disclose Leslie Jones, Houston, TX (*Abstract Co-Author*) Nothing to Disclose Ananth Annapragada, PhD, Houston, TX (*Abstract Co-Author*) Stockholder, Alzeca Biosciences, LLC; Stockholder, Sensulin, LLC; Stockholder, Abbott Laboratories; Stockholder, Johnson & Johnson; Research Grant, Alzeca Biosciences, LLC J. H. Kan, MD, Houston, TX (*Abstract Co-Author*) Nothing to Disclose

For information about this presentation, contact:

Zbigniew.Starosolski@TexasChildrens.org

PURPOSE

Fracture dating (acute vs healing) of various pediatric long bone fracture subtypes is routinely performed by human radiologists by identifying presence of periosteal reaction or callus. We evaluate if fracture acuity or evidence of healing can be accurately categorized in a heterogeneous group of pediatric long bone fractures using a properly designed and trained Convolutional Neural Network (CNN).

METHOD AND MATERIALS

Our IRB approved this retrospective study. Radiographs collected in a large pediatric hospital during 2018 were selected using a search of radiology reports containing keywords: humerus, tibia, fibula, radius, or femur. The radiographs were reviewed and manually labeled by a box overlaying the fracture location to facilitate CNN training. These fractures included Salter-Harris, oblique, transverse, and buckle fractures with or without varying degrees of displacement and angulation. These individual fractures were subclassified as healing or acute by two faculty pediatric radiologists and two radiology physician assistants with reference to the final signed radiology report. Healing was defined as any radiologically visible callus or early periosteal reaction. The resulting 3801 radiographs consisted of 1910 acute and 1891 healing fractures (mean age 7.2 years, male 55.6%). They were patched into 512x512 pixels subdomains, thus building training, validation and test sets with 3001/400/400 patches respectively, and an almost perfect 50/50 class balance in each set. Transfer learning CNN was utilized with an additional four fully connected top layers of the network. A 10-fold cross-validation approach was used by shifting each set (training/validation/test) sequentially. Trained networks classified single views from each study till all available views were classified, and a decision calculated based on the algebraic mean of results from all views.

RESULTS

The 3 best CNN's exhibit stable high accuracy of 92.02%, AUC-ROC of 0.96, with the best performing CNN achieving 94.35% accuracy and 0.97 AUC-ROC. The CNNs performance are summarized in table 1, confirming stable results.

CONCLUSION

CNN based pediatric long bone fracture acuity classification using a multi-view approach is highly accurate. The 10-fold cross-validation approach limits possible bias due to relatively low size of the dataset.

CLINICAL RELEVANCE/APPLICATION

 I his is the first study showing CNN's are capable of fracture subtype categorization.

SST08-03 Using a Dual-Input Convolutional Neural Network for Automated Detection of Pediatric Supracondylar Fracture on Conventional Radiography

Friday, Dec. 6 10:50AM - 11:00AM Room: E261

Participants

Jae Won Choi, MD, Seoul, Korea, Republic Of (*Presenter*) Nothing to Disclose Yeon Jin Cho, MD, Seoul, Korea, Republic Of (*Abstract Co-Author*) Nothing to Disclose Gayoung Choi, MD, Seoul, Korea, Republic Of (*Abstract Co-Author*) Nothing to Disclose Seulbi Lee, MD, Busan, Korea, Republic Of (*Abstract Co-Author*) Nothing to Disclose Seunghyun Lee, Seoul, Korea, Republic Of (*Abstract Co-Author*) Nothing to Disclose Young Hun Choi, MD, Seoul, Korea, Republic Of (*Abstract Co-Author*) Nothing to Disclose Jung-Eun Cheon, MD, Seoul, Korea, Republic Of (*Abstract Co-Author*) Nothing to Disclose Woo Sun Kim, MD, Seoul, Korea, Republic Of (*Abstract Co-Author*) Nothing to Disclose In-One Kim, MD, Seoul, Korea, Republic Of (*Abstract Co-Author*) Nothing to Disclose

For information about this presentation, contact:

djc0105@gmail.com

PURPOSE

The purpose of this study was to assess the feasibility and diagnostic performance of using a dual-input convolutional neural network (CNN)-based deep learning algorithm which utilizes both anteroposterior (AP) and lateral elbow radiographs for automated detection of pediatric supracondylar fracture on conventional radiography.

METHOD AND MATERIALS

For the development of deep learning model, 1,266 pairs of AP and lateral elbow radiographs examined between January 2013 and December 2017 at a single institution were split into a training set (1,012 pairs, 79.9%) and a validation set (254 pairs, 20.1%). We used 258 pairs of radiographs examined in 2018 at the same institution as a temporal test set and 95 examined between January 2016 and December 2018 at another hospital as a geographic test set. Images underwent preprocessing including cropping and histogram equalization and were passed into a dual-input neural network constructed by merging two ResNet models. Observer study by radiologists was performed on the geographic test set. The area under the receiver operating characteristic curve (AUC), sensitivity, specificity, positive predictive value (PPV), and negative predictive value (NPV) of the model and human readers were calculated.

RESULTS

Our trained model showed an AUC of 0.976 (95% CI, 0.949-0.991) in the validation set, 0.985 (95% CI, 0.962-0.996) in the temporal test set, and 0.992 (95% CI, 0.947-1.000) in the geographic test set; The AUCs of human readers in the geographic test set showed a range of 0.977 to 0.997. Using the optimal operating point derived from the validation set, the model showed a sensitivity of 93.9%, a specificity of 92.2%, a PPV of 80.5%, and a NPV of 97.8% in the temporal test set and a sensitivity of 100%, a specificity of 86.1%, a PPV of 69.7%, and a NPV of 100% in the geographical test set.

CONCLUSION

A dual-input deep learning model which interprets both AP and lateral elbow radiographs provided an accurate diagnosis of pediatric supracondylar fracture comparable to radiologists.

CLINICAL RELEVANCE/APPLICATION

Our study suggests a potential role of deep learning as triage in the management of pediatric elbow trauma, as our model showed high sensitivity and high negative predictive value in automated detection of a supracondylar fracture on elbow radiography.

SST08-04 Automatic Measurement of Leg Length Discrepancies in Pediatric Patients on X-Ray Imaging Using Deep Learning

Friday, Dec. 6 11:00AM - 11:10AM Room: E261

Participants

Qiang Zheng, Philadelphia, PA (*Presenter*) Nothing to Disclose Sphoorti Shellikeri, Philadelphia, PA (*Abstract Co-Author*) Nothing to Disclose Misun Hwang, MD, Ellicott City, MD (*Abstract Co-Author*) Nothing to Disclose Raymond W. Sze, MD, Philadelphia, PA (*Abstract Co-Author*) Nothing to Disclose

For information about this presentation, contact:

zhengq@email.chop.edu

PURPOSE

Leg length discrepancy studies are commonly ordered orthopedic conventional radiographic studies, which are simultaneously labor intensive and cognitively simple studies for pediatric radiologists, representing an inefficient use of the radiologist's time and expertise. The purpose of our study is to demonstrate that measuring and calculating differences in femur and tibia lengths on pediatric leg length discrepancy studies based on X-ray imaging can be automated and performed rapidly by a deep learning algorithm.

METHOD AND MATERIALS

The femora and tibiae of pediatric legs were segmented and measured by a cascaded coarse-fine convolutional neural network (CNN). Specifically, we trained a coarse CNN model to classify the leg to the left and right sides of subject, then the fine leg segmentation was performed on each side. In order to augment the training data and improve the segmentation accuracy, we adopted a leg shape based image registration method to generate more training samples after flipping the left side leg images vertically. The leg length was measured by extracting corresponding pixels on the edges and calculating the distances between

RESULTS

X-ray imaging scans of 103 subjects (48 male/ 55 females, mean age 12.99, SD 2.84) were identified in this study. We randomly selected 70 subjects as training data and 33 images as testing data. After the data augmentation by shape based image registration, the training data had 19600 samples. Results demonstrated that the cascaded coarse-fine deep learning method performed accurate segmentation on pediatric legs. On the testing data, the segmentation accuracy was 0.90, the correlation value between truth measurement from radiology reports and calculated measurements was 0.9772 (p<0.001), and the mean squared error was 1.4 mm. The automated measurements took less 1 second for each subject.

CONCLUSION

The deep learning algorithm can quickly perform the task of measuring leg lengths as accurately as subspecialty trained pediatric radiologists.

CLINICAL RELEVANCE/APPLICATION

The rapid and automated measurement of leg length as accurately as subspecialty trained pediatric radiologists will help make more efficient use of the radiologist's time and expertise. The automation of the labor intensive and cognitively undemanding task of measurement can enable radiologists to focus on seeking subtle additional findings such as bone tumors or metabolic disease.

SST08-05 Rethinking Greulich & Pyle: Deep Learning Models for Pediatric Bone Age Assessment

Friday, Dec. 6 11:10AM - 11:20AM Room: E261

Participants

Ian Pan, MA, Providence, RI (*Presenter*) Consultant, MD.ai Simukayi Mutasa, MD, New York, NY (*Abstract Co-Author*) Nothing to Disclose Derek Merck, PhD, Providence, RI (*Abstract Co-Author*) Nothing to Disclose Carrie B. Ruzal-Shapiro, MD, Bronx, NY (*Abstract Co-Author*) Nothing to Disclose Rama S. Ayyala, MD, Providence, RI (*Abstract Co-Author*) Nothing to Disclose David W. Swenson, MD, Providence, RI (*Abstract Co-Author*) Nothing to Disclose

For information about this presentation, contact:

ianpan358@gmail.com

PURPOSE

The Greulich & Pyle (G&P) atlas is the most common standard by which bone age assessment (BAA) is performed. This study compares G&P-based BAA (GP-BAA) with deep learning-based BAA (DL-BAA).

METHOD AND MATERIALS

DL-BAA uses a 3-model MobileNetV2 convolutional neural network (CNN) ensemble trained on 13,769 pediatric trauma hand radiographs (male: 6,889, female: 6,880, age range: 0-18 years, mean age: 11.1 years) from a large academic medical center using the patient's chronological age as ground truth. Separate models were trained for male and female patients. The test set comprised 214 pediatric trauma hand radiographs (male: 100, female: 114, age range: 1-18 years, mean age: 11.7 years) from a geographically distinct large academic children's hospital with chronological age as ground truth. Using mean absolute error (MAE), we compared performance of DL-BAA on the test set with that of 3 GP-BAA ratings, including two board-certified pediatric radiologists who each used G&P, and a CNN ensemble trained on G&P-labeled pediatric hand radiographs from the RSNA Pediatric Bone Age Machine Learning Challenge (RSNA-AI). The RSNA-AI had achieved a MAE of 4.35 months in the challenge. Statistical analysis was performed using the bootstrap method.

RESULTS

The MAE between radiologists 1 and 2 for the test set was 6.3 months; the MAEs between RSNA-AI and radiologists 1 and 2 were 8.6 months and 10.1 months, respectively. The MAEs in months of DL-BAA, radiologist 1, radiologist 2, and RSNA-AI were 11.8, 14.6, 16.0, and 14.2, respectively. For female (male) patients, the MAEs of DL-BAA and GP-BAA were 11.6 (12.0) months and 14.6-16.8 (13.5-15.0) months, respectively. All MAE differences between DL-BAA and GP-BAA were statistically significant with p < 1e-6. On average, all ratings overestimated chronological age by 5.2 to 8.3 months. DL-BAA and GP-BAA estimated bone ages within 12, 18, and 24 months of chronological age for 68% vs. 61-68%, 85% vs. 65-78%, and 94% vs. 85-87% of test cases.

CONCLUSION

DL-BAA performed with lower mean absolute error for a normal pediatric population than either pediatric radiologist or automated GP-BAA. Future work will validate this method on other patient populations with more test data.

CLINICAL RELEVANCE/APPLICATION

DL-BAA should be an integral part of the future of BAA, as it can achieve equal-to-superior performance versus conventional methods and easily be adapted to different patient populations.

SST08-06 Prediction of Neurodevelopmental Outcome in Preterm Neonates with Cerebral MR Spectroscopy and DTI Using Feed-Forward Neural Networks

Friday, Dec. 6 11:20AM - 11:30AM Room: E261

Participants

Tanja Janjic, Innsbruck, Austria (*Presenter*) Nothing to Disclose Sergiy Pereverzyev Jr, Innsbruck, Austria (*Abstract Co-Author*) Nothing to Disclose Lukas Lamplmayr, Innsbruck, Austria (*Abstract Co-Author*) Nothing to Disclose Vera Wallner, Innsbruck, Austria (*Abstract Co-Author*) Nothing to Disclose Ruth Steiger, Innsbruck, Austria (*Abstract Co-Author*) Nothing to Disclose Martina Zimmermann, Innsbruck, Austria (*Abstract Co-Author*) Nothing to Disclose Marlene Biermayr, Innsbruck, Austria (*Abstract Co-Author*) Nothing to Disclose Vera Neubauer, Innsbruck, Austria (*Abstract Co-Author*) Nothing to Disclose Ursula Kiechl-Kohlendorfer, Innsbruck, Austria (*Abstract Co-Author*) Nothing to Disclose Anna Buchheim, Innsbruck, Austria (*Abstract Co-Author*) Nothing to Disclose Astrid Grams, MD, Innsbruck, Austria (*Abstract Co-Author*) Nothing to Disclose Elke R. Gizewski, MD, PhD, Innsbruck, Austria (*Abstract Co-Author*) Nothing to Disclose

For information about this presentation, contact:

tanja.janjic@i-med.ac.at

PURPOSE

We aimed to evaluate if proton magnetic resonance spectroscopy (1H-MRS) and diffusion tensor images (DTI) performed in very preterm neonates (PNs) at term equivalent age (TEA) can predict their neurodevelopmental outcome (NDO) at the corrected age of 12 months using feed-forward neural-networks (fNNs).

METHOD AND MATERIALS

From 346 PNs born before 32 gestational weeks, 246 were excluded due to missing or poor-quality spectroscopy data and/or missing neurodevelopmental tests at 12 months corrected age. The data sets of 100 PNs were considered for motoric and cognitive development, of whom 8 and 5, respectively were categorized as underdeveloped. We evaluated five potentially relevant metabolite ratios and two DTI characteristics, each in six different areas of the brain. We performed a feature selection algorithm for receiving a subset of those characteristics that we could assume as significant. To reduce bias by unbalanced classes, only PNs that share approximate values of those characteristics with ones that had shown underdevelopment were considered for further calculations. On those smaller sets of PNs, we finally constructed predictors using fNNs, which were able to predict underdevelopment in PNs after considering the characteristics selected previously.

RESULTS

The constructed predictors give a 100% accuracy in the case of the motoric underdevelopment. In the case of cognitive underdevelopment, we obtain a true positive rate of 100% and a positive predictive value of 83,3 %.

CONCLUSION

1H-MRS and DTI obtained at TEA in PNs allow prediction of their motoric and cognitive development at the corrected age of 12 months. The proposed approach using fNNs promises its use in clinical practice and could be useful for spotting those PNs, who would mostly benefit from early intervention services.

CLINICAL RELEVANCE/APPLICATION

1H-MRS and DTI obtained at term equvalent age in very preterm neonates allow prediction of their motoric and cognitive development at the corrected age of 12 months, and the proposed approach using fNNs could be useful for spotting those preterm neonates, who would mostly benefit from early intervention services.

SST08-07 MRI Radiomics Profiling of Pediatric Medulloblastoma Improves Risk Stratification Beyond Clinical and Conventional MR Imaging Features

Friday, Dec. 6 11:30AM - 11:40AM Room: E261

Participants

Hui Zheng, Shanghai, China (*Presenter*) Nothing to Disclose Yuhua Li, Shanghai, China (*Abstract Co-Author*) Nothing to Disclose Huanhuan Liu, Shanghai, China (*Abstract Co-Author*) Nothing to Disclose Ming Liu, Shanghai, China (*Abstract Co-Author*) Nothing to Disclose Dengbin Wang, MD, Shanghai, China (*Abstract Co-Author*) Nothing to Disclose

For information about this presentation, contact:

zhenghui@xinhuamed.com.cn

PURPOSE

Radimoics is a powerful and promising approach to predict the disease prognosis. Our purpose was to evaluate magnetic resonance imaging (MRI) radiomics signature in stratifying the risk of pediatric medulloblastoma with overall survival (OS).

METHOD AND MATERIALS

Eighty-two children (mean age: 5.9 ± 3.1 years) with pathologically confirmed medulloblastoma and preoperative MR images were retrieved from the database of our hospital from November 2006 to October 2017. Three hundreds and eighty-five radiomics features were extracted from postcontrast T1 weighted images and the features correlated with OS of pediatric medulloblastoma were identified using the least absolute shrinkage and selection operator (LASSO) Cox regression model. Five-fold cross validation was used to test steadiness of selected features. The radimoics signature (Ras-score) was generated and the incremental value of the radimoics signature to the clinical and conventional MR imaging features for personalized OS estimation was calculated by comparing the models in different layers.

RESULTS

Seven selected radiomics features-based Rad-score could enable the stratification of medulloblastoma for OS (HR: 5.8; [CI]: 2.07, 16.27; P<0.01). Among the models from different layers, the integrative model combined Rad-score, clinical and conventional imaging features was the most accurate model in predicting the OS of children with medulloblastoma (C-index:0.928).

CONCLUSION

Rad-score radiomics allow predicting OS of the pediatric patients with medulloblastoma. And the predictive performance can be improved when combined with the clinical and conventional MR imaging characteristics.

CLINICAL RELEVANCE/APPLICATION

Radiomics is an approach which can provide a great deal of quantitative features reflecting intratumoral heterogeneity. Combined with clinical and conventional MR imaging features, radiomics could increase predictive accurancy for children with medulloblastoma.

SST08-08 CT-Based Radiomics Signature: A Potential Non-Invasive Biomarker for Predicting MYCN Amplification in Neuroblastomas in Children

Friday, Dec. 6 11:40AM - 11:50AM Room: E261

Participants

Haoting Wu, Shanghai, China (*Presenter*) Nothing to Disclose Hui Zheng, Shanghai, China (*Abstract Co-Author*) Nothing to Disclose Chenqing Wu, Shanghai, China (*Abstract Co-Author*) Nothing to Disclose Huanhuan Liu, Shanghai, China (*Abstract Co-Author*) Nothing to Disclose Li Jun Wang, MMedSc, BMedSc, Shanghai, China (*Abstract Co-Author*) Nothing to Disclose Wenbin Guan, Shanghai, China (*Abstract Co-Author*) Nothing to Disclose Shaofeng Duan, Shanghai, China (*Abstract Co-Author*) Nothing to Disclose Lei Wang, Shanghai, China (*Abstract Co-Author*) Nothing to Disclose Dengbin Wang, MD, Shanghai, China (*Abstract Co-Author*) Nothing to Disclose

For information about this presentation, contact:

15057536257@163.com

PURPOSE

To develop a CT-based radiomics signature and evaluate its capability for predicting the MYCN-amplification (MNA) in neuroblastomas (NBs) in children.

METHOD AND MATERIALS

This retrospective study included 77 children with histopathological-confirmed neuroblastomas (39 in training group and 38 in test group). Clinical information were recorded for each child.Children underwent MYCN gene detection and contrast-enhanced CT before treatment. Region of interest (ROI) was manually delineated in pre-contrast phase, arterial phase, and venous phase with five slices of primary tumor, and 396 CT-based radiomics features were extracted from each phase respectively. The synthetic minority oversampling technique (SMOTE) was used to balance the sample number in training group (MNA vs non-MNA, 7 vs 32). Four radiomics signatures were built by the least absolute shrinkage and selection operator (LASSO) logistic regression model based on the 3 phases and combined phase, respectively. The receiver operating characteristics curve (ROC) analysis and 10-fold aross validation were conducted to evaluate the predictive performance of them. The developed radiomics signature was further validated for its predictability in the test group.

RESULTS

All of four CT-based radiomics signatures were developed as an independent predictor for MNA in NBs. The best predicting performance of MNA was from the combination of pre- and post-phases. The sensitivity, specificity, accuracy and area under the curve of training group were 96.4%, 100%, 98.0%, and 1.00, while 93.8%, 100%, 94.9%, and 0.98 in the test group, respectively.

CONCLUSION

The proposed CT-based radiomic signature can potentially help in predicting MNA in pretreated NBs in children. Combination of images in the pre- and post-contrast phase can serve as a better non-invasive biomaker for the identification of MNA.

CLINICAL RELEVANCE/APPLICATION

This study is designed to developing a CT-based radiomics signature and evaluating its capability for predicting the MYCNamplification (MNA) in neuroblastomas (NBs) in children. The proposed CT-based radiomic signature can potentially serve as a noninvasive biomaker for the identification of MNA.

SST08-09 CT-Based Radiomic Analysis Predicts Prognosis in Pediatric Malignant Peripheral Neuroblastic Tumors: A Single Center Retrospective Study

Friday, Dec. 6 11:50AM - 12:00PM Room: E261

Participants

Xiao Xia Wang, Shanghai, China (*Presenter*) Nothing to Disclose Xinrong Wang, Shanghai , China (*Abstract Co-Author*) Nothing to Disclose Ling Chen, Shanghai, China (*Abstract Co-Author*) Nothing to Disclose Yumin Zhong, MD, Shanghai, China (*Abstract Co-Author*) Nothing to Disclose Xin Li, Shanghai, China (*Abstract Co-Author*) Nothing to Disclose

For information about this presentation, contact:

wangxiaoxia0430@hotmail.com

PURPOSE

The aim of this study was to develop and validate a preoperative radiomics analysis system based on CT images to predict outcome in pediatric malignant PNTs.

METHOD AND MATERIALS

A total of 405 patients (training cohort: n = 280; validation cohort: n = 121) pathologically diagnosed as malignant PNTs including neuroblastoma (NB) and ganglioneuroblastoma (GNB) were retrospectively studied between January 2010 and June 2018. Every patient underwent post-contrast enhanced CT examination before any treatment. Patients were divided into low-, intermediate-, and high-risk groups according to clinical prognostic factors. All radiomics features were extracted from manually segmented tumors in artery phase of CT images in all cases, and they were derived from first-order histogram, tumor shape, gray-level co-occurrence matrix (GLCM), gray-level run length matrix (GLRLM), gray-level size zone matrix (GLSZM), neighboring gray-tone difference matrix (NGTDM), gray-level dependence matrix (GLDM). Spearman's rank order correlation with 0.9 threshold and least absolute shrinkage and selection operator (LASSO) were used for redundancy elimination and feature selection, respectively. To build a classifier for stratifying three groups of risk, two logistics regression models were applied in a cascade way. The first model (model1) was used for classifying high-risk group and the rest, while the rest were classified into intermediate- and low-risk groups by the second model (model2). The performance of the predictive models was evaluated with the respect to the receiver operating characteristics (ROC) curve. Above works were completed by IFoundry (Intelligence Foundry 1.1, GE Healthcare).

RESULTS

18 and 32 features were obtained after the process of redundancy elimination and feature selection for model1 and model2 respectively. The models demonstrated good discrimination in both training cohort and validation cohort, with AUC of 0.826 for model1 and that of 0.811 for model2.

CONCLUSION

Radiomics analysis based on preoperative CT images has the potential to predict clinical prognosis and aid to stratify individualized treatments of pediatric malignant PNTs. Future studies are needed to validate these findings.

CLINICAL RELEVANCE/APPLICATION

Radiomics approach may be used to aid intratumoral heterogeneity detection and outcome prediction in malignant PNTs children.

Printed on: 10/29/20







SST09

Physics (CT - Artifact Reduction)

Friday, Dec. 6 10:30AM - 12:00PM Room: E351



AMA PRA Category 1 Credits ™: 1.50 ARRT Category A+ Credit: 1.75

FDA Discussions may include off-label uses.

Participants

Xiaochuan Pan, PhD, Chicago, IL (*Moderator*) Founder, XP Imaging, LLC; Shareholder, XP Imaging, LLC; Founder, XPIM, LLC; Shareholder, XPIM, LLC; Founder, Clarix Imaging Corp; Shareholder, Clarix Imaging Corp Shuai Leng, PHD, Rochester, MN (*Moderator*) Nothing to Disclose

Sub-Events

SST09-01 A Deep Learning-Based Dual-Domain Model for Reducing Metal Artifacts in Clinical CT Images

Friday, Dec. 6 10:30AM - 10:40AM Room: E351

Participants

Yuanyuan Lyu, Zushou, China (*Abstract Co-Author*) Z2AI Corporation Wei-An Lin, College Park, MD (*Abstract Co-Author*) Nothing to Disclose Haofu Liao, Rochester, NY (*Abstract Co-Author*) Nothing to Disclose Jingjing Lu, MD, Boston, MA (*Abstract Co-Author*) Nothing to Disclose Lei Wang, Beijing, China (*Abstract Co-Author*) Nothing to Disclose S. Kevin Zhou, Princeton, NJ (*Presenter*) Employee, Siemens AG

For information about this presentation, contact:

lvyuanyuanoo@gmail.com

CONCLUSION

Our proposed deep learning model yields better metal artifact reduction performance than other state-of-the-art methods and can be applied in the real word.

Background

Metallic implants cause severe streak and beam hardening artifacts in CT scans. Traditional methods, like linear interpolation (LI) and NMAR, inpaint affected sinogram to reduce artifact, but induce secondary artifacts or suffer from false tissue segmentation. Recently, deep learning based method, cGan-CT, tries to reduce artifacts in image domain but the effect is limited. Here, we propose a Dual-Domain Network (DuDoNet) and demonstrate its application to clinical data.

Evaluation

DuDoNet consists of a sinogram enhancement network (SE-Net), a differentiable Radon inversion layer (RL) and an image enhancement network (IE-Net). The SE-Net learns to restore sinogram data via a mask pyramid U-Net. RL reconstructs images from sinograms and allows joint learning of the two networks. The IE-Net further refines the images by a U-Net with residual learning. The learning of DuDoNet, which takes metal affected sinograms and corresponding metal traces as inputs, is supervised with clean sinograms and images. We synthesize 360,000 training and 2,000 validation samples based on DeepLesion. In synthesized data, DuDoNet restores the most details among all methods, with a PSNR of 32.29dB and a SSIM of 0.959. Our model successfully reduces the streak and shadowing artifacts and alleviates drawbacks of single domain methods. Then, DuDoNet trained on simulated data is applied to a total of 100 clinical images from DeepLesion and SpineWeb. Visual comparison shows that DuDoNet effectively suppresses the secondary artifacts and avoids false structural segmentation problem in prior based methods. Blinded qualitative evaluation by radiologists shows DuDoNet achieves the best performance (rank: 3.13) and significantly outperforms LI, NMAR, cGan-CT (p<0.028).

Discussion

In DuDoNet, SE-Net first recovers inconsistent sinograms and IE-Net further reduces secondary artifacts. Our model effectively reduces metal artifacts in both simulated and clinical scans and achieves better image quality than other single domain approaches.

SST09-02 Reduction of Artifacts from High-Density Moving Objects in C-arm CBCT Using a Deep Learning-Based Segmentation Approach

Friday, Dec. 6 10:40AM - 10:50AM Room: E351

Participants

Daniel Gomez-Cardona, PhD, Rochester, MN (*Presenter*) Nothing to Disclose Shuai Leng, PHD, Rochester, MN (*Abstract Co-Author*) Nothing to Disclose Christopher P. Favazza, PhD, Rochester, MN (*Abstract Co-Author*) Nothing to Disclose Beth A. Schueler, PhD, Zumbrota, MN (*Abstract Co-Author*) Nothing to Disclose Kenneth A. Fetterly, PhD, Rochester, MN (*Abstract Co-Author*) Nothing to Disclose

For information about this presentation, contact:

gomezcardona.daniel@mayo.edu

PURPOSE

Moving, high-density objects in the heart, including catheters and pacemaker leads, cause substantial artifacts in cone beam CT (CBCT) images. The purpose of this work was to exploit a deep learning method to efficiently segment and remove these objects from projection rotational angiography (RA) images, thereby reducing artifacts in cardiovascular CBCT images.

METHOD AND MATERIALS

Segmentation of the high-density objects from the RA images was performed using a deep convolutional neural network with an encoder-decoder architecture based on the VGG-16 network. Synthetic training (3,000) and validation (2,000) images were created by adding augmented RA images of a pigtail catheter to RA images of an anthropomorphic phantom acquired with a clinical angiography system. The model trained with the synthetic images was then used as a starting point to learn to label pacemaker leads and different type of catheters in two real patient data sets. The new image set consisted of 450 and 50 RA images in total for training and validation, respectively. Data was augmented by reflection, translation, size scaling, rotation, and noise addition in both image sets. To remove high-density object artifacts, the segmented image pixels were inpainted by solving the Dirichlet boundary value problem. Correlated Poisson noise was then added to the inpainted pixels to match image texture. The original and modified RA images were reconstructed using filtered back-projection to create CBCT images.

RESULTS

Training for the synthetic and patient images took 25 and 2 hours, respectively. A Sørenson-Dice coefficient of 80.8% and 75.6% was obtained for each set, respectively. These values are partly explained by the model output which extended modestly beyond the edges of the ground truth representation of the objects. Visual inspection of the resultant patient CBCT images demonstrated that artifacts associated with moving catheters and pacemaker leads were nearly completely resolved without introduction of other image defects.

CONCLUSION

A deep learning method to segment catheters and pacemaker leads in projection RA images of the heart was implemented and used to mitigate associated artifacts in CBCT images of the heart.

CLINICAL RELEVANCE/APPLICATION

This work demonstrates a deep learning segmentation method to mitigate the artifacts caused by moving high-density objects in the heart, thereby providing substantially improved CBCT images.

SST09-03 Dental Artifact Reduction Using a Three-Stage Projection-Based Metal Artifact Reduction Algorithm for Spectral Imaging: A Phantom Study

Friday, Dec. 6 10:50AM - 11:00AM Room: E351

Participants

Nikesh Muthukrishnan, Montreal, QC (*Presenter*) Nothing to Disclose Elizabeth Nett, Waukesha, WI (*Abstract Co-Author*) Employee, General Electric Company Sahir Bhatnagar, PhD, Montreal, QC (*Abstract Co-Author*) Nothing to Disclose Deborah R. Shatzkes, MD, New York, NY (*Abstract Co-Author*) Nothing to Disclose C. Douglas Phillips, MD, New York, NY (*Abstract Co-Author*) Nothing to Disclose Griselda T. Romero Sanchez, MD, Montreal, QC (*Abstract Co-Author*) Nothing to Disclose Rajiv Gupta, PhD, MD, Boston, MA (*Abstract Co-Author*) Nothing to Disclose Reza Forghani, MD,PhD, Cote Saint-Luc, QC (*Abstract Co-Author*) Researcher, General Electric Company; Institutional research collaboration, General Electric Company; Consultant, General Electric Company; Speaker, General Electric Company ; Founder, 4intelligent Inc; Stockholder, 4intelligent Inc; Stockholder, Real-Time Medical, Inc

For information about this presentation, contact:

nikesh.muthukrishnan@mail.mcgill.ca

PURPOSE

Dental artifact remains a significant challenge on neck computed tomography. The purpose of this study is to evaluate a novel three-stage projection-based metal artifact reduction (GSI MAR) algorithm for reducing dental artifact using a phantom. The study evaluates the effectiveness of the MAR algorithm on dual energy acquisitions, the impact of radiation dose and the impact of MAR on multiple iodine concentrations.

METHOD AND MATERIALS

Two dental amalgams were inserted in a phantom next to five varying iodine concentrations to simulate the effects of artifact on enhancing tissues. Scans were acquired at five different doses and reconstructed without or with GSI MAR. Quantitative analysis was performed using standard deviation (SD), signal-to-noise ratio (SNR) and contrast-to-noise ratio (CNR) of strategically located regions of interest (ROI). The impact across 40 keV to 140 keV virtual monochromatic image (VMI) were evaluated. Qualitative analysis was performed by two external radiologists, estimating artifact reduction, anatomical and contrast improvement. Lastly, material decomposition maps were used for estimating iodine content.

RESULTS

Quantitative results indicated that the GSI MAR significantly lowered noise at all energy levels. Noise reduction percentage was highest at 70.72 % in the 135 keV VMI and the lowest at 58.70% in the 40 keV VMI. Iodine conspicuity was highest at low energy levels. A 348.58 % CNR and 294.35 % SNR increase was calculated at 40 keV VMI and a 18.5 % CNR and 14.25 % SNR increase in the 140 keV VMI. GSI-MAR improved the iodine estimation error from 146.95% to 62.82%. Subjective analysis indicated that the MAR provided higher quality acquisitions with an average artifact reduction between 51-75%.

CONCLUSION

Quantitative analysis of GSI MAR indicated an improvement of image quality across all energy levels. Lowest noise was found at higher energy levels and highest CNR and SNR was found at lower energy levels. Furthermore, subjective review indicated that MAR reconstructions provided higher quality images. Finally, GSI MAR was found to improve iodine concentration estimation.

CLINICAL RELEVANCE/APPLICATION

Dental artifact remains a significant challenge on neck computed tomography. This study evaluates the effectiveness of a novel metal artifact reduction algorithm.

ssT09-04 CT Image Quality for Five Different Metal Artifact Reduction Algorithms

Friday, Dec. 6 11:00AM - 11:10AM Room: E351

Participants

Mercy Victoria Kataike, Oslo, Norway (*Abstract Co-Author*) Nothing to Disclose Matt Whitaker, Salem, NY (*Abstract Co-Author*) Employee, Image Owl, Inc Hilde K. Andersen, MSc, Oslo, Norway (*Abstract Co-Author*) Nothing to Disclose Caroline Stokke, PhD, Oslo, Norway (*Abstract Co-Author*) Nothing to Disclose Anne C. Martinsen, Oslo, Norway (*Presenter*) Nothing to Disclose

PURPOSE

To evaluate the effectiveness of five CT Metal Artifact Reduction (MAR) Algorithms from four vendors in improving the image quality using a novel phantom for Metal Artifact Analysis.

METHOD AND MATERIALS

A Catphan 605 phantom with extension ring was scanned with different inserts (Hard Steel, Titanium, and Water) on 5 CT scanners reconstructed with and without MAR algorithms. The MAR algorithms used; GSI MAR (GE Revolution CT), Smart MAR (GE Revolution Frontier), O-MAR (Philips Ingenuity CT), iMAR (Siemens Somatom Drive) and SEMAR (Toshiba Aquilion One Genesis). Phantom was scanned at 120kV and at 120 kVp equivalent for GSI MAR and iMAR. Image quality was assessed by obtaining Contrast to Noise Ratio (CNR), Metal Artifact Analysis and Noise Power Spectrum (NPS). The parameters were obtained from ImageOwl Catphan QA software and Matlab.

RESULTS

For Titanium, Smart MAR, iMAR and SEMAR images had more noise than the images without MAR algorithms, while GSI MAR and O-MAR images had less noise than the images without MAR. MAR images had a lower CNR than the corresponding images without MAR, except GSI MAR images which had higher CNR than the images without MAR. For water, there was no difference in CNR for images with and without MAR, except iMAR and SEMAR. Metal Artifact Analysis showed artifact reduction around the insert and at a distance from the insert for all MAR algorithms in like manner. For titanium, GSI MAR showed the largest artifact reduction (87%, 73% respectively) followed by Smart MAR, SEMAR, O-MAR and iMAR. For hard steel, Smart MAR showed the largest artifact reduction (92%, 82%) followed by GSI MAR, SEMAR, iMAR, and O-MAR.There was no difference in NPS with and without MAR.

CONCLUSION

GSI MAR showed the most consistent performance under different conditions. Different MAR algorithms compensate differently for metal artifacts under different conditions. Thus, it is important to know the effects of the algorithms on image quality. Images obtained with MAR algorithms should be compared with those without MAR algorithms.

CLINICAL RELEVANCE/APPLICATION

Different MAR algorithms compensate for metal artifacts differently under different conditions. Thus, it is important to know the effects of the algorithms on image quality.

SST09-05 Image Quality Assessment of Metal Artefact Reduction in CT Using a Novel Abdominal Phantom

Friday, Dec. 6 11:10AM - 11:20AM Room: E351

Participants Mercy Afadzi, PhD, Olso, Norway (*Presenter*) Nothing to Disclose Oyvind T. Overbo, Oslo, Norway (*Abstract Co-Author*) Nothing to Disclose Kristin Jensen, Oslo, Norway (*Abstract Co-Author*) Nothing to Disclose Anne C. Martinsen, Oslo, Norway (*Abstract Co-Author*) Nothing to Disclose

PURPOSE

To evaluate a novel anthropomorphic abdominal phantom specially designed for qualitative and quantitative metal artefact assessment in CT for two different metal artefact reduction technologies.

METHOD AND MATERIALS

A anthropomorphic abdominal phantom with different inserts (bone with metal, low contrast, spatial resolution and homogeneity) was used in this study. Titanium, Hard and stainless steel inserts were placed in the center of the bone insert. All scans were performed on a GE Revolution CT at 15 and 20 mGy CTDIvol, 40 mm collimation, 120 kVp (+/- HiRes) and spectral imaging (GSI). Images were reconstructed with standard kernel, 2.5 mm slices, ASIR-V 50% and +/- MAR. Four observers evaluated lesion conspicuity and scored artefacts on a 4-point scale for all reconstructions. HU uniformity, coefficient of variation, reduction in noise streaks (range and standard deviations (SD)), noise power spectrum (NPS) and modulation transfer function (MTF) were evaluated for all reconstructions.

RESULTS

Preliminary quantitative and qualitative results showed that both single energy MAR (SMAR) and GSI MAR (GSIMAR) reduced streaks artefacts surrounding (2123-7019 vs 1267-5993 HU) and at a distance (196-251 vs 78-83 HU). Lesion conspicuity was not affected by MAR. HU uniformity and SD around the metals (223.08-438.76 vs 105.02-260.75 HU) and the bone insert (SD: 71.48 -143.17 vs 39.59 - 69.97 HU) were improved by the use of both SMAR and GSIMAR. These improvements were independent of dose. The use of only HiRes without MAR did not reduce streaks artefact, noise or HU uniformity. MAR hardly affected the MTF@50%. NPS profile

CONCLUSION

Both SMAR and GSIMAR reduced metal artefact and improved image quality. Anthropomorphic phantom designed for qualitative and quantitative image quality analysis evaluation of metal artefact reduction should be used to assess image quality and lesion detection when MAR is introduced in daily routine to ensure that pathology is not missing after MAR has been applied.

CLINICAL RELEVANCE/APPLICATION

New anthropomorphic phantom specially designed for quantitative and qualitative assessment of metal artefact reduction in CT is important to ensure that pathology is not missing when MAR is applied.

ssT09-06 Reduction of Cone-Beam Artifacts in Axial CT Systems with Large Detector Coverage

Friday, Dec. 6 11:20AM - 11:30AM Room: E351

Participants

Stanislav Zabic, PhD, Mayfield Village, OH (*Presenter*) Employee, UIH America, Inc Hao Zhao, Shanghai, China (*Abstract Co-Author*) Employee, Shanghai United Imaging Healthcare Co, Ltd Rengcai Yang, Shanghai, China (*Abstract Co-Author*) Employee, Shanghai United Imaging Healthcare Co, Ltd

PURPOSE

We report cone-beam artifact reduction on axial scans with a 16cm coverage CT system using a recursive application of 3D filtered backprojection (FBP).

METHOD AND MATERIALS

Axial CT for voxels outside the acquisition plane does not satisfy a fundamental completeness condition, which leads to cone-beam artifacts. This is particularly evident in systems with large detectors. Previously published re-projection based recursive application of FBP was used to improve image quality in large pitch helical scans. We revisit this approach, apply it to the axial 3D FBP reconstruction and explain the effectiveness of the algorithm using a new argument based on the minimization of Bregman distances. The theoretical result is tested with analytic simulations and clinical data sets, reused from the previous clinical trials.

RESULTS

Recursive FBP algorithm reduced the low frequency artifacts in simulations effectively, returning images which are approaching the analytic ground-truth with every repeated recursive step. In clinical data, cone beam artifacts were considerably reduced with a more pragmatic combination of image processing and one recursive FBP application.

CONCLUSION

Bregman distance minimization algorithm leads to a previously known recursive 3D FBP algorithm, which proves to be effective for axial scans on systems with large detector coverage, offering a strong, new theoretical foundation for this algorithm. A pragmatic combination of recursive FBP with image processing returns high quality results from single-shot axial scans with improved bone clarity and more accurate CT numbers in the soft tissue.

CLINICAL RELEVANCE/APPLICATION

Cardiac scans can be performed within a single heartbeat using an axial CT with 0.25s rotation time and 16cm detector coverage. Tilted single shot axial head scanning ensures an efficient protection against excessive x-ray dose delivered to the eye lenses. Efficient reduction of cone-beam artifacts for both of these protocols is necessary.

SST09-07 Reduction of Artifact Caused by Embolization Coil Implant in Spectral CT Examination by Means of Virtual Monochromatic Imaging (VMI) and Monochromatic Imaging Combined with Metal Artifact Reduction Software (MARs)

Friday, Dec. 6 11:30AM - 11:40AM Room: E351

Participants Zhipeng Yao, Beijing, China (*Presenter*) Nothing to Disclose Yahui Peng, PhD, Chicago, IL (*Abstract Co-Author*) Nothing to Disclose

PURPOSE

To evaluate the reduction of artifact from embolization coil implant using VMI and VMI combined with MARs in spectral CT.

METHOD AND MATERIALS

Embolization coil implant was placed in an intermediate tube of the Quantitative Standard Pulsating Phantom (QSP) that contained an Iodine solution of 7 mgI/ml (CT value = 160HU at 120 kVp, representing the portal vein attenuation in the portal vein phase). Subsequently, 20 ml of sodium chloride solution was contained in eight tubes and inserted into the QSP. Two spectral CT scan protocols were used for image acquisition: conventional CT scan with tube voltage of 120 kVp(Group A); Spectral Imaging scan (Group B). A conventional image (CI) and virtual monochromatic images (70 - 140 keV, of 10 keV interval) with and without MARs were reconstructed, respectively. In each of the images, a measurement region of interest (ROI) was placed around the tube , including all pixels contaminated by the metal artifact but excluding the pixels inside the tube(ROItube). Besides, a background ROI was placed above the tube not influenced by the artifact, from where mean CT number(NCT) and standard deviation (SD) were measured. Δ CT was defined as the absolute value of NCT in hyperdense or hypodense artifact minus NCT in background ROI.

RESULTS

VMIMARs showed a significant decrease of hyperdense artifact (p<0.05)and hypodense artifact(p<0.05)in term of lower Δ CT as compared to 120kVp imaging. With increasing of KeV , Δ CT and SD of artifact were decreasing in VMIMARs.In addition, noise image in VMIMARs exhibited a decreasing trend with increasing keV level. Whereas VMI only showed a significant decrease of hyperdense artifact (p<0.05). VMIMARs at 70 keV -140keV could show a better effect on the reduction of metal artifact as compared VMI at 140keV(p<0.05).

CONCLUSION

Compared with conventional CT scanning, VMIMARs by using spectral CT could significantly reduce metal artifacts caused by embolization coil implants and provide better image noise.

CLINICAL RELEVANCE/APPLICATION

When using spectral CT for patients underwent Gastric coronary vein embolization(GCVE) produre, VMIMARs could significantly reduce metal artifacts caused by embolization coil implants in portal vein phase.

SST09-08 Ability of a Single Adaptive Iterative Metal Artifact Reduction Algorithm to Improve CT Image Quality in Patients with Multiple Metal Implants

Friday, Dec. 6 11:40AM - 11:50AM Room: E351

Participants

Julian A. Hagen, BSC, Malvern, PA (*Presenter*) Employee, Siemens AG
Christian Hofmann, Erlangen, Germany (*Abstract Co-Author*) Employee, Siemens AG
Payam Mohammadinejad, MD, Rochester, MN (*Abstract Co-Author*) Nothing to Disclose
Joel G. Fletcher, MD, Rochester, MN (*Abstract Co-Author*) Grant, Siemens AG; Consultant, Medtronic plc; Consultant, Takeda
Pharmaceutical Company Limited; Grant, Takeda Pharmaceutical Company Limited; ;
Zaiyang Long, PhD, Rochester, MN (*Abstract Co-Author*) Nothing to Disclose
Andreas Maier, DIPLENG, Erlangen, Germany (*Abstract Co-Author*) Nothing to Disclose
Ashish R. Khandelwal, MD, Rochester, MN (*Abstract Co-Author*) Nothing to Disclose
Cynthia H. McCollough, PhD, Rochester, MN (*Abstract Co-Author*) Nothing to Disclose
Cynthia H. McCollough, PhD, Rochester, MN (*Abstract Co-Author*) Research Grant, Siemens AG
Ahmed Halaweish, PhD, Rochester, MN (*Abstract Co-Author*) Research Grant, Siemens AG

PURPOSE

To compare performance of a single, adaptive iterative metal artifact reduction (AiMAR) algorithm applied to an entire patient's CT exam to 7 anatomically specific iMAR presets, in patients with multiple metal implants.

METHOD AND MATERIALS

In 30 patients with 72 types of implants, CT images were reconstructed with different strength settings of a single AiMAR algorithm and 2 - 3 iMAR presets (selected for body part/implant). The AiMAR algorithm enables real-time image-based measurements to adapt the degree and level of artifact reduction. In separate sessions, 2 trained radiologists evaluated artifacts (0 - 5), visualization of critical anatomic structures (1 - 5) and diagnostic confidence (1 - 5) in the region of each implant, also assigning an overall 'whole body' image quality score (1 - 5), considering all evaluated regions, with lower values for all scales being better. The optimal AiMAR strength was determined by comparing whole body image quality scores with individual iMAR presets in each body region. Significance was tested by Wilcoxon Signed rank test for paired samples.

RESULTS

Optimized results using AiMAR were achieved using strength settings 4 and 5 for head&neck, thoracic and extremity areas (dental, neuro, cervical spine,shoulder, thoracic spine, cardiac,arms/elbow, legs/knee). For abdomen/pelvis (hip, lumbar spine), preferred AiMAR strengths varied between 2 - 5, with the lower strengths providing higher diagnostic confidence and the higher strengths providing better artifact reduction. AiMAR strength 5 setting was preferred over lower strengths (p<0.05) when evaluating whole body image quality scores. For every body region, AiMAR strength 4 and 5 settings demonstrated widely overlapping (p>0.05) diagnostic confidence, visualization and artifact performance with the dedicated anatomically specific iMAR presets (figure).

CONCLUSION

In patients with multiple metal implants, a strength based adaptive implementation of artifact reduction (AiMAR) permits a single reconstruction of the entire body that provides a diagnostic quality anatomic evaluation and metal artifact reduction of similar quality compared to multiple reconstructions using separate body part specific iMAR presets.

CLINICAL RELEVANCE/APPLICATION

AiMAR can dramatically improve clinical workflow by minimizing the need for body-part specific iMAR reconstructions without compromising image quality, diagnostic confidence or artifact reduction.

SST09-09 Reproducibility and Validity of Approaches for Artifact Quantification in CT Imaging

Friday, Dec. 6 11:50AM - 12:00PM Room: E351

Participants

Nils Grosse Hokamp, MD, Koln, Germany (*Presenter*) Speakers Bureau, Koninklijke Philips NV Brendan Eck, Eaton, OH (*Abstract Co-Author*) Research Grant, Koninklijke Philips NV Florian Siedek, MD, Stanford, CA (*Abstract Co-Author*) Nothing to Disclose Daniel Pinto dos Santos, MD, Mainz, Germany (*Abstract Co-Author*) Nothing to Disclose Jasmin A. Holz, PhD, Cologne, Germany (*Abstract Co-Author*) Nothing to Disclose Zhouping Wei, Cleveland, OH (*Abstract Co-Author*) Nothing to Disclose David C. Maintz, MD, Koln, Germany (*Abstract Co-Author*) Nothing to Disclose Stefan Haneder, MD, Cologne, Germany (*Abstract Co-Author*) Nothing to Disclose

For information about this presentation, contact:

nils.grosse-hokamp@uk-koeln.de

PURPOSE

To objectify metal artifact reduction, numerous methods and approaches have been suggested. We aimed to compare results of such methods to visual perception of artifacts in order to establish a standard for artifact quantification in CT imaging.

METHOD AND MATERIALS

Two titanium rods (5 and 10mm) were examined with 25 different scanning and image reconstruction parameters to obtain a reference database of different types and extents of artifacts. 4 radiologists separately evaluated every image against each other (2-pair forced choice) using an in-house developed software. Rating was repeated two times (2400 comparisons = 2 times x 4 readers x 300 comparisons). Rankings were combined to obtain a reference ranking reaching from best to worst image. Proposed approaches for artifact quantification have been identified in literature, including manual measurement of artifact attenuation, standard deviation and noise as well as sophisticated algorithm-based approaches within the image- and frequency-domain (ImgD and FreqD, respectively). Two radiologists conducted manual measurements twice while the aforementioned algorithms were developed within the Matlab-Environment allowing for automated image analysis. The reference ranking was compared to all aforementioned methods for artifact quantification to identify suited and less-suited approaches. Besides visual analysis, Kappa-statistics were used to evaluate agreement between quantitative methods and visual perception. Intraclass correlation coefficients (ICC) indicated intra- and interreader agreement.

RESULTS

Intra- and Interreader agreement of visual artifact perception were excellent (ICC 0.85-0.92). No quantitative method was able to represent the exact ranking of visually perceived artifacts; however, ICC for manual measurements were low (ICC 0,25-0,97). The methods that showed best correspondence and reproducibility were ImgD and FreqD-based.

CONCLUSION

Artifact quantification in CT is challenging. Manual measurements show a limited reproducibility. We propose two methods that quantify artifacts in the image- and frequency-domain and that correspond closely to visual artifact perception.

CLINICAL RELEVANCE/APPLICATION

Automated measurements of artifact extent should be preferred over manual measurements as they correspond close to visual perception while the latter show a limited reproducibility.

Printed on: 10/29/20





SST10

Vascular/Interventional (Tumor Ablation & Biopsy)

Friday, Dec. 6 10:30AM - 12:00PM Room: E451B



AMA PRA Category 1 Credits ™: 1.50 ARRT Category A+ Credit: 1.75

FDA Discussions may include off-label uses.

Participants

Jennifer Montgomery, MD,PhD, Cleveland, OH (*Moderator*) Nothing to Disclose Nikunj R. Chauhan, MD, Cleveland, OH (*Moderator*) Nothing to Disclose

Sub-Events

SST10-01 Accuracy and Effectiveness of Transoral Contrast-Enhanced Ultrasound Guided Core Needle Biopsy for Oral Lesions

Friday, Dec. 6 10:30AM - 10:40AM Room: E451B

Participants Ting Wei, Chengdu, China (*Presenter*) Nothing to Disclose Man Lu, PhD, Chengdu, China (*Abstract Co-Author*) Nothing to Disclose

For information about this presentation, contact:

graceof@163.com

PURPOSE

To determine the accuracy and effectiveness of transoral contrast-enhanced ultrasound (CEUS) guided core needle biopsy (CNB) for oral lesions that could not be accurately identified or had a previously non-diagnostic cyto-histological biopsy.

METHOD AND MATERIALS

A consecutive series of 29 patients (age range, 31-81 years; mean 61±12 years; 18 male and 11 female) who underwent transoral CEUS-guided CNB of oral lesions at our hospital were evaluated retrospectively. Among them, 10(34.5%) lesions were inconspicuous and 19(65.5%) patients had a previously non-diagnostic cyto-histological exam by endoscopic or surgical incisional biopsy. Transoral CEUS-guided CNB was performed by using an endocavitary transducer and needle guide device attached to the transducer shaft. The CEUS characteristics, successful biopsy rate, diagnostic performance and complications were assessed and recorded.

RESULTS

Of the 29 lesions (median size: 31.5 ± 14.3 mm; range: 9-58mm), 18 lesions were located in oral cavity (oral tongue (n=6), floor of the mouth (n=5), gingiva (n=5), hard palate (n=1) and lip (n=1)) and 11 lesions were located in oropharynx (base of the tongue (n=6), parapharyngeal space (n=4), and tonsil (n=1)). CEUS improved the conspicuity of target lesions and detection rate of internal liquefied necrosis comparing with transoral US (p <0.05). Successful biopsy rate was 100%. Based on the final diagnosis: 19 malignant lesions (15 squamous cell carcinomas, 2 adenoid cystic carcinomas, one mucoepidermoid carcinoma and one melanoma) and 10 benign lesions (5 inflammatory lesions, 3 pleomorphic adenomas, one schwannoma and one hematoma), the diagnostic sensitivity, specificity, positive predictive value (PPV), negative predictive value (NPV), and accuracy of this technique for the diagnosis of oral lesions were 94.7%, 100%, 100%, 90.9% and 96.6% respectively. No serious complications were observed.

CONCLUSION

Transoral CEUS-guided CNB can be considered as a complementary technology for pathological diagnosis of oral lesions that could not be accurately identified or had a previously non-diagnostic cyto-histological biopsy.

CLINICAL RELEVANCE/APPLICATION

Transoral CEUS-guided CNB can serve as a safe, feasible and accurate technique for pathological diagnosis and decision making of oral lesions.

SST10-02 HighNoon CT-Guided Needle Navigation Device: Preliminary Experience

Friday, Dec. 6 10:40AM - 10:50AM Room: E451B

Participants

Siddharth S. Vijayakumar, MBBS, Chennai, India (*Presenter*) Nothing to Disclose Roy J. Santosham, MD, Chennai, India (*Abstract Co-Author*) Inventor, HigHNooN; Director, Kornerstone Pvt Ltd Bhawna Dev, MD, Chennai, India (*Abstract Co-Author*) Nothing to Disclose Ritesh Santosham, MBBS, Chennai, India (*Abstract Co-Author*) Nothing to Disclose Shanthakumar Devakaran, BSC, Chennai, India (*Abstract Co-Author*) Director, Kornerstone Devices Pvt Ltd; Managing Director, Vital Bio-Systems Pvt Ltd Azhagu Palaniappan, Chennai, India (*Abstract Co-Author*) Technical Coordinator, Kornerstone Devices Pvt Ltd

For information about this presentation, contact:

santoshamroy@yahoo.com

PURPOSE

To establish the clinical utility in terms of safety, less time consumption & practicality of high noon in simple & complex CT guided needle placement - biopsies & procedures.

METHOD AND MATERIALS

HighNooN - Shadow based needle navigation device is used to perform high precision percutaneous CT guided needle placement. The devices is ceiling mounted and can be guided easily to area of action. Device has central camera, four sources of light at right angle to each other and a laser source which project a crosier on the patient. The device can make left to right and head to toe swinging motion.140 biopsies were performed on mannequins under Ct guidance following which detailed results were presented to the ethics committee. After approval from ethics committee 55 cases are done using HighNoon prototype.

RESULTS

We are presenting here the results of our initial 55 patients. In these 55 Patients Average target accuracy achieved was 1mm as compared to 5mm without needle guidance device . Average manipulations done was 3%, average no of check scans was 1.24 using High Noon when compared to free hand biopsies where it was 5-10% & 0.4 - 6 respectively. Average wheel in & wheel out time was 26 mins with High noon and between 35 to 50 mins without needle guidance. Patient movement can be identified and corrected and respiratory misregisteration can be avoided using visual feedback for raddiologist & bagging anestheteist .

CONCLUSION

The 'High noon device 'helps to place the needle/device with precise angles of incidence from the point of entry in both axis (X & Z axis), thereby adding to accuracy, reducing the number of insertions, pain, discomfort, radiation, and complications.

CLINICAL RELEVANCE/APPLICATION

WHO states that 9.6 million deaths occurred globally in 2018, 30 % increase in cancer cases is expected in 2030. As the cancer mortality is decreased by early detection -the action plan of WHO is to develop tools to help early detection.HighNooN can help in assessing the smaller lesions in easy & difficult locations to be biopsied and reach the final histopathological diagnosis leading to timely, correct treatment saving lives. Also in countries like India where tuberculosis including extra pulmonary tuberculosis mimicking malignancy is very common - deep seated mediastinal lymph nodes & vertebral lesions can be easily accessed by HighNoon alleviating the unnecessary apprehension and and initiating the correct medication .

SST10-03 Video Augmented Reality Percutaneous Needle Intervention Decreases Radiation Dose While Maintaining Accuracy Compared to C-Arm Cone Beam CT with Fluoroscopy Overlay: A Prospective Clinical Study with a Matched Control

Friday, Dec. 6 10:50AM - 11:00AM Room: E451B

Participants

John M. Racadio, MD, Cincinnati, OH (*Presenter*) Institutional research agreement, Koninklijke Philips NV Neil D. Johnson, MD, Cincinnati, OH (*Abstract Co-Author*) Institutional research agreement, Koninklijke Philips NV Manish N. Patel, DO, Cincinnati, OH (*Abstract Co-Author*) Institutional research agreement, Koninklijke Philips NV Nicole Hilvert, Cincinnati, OH (*Abstract Co-Author*) Institutional research agreement, Koninklijke Philips NV Drazenko Babic, MD, Best, Netherlands (*Abstract Co-Author*) Employee, Koninklijke Philips NV Robert Homan, MSc, Best, Netherlands (*Abstract Co-Author*) Employee, Koninklijke Philips NV Jurgen Hoppenbrouwers, Best, Netherlands (*Abstract Co-Author*) Employee, Koninklijke Philips NV

For information about this presentation, contact:

john.racadio@cchmc.org

PURPOSE

To compare navigational accuracy and radiation dose during percutaneous needle intervention for video augmented reality (AR) guidance (study group) versus c-arm cone beam computed tomography (CT) with fluoroscopy overlay (control group)

METHOD AND MATERIALS

This is an IRB approved prospective study with a retrospective matched-control group. Matching was performed for clinical indication. Patients requiring c-arm cone beam CT and integrated fluoroscopy overlay guidance for biopsy, drainage, injection, or ablation were eligible to be prospectively enrolled for the procedure to be performed with video AR. Three interventional radiologists performed 15 video AR procedures in 11 patients. The video AR procedures were compared to an equal number of procedures and patients using c-arm cone beam CT with fluoroscopy overlay. Accuracy of needle guidance was defined as distance between the needle tip and planned anatomic target. Target depth from skin surface, fluoroscopy time, and complications were recorded. Correlation between accuracy and depth of target was assessed using Pearson correlation coefficient. Student's t-test was applied to evaluate statistical difference between groups for each continuous variable.

RESULTS

Age in the study and control groups was 19±6 yrs and 14±4 yrs (p<0.05), respectively. There were 6 biopsies (3 ilium, 1 femur, 1 tibia, 1 sternum) and 9 injections (4 pars interarticularis, 3 sacroiliac, 1 hip, 1 sternum) in each group. Accuracy in the study group was superior to the control group ($2.9\pm2.3 \text{ mm vs}$. $5.6\pm5.0 \text{ mm}$) although not statistically significant (p=0.07). Fluoroscopy time was significantly lower in the study group compared to the control group ($0.8\pm1.0 \text{ min vs}$. $2.1\pm2.0 \text{ min}$, p<0.05). Target depth in the study group ($48\pm20 \text{ mm}$) and control group ($60\pm27 \text{ mm}$) were not statistically different (p=0.18). There was higher negative correlation between the accuracy and the depth of the anatomic target in control group compared to the study group. There were no complications in either group.

CONCLUSION

Video augmented reality percutaneous needle intervention decreases radiation dose while maintaining accuracy compared to c-arm cone beam CT with fluoroscopy overlay.

CLINICAL RELEVANCE/APPLICATION

Replacing fluoroscopy with video AR guidance decreases x-ray dose to patients and interventionalists without compromising accuracy or clinical outcome.

SST10-04 Comparison of the Complications of Percutaneous versus Transjugular Liver Biopsies Performed at a Single Institution

Friday, Dec. 6 11:00AM - 11:10AM Room: E451B

Participants

Andrew P. Mai, Houston, TX (*Presenter*) Nothing to Disclose Peyton Cramer, BS, Houston, TX (*Abstract Co-Author*) Nothing to Disclose Anil K. Pillai, MD, Houston, TX (*Abstract Co-Author*) Nothing to Disclose

PURPOSE

Transjugular liver biopsy (TJLB) is safer than percutaneous liver biopsy (PLB) in patients with increased risk for hemorrhage. Few clinical studies have directly compared the complication rates between the two procedures. The aim of this study was to retrospectively review patients who underwent liver biopsy and compare the incidence of adverse events and patient factors that were associated with complications.

METHOD AND MATERIALS

Institutional approval was obtained for this study. Data was collected from 158 patients diagnosed with cirrhosis that underwent non-targeted liver biopsies from January 2016 to April 2018. Information included patient demographics, coagulation status, biopsy method, operative findings, and immediate complications (<30 day). Statistical analyses with Fisher's exact test and Wilcoxon rank sum test were then performed to compare the outcomes of the two procedures.

RESULTS

Complications occurred in 7.3%(7/96) who underwent TJLB and included self-limiting post-operative pain (n=4, 4.2%) and major vascular complications (n=3, 3.1%) such as AV fistula and hemoperitoneum. 4.8% (3/62) of patients in the PLBs developed procedural complications including post-operative pain (n=2, 3.2%) and major vascular complications (n=1, 1.6%). The difference in complication rates between the two techniques was not statistically significant (p = 1), nor was there a clinically significant difference in patient demographics, INR, PTT, or PT between the two groups. A larger number of patients who received TJLB were on anticoagulation therapy.

CONCLUSION

Our results show that both TJLB and PLB are safe procedures and there is no significant difference in complication rates between the two biopsy techniques. Although not statistically significant, there was a higher number of major vascular complications with TJLB biopsies. This suggests that the conventional belief of TJLB being the inherently safer approach is not necessarily true in clinical practice.

CLINICAL RELEVANCE/APPLICATION

Transjugular and percutaneous liver biopsies are minimally invasive techniques that allow for hepatic tissue sampling and both are used in the diagnosis and management of cirrhosis.

SST10-05 Power of Lipiodol-Enhancement in CT-Guided Biopsies of Unspecified Suspect Intrahepatic Lesions: Improvement of Accuracy and Safeness

Friday, Dec. 6 11:10AM - 11:20AM Room: E451B

Participants

Marcel C. Langenbach, MD, Cologne, Germany (*Presenter*) Research Grant, Guerbet SA Thomas J. Vogl, MD, PhD, Frankfurt, Germany (*Abstract Co-Author*) Nothing to Disclose Amelie Buchinger, MS, Frankfurt, Germany (*Abstract Co-Author*) Nothing to Disclose Lajos M. Basten, Frankfurt am Main, Germany (*Abstract Co-Author*) Nothing to Disclose Renate M. Hammerstingl, MD, Frankfurt am Main, Germany (*Abstract Co-Author*) Nothing to Disclose Tatjana Gruber-Rouh, Frankfurt am Main, Germany (*Abstract Co-Author*) Nothing to Disclose

For information about this presentation, contact:

marcel.langenbach@me.com

PURPOSE

To evaluate the power of Lipiodol in improving the rate of successful biopsies of suspect intrahepatic lesion which is often challenging in native CT-scans. Lipiodol, commonly applied in angiography for tumor embolization, might improve the success rate.

METHOD AND MATERIALS

Six-hundred-seven patients (men: 358, women: 259) with unclear suspect liver lesions were retrospectively evaluated. All patients received a CT-guided liver biopsy and results were histopathological analysed. Successful punctuations were defined by positive pathological findings. Data were ascertain regarding the use of contrast media, lipiodol or common intravenous contrast, or native performance. Lesion hitting rate and influencing factors like lesion size or liver cirrhosis were insulated. Procedure was performed with the same 128-multislice CT-scanner. Correlation was calculated according to Spearman-Rho, results compared using Wilcoxon-Man-Whitney t-test and Chi-square-test. P<0.05 was considered as statistically significant.

RESULTS

Losion hitting rate was significantly higher using Liniadal (79 604) compared to native hiensy (72 204) or the use of intravenous

Lesion nutring rate was significantly higher using Liploud (70.0%) compared to hative plopsy (73.2%) of the use of intravenous contrast agent (65.2%) (p=0.038). For lesions with a size <20mm, the benefit regarding the hitting rate was even higher for Liplodol (71.2% vs 47.7% vs. 65.5%) (p=0.021). For patients with an existing liver cirrhosis in comparison of all three groups were seen. (p=0.97). No major complications occurred during the interventions.

CONCLUSION

Pre-puncture marking using Lipiodol in angiography increases the lesion hitting rate significantly, especially for small suspect liver lesions (<20mm), combines with a lower rate of re-biopsy and a higher safeness for the patient.

CLINICAL RELEVANCE/APPLICATION

Pre-puncture marking of unclear intrahepatic lesions using Lipiodol increases the hitting rate and safeness of liver biopsies and is recommended for hardly detectable liver lesions in CT.

SST10-06 Real-Time Intravascular Device Guidance for Procedures in the Thorax and Abdomen Using Motion-Compensated Roadmaps

Friday, Dec. 6 11:20AM - 11:30AM Room: E451B

Participants

Martin Wagner, Madison, WI (*Presenter*) Shareholder, LiteRay Medical LLC Sarvesh Periyasamy, MS, Madison, WI (*Abstract Co-Author*) Nothing to Disclose Joe F. Whitehead, BS, Madison, WI (*Abstract Co-Author*) Nothing to Disclose Michael Speidel, PhD, Madison, WI (*Abstract Co-Author*) Nothing to Disclose Paul F. Laeseke, MD, PhD, Madison, WI (*Abstract Co-Author*) Consultant, NeuWave Medical, Inc ; Shareholder, Elucent Medical ; Consultant, Elucent Medical ; Shareholder, HistoSonics, Inc; Consultant, HistoSonics, Inc; Shareholder, McGinley Orthopaedic Innovations, LLC; Grant, Siemens AG

For information about this presentation, contact:

mwagner9@wisc.edu

PURPOSE

Vascular roadmaps have limited utility for intravascular procedures in the thorax and abdomen due to severe subtraction artifacts and changes in vessel shape and position caused by respiratory motion. Instead, most interventional radiologists navigate devices (eg. guidewires and catheters) without vascular overlay. This procedure is time consuming and requires experienced interventional radiologists. The purpose of this study was to test the accuracy of a recently developed system that provides real-time motioncompensated vascular overlays for device navigation.

METHOD AND MATERIALS

The proposed system creates a dynamic motion model from contrast enhanced x-ray images acquired under free breathing conditions. During device navigation, a motion-compensated vessel roadmap is created based on respiratory motion estimations from live x-ray images. The device is extracted from the x-ray images and superimposed on the motion compensated roadmap. Alternatively, the system can apply respiratory motion compensation to the device and display a static vascular roadmap. A porcine study was conducted with 3 animals, where a real-time prototype of the system was used to navigate a guidewire within the hepatic arteries. An EM-tracking sensor was placed in different branches of the vasculature to measure motion and compare it to the deformation estimated by the proposed approach.

RESULTS

The average difference between the measured EM-sensor motion and the estimated vessel motion was 1.59 ± 0.64 mm at the detector. The Pearson correlation was 0.94 (p < 0.01). The prototype was able to display the guidewire within the correct vascular branches despite respiratory motion. In some cases, the proximal and less flexible part of the device deforms the surrounding vessels, but the distal part, most relevant for device navigation, is still displayed correctly.

CONCLUSION

Our real-time motion compensated device guidance system provides an intuitive way to accurately navigate devices during intravascular procedures in the abdomen. This could reduce procedure times and therefore decrease risk and radiation exposure to the patient.

CLINICAL RELEVANCE/APPLICATION

Real-time motion compensated roadmaps provide the device position in the vasculature during procedures in the abdomen. This could reduce procedure times and decrease radiation and risk to patients.

SST10-07 Role of Contrast-Enhanced Ultrasound (CEUS) in the Detection of Complications Ensuing US-Guided Interventional Procedures: A Multi-Center Study

Friday, Dec. 6 11:30AM - 11:40AM Room: E451B

Participants

Giampiero Francica, MD, Castel Voltumo, Italy (*Presenter*) Research Consultant, Shenzhen Mindray Bio-Medical Electronics Co, Ltd Maria Franca Meloni, Basiglio, Italy (*Abstract Co-Author*) Nothing to Disclose Laura Riccardi, Roma, Italy (*Abstract Co-Author*) Nothing to Disclose Eugenio Caturelli, Viterbo, Italy (*Abstract Co-Author*) Nothing to Disclose Ilario De Sio, Naples , Italy (*Abstract Co-Author*) Nothing to Disclose Francesco Giangregorio, MD, Piacenza, Italy (*Abstract Co-Author*) Nothing to Disclose Fulvia Terracciano, San Giovanni Rotondo, Italy (*Abstract Co-Author*) Nothing to Disclose Maurizio Pompili, MD, Roma, Italy (*Abstract Co-Author*) Nothing to Disclose

For information about this presentation, contact:

PURPOSE

Aim of this study was to assess the contribution of CEUS to the detection of complications ensuing US-guided hepatic interventional procedures in field practice of 7 interventional ultrasound centers

METHOD AND MATERIALS

The participating centers retrospectively selected all patients in whom CEUS detected complications after US-guided liver biopsy for diffuse liver disease or focal liver lesions (FLL) and after ablation of liver tumors over the last decade.

RESULTS

22 patients (13 M/ 9F, median age 73 yrs.) experienced complications after 5 liver biopsies with 18g cutting needles (3 for FLL) and 17 ablations of liver tumors (16 HCC) carried out with PEI (2), MW (2), RF (13). Median size of the 20 biopsied/ablated nodules was 22.5 mm (range 15-39 mm). In 10 cases CEUS was performed at the end of ablation (2 PEI, 2 MW, 6 RF) and demonstrated 6 sub-segmental/segmental infarcts, 3 active bleedings (2 capsular tears with hemoperitoneum, 1 hemobilia), and 1 subcapsular hepatic hematoma (SHH). Only 2 patients underwent RF to achieve hemostasis. In 5 symptomatic cases CEUS was performed within 6 hours after biopsy and displayed 1 actively bleeding capsular tear with hemoperitoneum, 1 hemobilia and 3 SHHs, one of which actively bleeding. In the latter case transarterial embolization (TAE) was carried out and another patient needed blood transfusion (BT). Finally, in 7 cases CEUS was performed 24-48 hours after interventional maneuvers. In 5 symptomatic cases CEUS showed 1 actively bleeding capsular tear with hemotherax (due to actively bleeding intercostal artery), 1 pseudoaneurysm of a right arterial branch, 1 segmental infarct, 2 abscessed ablated areas; in the remaining case, routine CEUS check at 24 hours displayed 1 SHH. 5 out of 7 patients in this group were treated with TAE (2 cases), percutaneous abscess drainage (2 cases), and BT plus TAE (1 case).

CONCLUSION

This multicenter survey highlights the potential role of CEUS in the detection of immediate and early (<6 hours) complications ensuing US-guided liver biopsy or ablation. Iatrogenic hemorrhagic complications even with active bleeding and ischemic segmental areas can be successfully demonstrated by CEUS and promptly treated if clinically needed.

CLINICAL RELEVANCE/APPLICATION

CEUS should be considered as an useful tool to detect iatrogenic complications mainly of ischemic and hemorrhagic type occurring after US-guided hepatic interventional procedures.

SST10-08 Detection of Bleeding Complications After Instituting a 1-Hour Post-Procedure Recovery Time Following Renal Transplant Biopsy

Friday, Dec. 6 11:40AM - 11:50AM Room: E451B

Participants

Maitray D. Patel, MD, Paradise Valley, AZ (*Abstract Co-Author*) Nothing to Disclose Jeffry S. Kriegshauser, MD, Phoenix, AZ (*Presenter*) Research support, General Electric Company Nirvikar Dahiya, MD, Phoenix, AZ (*Abstract Co-Author*) Nothing to Disclose Scott W. Young, MD, Phoenix, AZ (*Abstract Co-Author*) Nothing to Disclose

For information about this presentation, contact:

patel.maitray@mayo.edu

PURPOSE

To analyze the timing of major bleeding complications following renal transplant biopsy in the context of a standardized 1-hour post-procedure observation protocol.

METHOD AND MATERIALS

We retrospectively reviewed the electronic medical record for 4519 consecutive US-guided renal transplant biopsies (769 women, 1055 men) from 01/01/2012 to 12/31/2017, after initiating a post-procedural protocol limited to 1 hour of routine observation, additional observation only if symptoms present at 1 hour, and subsequent patient contact within 24 hours after discharge. The development of a major bleeding complication (CTCAE Class 3 or higher) was recorded, along with all available details regarding the time course of patient symptoms and presentation.

RESULTS

There were 11 CTCAE Class 3 complications (11/4519, 0.24%). Seven patients (7/11, 63.6%) were asymptomatic after 1 hour of observation and were discharged. Of these, two (2/11, 18.2%) were admitted after symptoms began 4-8 hours after biopsy; the remaining five (5/11, 45.5%) were admitted after developing symptoms more than 8 hours after biopsy. Four patients (4/11, 36.3%) had symptoms in the 1 hour observation period; of these, two (2/11, 18.2%) had pain combined with hemodynamic alterations, leading to hospital admission. The other 2 patients (2/11, 18.2%) had pain without hemodynamic alterations, leading to an additional hour of observation, and subsequent discharge due to successful pain control with oral analgesics; these 2 patients were later admitted when symptoms returned 4- 8 hours after biopsy.

CONCLUSION

Major bleeding complications following US-guided renal transplant biopsy are rare, occurring in 0.24% of patients in this study, and most are not clinically apparent within 4 hours of biopsy. One-third of patients who develop significant hemorrhage have early manifestations, but approximately two-thirds of patients do not have unusual symptomatic manifestations of hemorrhage until more than 4 hours after biopsy. Almost half of all patients do not have unusual symptoms until more than 8 hours after biopsy.

CLINICAL RELEVANCE/APPLICATION

A recovery protocol with only 1 hour of routine observation after uneventful renal transplant biopsy can be safely implemented when combined with routine follow-up patient contact. Requiring routine post-procedure observation for 4 hours as used at some facilities uses more resources without improving care.

SST10-09 High-Intensity Focused Ultrasound (HIFU) Focal Therapy to Primary Treatment of Localized Prostate Cancer Using 68Ga-PSMA PET/MR as Main Guidance: Innovative Experience in 14 Patients

Friday, Dec. 6 11:50AM - 12:00PM Room: E451B

Participants

Guilherme C. Mariotti, MD, Jundiai, Brazil (*Presenter*) Nothing to Disclose Paulo Kayano, Sao Paulo, Brazil (*Abstract Co-Author*) Nothing to Disclose Priscila M. Falsarella, Sao Paulo, Brazil (*Abstract Co-Author*) Nothing to Disclose Oliver R. Claros, Sao Paulo, Brazil (*Abstract Co-Author*) Nothing to Disclose Marcelo L. Cunha, MD, Sao Paulo, Brazil (*Abstract Co-Author*) Nothing to Disclose Gustavo C. Lemos, Sao Paulo, Brazil (*Abstract Co-Author*) Nothing to Disclose Marcos R. Queiroz, MD, Barueri, Brazil (*Abstract Co-Author*) Nothing to Disclose Rodrigo G. Garcia, MD, Sao Paulo, Brazil (*Abstract Co-Author*) Nothing to Disclose Ronaldo H. Baroni, MD, Sao Paulo, Brazil (*Abstract Co-Author*) Nothing to Disclose Arie Carneiro, Sao Paulo, Brazil (*Abstract Co-Author*) Nothing to Disclose

For information about this presentation, contact:

guilherme.mariotti@einstein.br

PURPOSE

To identify candidates to High-intensity focused ultrasound (HIFU) focal therapy (FT) for localized prostate cancers (pCa), the following inclusion criteria are commonly used: serum PSA (<15 ng/ml), Gleason score (ISUP 1-3), multiparametric magnetic resonance imaging (mpMRI) with no extracapsular extension, no seminal vesicle invasion or pelvic lymph node disease and negative bone scintigraphy; however, to the best of our knowledge, no prior study has used 68Ga-PSMA PET/MR as the main feature to indicate and guide HIFU procedures.

METHOD AND MATERIALS

A single-center prospective analysis of initial 14 patients, candidates for FT (hemi-gland or super-focal ablation) as the primary treatment option, from August 2018 to March 2019. All patients were re-evaluated by mpMRI and transrectal US/MR fusion prostate biopsy and follow-up 68Ga-PSMA PET/MR to better understand the indication of HIFU before the procedure.

RESULTS

Mean prostatic volume, age, PSA and region of interest volumes were: 47.9 cc, 68 years, 4.56 ng/dl and 1.1 cm; respectively. Preprocedure mpMRI showed 7.1% of PIRADS 2, 21.4% of PIRADS 3, 57.3% of PIRADS 4 and 14.2% of PIRADS 5. US-guided fusion + systematic biopsy showed 3 patients with unilateral ISUP 1, 8 patients wth unilateral ISUP 2 and 3 patients with ISUP 3. Ten patients (71.4%) had concordant findings between pre-procedure mpMRI, 68Ga-PSMA PET/MR and biopsy. Four patients (28.5%) had discordant findings, altering the treatment planning or contraindicating the procedure, for the following reasons: 2 patients had larger unilateral multifocal disease on 68Ga-PSMA PET/MR than on MRI or US-MR fusion biopsy, with need to extend the treatment area; One patient presented a smaller extent of disease in 68Ga-PSMA PET/MR than in MRI, allowing a reduction of the expected area of treatment; One patient had extensive bilateral disease in 68Ga-PSMA PET/MR that was not suspected in MRI, confirmed by biopsy, contraindicating the procedure.

CONCLUSION

In conclusion, 68Ga-PSMA PET/MR may play a fundamental role in the indication and planning of focal ablative prostatic therapy and might be introduced in the inclusion criteria for cases indicated for HIFU.

CLINICAL RELEVANCE/APPLICATION

High-intensity focused ultrasound is a promising novel technique but new diagnostic procedures, such as 68Ga-PSMA PET/MR for selection of patients and correct planning of the procedure may alter the oncological outcome and mortality.

Printed on: 10/29/20





SPFR61

Friday Imaging Symposium: Healthy Aging Reimagined - A Multidisciplinary Approach

Friday, Dec. 6 12:30PM - 3:00PM Room: E253CD

от

AMA PRA Category 1 Credits ™: 2.50 ARRT Category A+ Credits: 3.00

FDA Discussions may include off-label uses.

Participants

Leon Lenchik, MD, Winston-salem, NC (*Moderator*) Nothing to Disclose Stephen B. Kritchevsky, PhD, Winston-Salem, NC (*Moderator*) Nothing to Disclose

For information about this presentation, contact:

llenchik@wakehealth.edu

LEARNING OBJECTIVES

1) Provide a multidisciplinary perspective on healthy aging, including optimal strategies for imaging, lessons from population health, and insights from research into biologic determinants.

Sub-Events

SPFR61A Reimagining Imaging and Aging

Participants Leon Lenchik, MD, Winston-salem, NC (*Presenter*) Nothing to Disclose

For information about this presentation, contact:

llenchik@wakehealth.edu

LEARNING OBJECTIVES

1) Describe current trends in imaging of aging.

SPFR61B Keynote: Aging Organs and Aging Systems - A Population Health Perspective

Participants

Stephen B. Kritchevsky, PhD, Winston-Salem, NC (Presenter) Nothing to Disclose

For information about this presentation, contact:

skritche@wakehealth.edu

LEARNING OBJECTIVES

1) Understand the limitations of chronological age in understanding health risks for older adults. 2) Identify several strategies for assigning biologic age to persons of similar chronologic age. 3) Discuss radiological phenotypes that might help predict functional trajectories in older adults.

SPFR61C Role of Body Composition Imaging in Healthy Aging

Participants Robert D. Boutin, MD, Davis, CA (*Presenter*) Nothing to Disclose

LEARNING OBJECTIVES

1) Highlight the role of routine imaging techniques to evaluate changes in bone, fat, and muscle that occur with aging.

SPFR61D Role of Cardiovascular Imaging in Healthy Aging

Participants

John J. Carr, MD, MS, Nashville, TN (Presenter) Nothing to Disclose

For information about this presentation, contact:

j.jeffrey.carr@vanderbilt.edu

LEARNING OBJECTIVES

1) Identify activities that support ideal cardiovascular health from conception, childhood and across adult life.

ABSTRACT

Cardiovascular health across the lifespan is important to maximizing an individuals opportunity for healthy aging.

SPFR61E Role of Brain Imaging in Healthy Aging

Participants

Cyrus Raji, MD,PhD, St. Louis, MO (Presenter) Consultant, Brainreader ApS; Consultant, Neuroevolution LLC

SPFR61F Keynote: Biologic Determinants of Aging

Participants

Osvaldo Delbono, Winston Salem, NC (Presenter) Nothing to Disclose

LEARNING OBJECTIVES

1) To categorize the cellular and molecular determinants of aging. 2) To identify altered intercellular communication as a major driver of loss in tissue composition and function with aging. 3) To discuss the role of cellular imaging in identifying biological processes leading to age-associated diseases.

SPFR61G Deep Learning and the Imaging of Aging

Participants

Albert Hsiao, MD,PhD, La Jolla, CA (*Presenter*) Founder, Arterys, Inc; Consultant, Arterys, Inc; Shareholder, Arterys, Inc; Speaker, Bayer AG; Research Grant, Bayer AG; Speaker, General Electric Company; Research Grant, General Electric Company;

LEARNING OBJECTIVES

1) Review the potential for deep learning technology to transform imaging diagnosis. 2) Examine the opportunities for deep learning to perform opportunistic screening and quantification of imaging biomarkers of aging.

SPFR61H Mind-Body Connection in Aging

Participants Leon Lenchik, MD, Winston-salem, NC (*Presenter*) Nothing to Disclose

For information about this presentation, contact:

llenchik@wakehealth.edu

LEARNING OBJECTIVES

1) Describe the relationship between mind and body in older adults.

SPFR61I Panel Discussion

Printed on: 10/29/20